Fermi National Accelerator Laboratory

FERMILAB-Pub-92/202-A
June 1992

NATURAL INFLATION: PARTICLE PHYSICS MODELS, POWER LAW SPECTRA FOR LARGE-SCALE STRUCTURE, AND CONSTRAINTS FROM COBE

Fred C. Adams[1,5], J. Richard Bond[2], Katherine Freese[1,5,6]
Joshua A. Frieman[3,5] and Angela V. Olinto[4,5]

[1] *Physics Department, University of Michigan*
Ann Arbor, MI 48109

[2] *CIAR Cosmology Program*
Canadian Institute for Theoretical Astrophysics
University of Toronto, Toronto, ON M5S 1A1, Canada

[3] *NASA/Fermilab Astrophysics Center*
Fermi National Accelerator Laboratory
P.O. Box 500, Batavia, IL 60510

[4] *Department of Astronomy and Astrophysics*
University of Chicago
Chicago, IL 60637

[5] *Institute for Theoretical Physics*
University of California, Santa Barbara
Santa Barbara, CA

[6] *Presidential Young Investigator*
and Sloan Foundation Fellow

Operated by Universities Research Association Inc. under contract with the United States Department of Energy

ABSTRACT

We discuss the particle physics basis for models of natural inflation with pseudo-Nambu-Goldstone bosons and study the consequences for large-scale structure of the non-scale-invariant density fluctuation spectra that arise in natural inflation and other models. A pseudo-Nambu-Goldstone boson, with a potential of the form $V(\phi) = \Lambda^4[1 \pm \cos(\phi/f)]$, can naturally give rise to an epoch of inflation in the early universe, if $f \sim M_{Pl}$ and $\Lambda \sim M_{GUT}$. Such mass scales arise in particle physics models with a gauge group that becomes strongly interacting at the GUT scale. We work out a specific particle physics example based on the multiple gaugino condensation scenario in superstring/supergravity theory. We then study the cosmological evolution of and constraints upon these inflation models numerically and analytically. To obtain sufficient inflation with a probability $\mathcal{O}(1)$ and a high enough post-inflation reheat temperature for baryogenesis, we require $f \gtrsim 0.3 M_{pl}$.

The primordial density fluctuation spectrum generated by quantum fluctuations in ϕ is a non-scale-invariant power law, $P(k) \propto k^{n_s}$, with $n_s \simeq 1 - (M_{Pl}^2/8\pi f^2)$, leading to more power on large length scales than the $n_s = 1$ Harrison-Zeldovich spectrum. (For the reader primarily interested in large-scale structure, the discussion of this topic is presented in Section IV and is intended to be nearly self-contained.) We pay special attention to the prospects of using the enhanced power to explain the otherwise puzzling large-scale clustering of galaxies and clusters and their flows. We find that the standard cold dark matter (CDM) model with $0 \lesssim n_s \lesssim 0.6$ could in principle explain these clustering data, such as the APM galaxy angular correlation function. However, the microwave background anisotropies recently detected by COBE imply such low primordial amplitudes for these CDM models (that is, bias factors $b_8 \gtrsim 2$ for $n_s \lesssim 0.6$) that galaxy formation would occur too late to be viable and the large-scale galaxy velocities would be too small. In fact, combining the COBE results with the requirement of sufficiently early galaxy formation ($z_{gf} > 2$) leads to the constraint $n_s \gtrsim 0.63$, which corresponds to $f \gtrsim 0.3 M_{Pl}$ for natural inflation (virtually the same as the sufficient reheating constraint). A comparable bound, $n_s \gtrsim 0.72$, arises by combining COBE with the inferred large-scale flows. For other inflation models, such as extended inflation and inflation with exponential potentials, which give rise to initial fluctuation spectra that are power laws through the 3 decades in wavelength probed by large scale observations, gravity waves can produce a significant fraction of the COBE signal (while they are negigible for natural inflation); for these models, our corresponding COBE constraints on n_s are therefore tighter, $n_s > 0.76$ (from $z_{gf} > 2$) and $n_s > 0.89$ (from large-scale flows). Combined with other constraints on the Brans-Dicke parameter (which effectively imply $n_s < 0.77 - 0.84$), this leaves little or no room for most extended inflation models. Chaotic inflation models with power law potentials have $n_s \gtrsim 0.95$ over observable wavelengths and so are not affected. Although no single value of the spectral index n_s in the standard cold dark matter model universally fits the data, a value $n_s \leq 1$ may be combined with other variations of the standard CDM framework to explain the large-scale structure. For example, if the baryon density is as high as $\Omega_b = 0.1$ or the Hubble parameter as low as $H_0 = 40$ km/sec/Mpc, then $n_s \sim 0.7$ with CDM would be at least marginally consistent with the large-scale clustering data, COBE, large-scale velocities, and the requirement of sufficiently early structure formation.

I. INTRODUCTION

In recent years, the inflationary universe has been in a state of theoretical limbo: it is a beautiful idea in search of a compelling model. The idea is remarkably elegant[1]: if the early universe undergoes an epoch of quasi-exponential expansion during which the Robertson-Walker scale factor $a(t)$ increases by a factor of at least e^{60}, then a small causally connected region grows to a sufficiently large size to explain the observed homogeneity and isotropy of the universe, to dilute any overdensity of magnetic monopoles or other unwanted relics, and to flatten the spatial hypersurfaces, $\Omega \equiv 8\pi G\rho/3H^2 \rightarrow 1$ (where the density ρ includes all forms of stress-energy, including the vacuum [the cosmological constant], and H is the Hubble parameter). As a bonus, quantum fluctuations during inflation can causally generate large-scale density fluctuations, which are required for galaxy formation[2].

During the inflationary epoch, the energy density of the universe is dominated by the (nearly constant) potential energy density $V(\phi)$ associated with a slowly rolling scalar field ϕ, the *inflaton*[3]. The combination of two constraints – that the universe inflate sufficiently, and that perturbations in the cosmic microwave background radiation (CMBR) are not produced in excess of observations – requires the potential of the inflaton to be very flat. Consequently, the field ϕ must be extremely weakly self-coupled, with effective quartic self-coupling constant $\lambda_\phi < \mathcal{O}(10^{-8})$ [4] (and with $\lambda_\phi < 10^{-12}$ in most models).

Density fluctuations in inflation are thus a blessing for astronomers but a curse for particle physicists, because the theory must contain a very small dimensionless number. Attitudes concerning this problem vary widely among inflation theorists: to some this represents unacceptable 'fine tuning'; to others, it is not an issue of great concern because we know there exist other small numbers in physics, like lepton and quark Yukawa couplings $g_Y \sim 10^{-5}$ and the ratio $M_{weak}/M_{Pl} \sim 10^{-17}$. Partly as a consequence of the latter view, in recent years, it has become customary to decouple the inflaton completely from particle physics models, to specify an 'inflaton sector' with the requisite properties, with little or no regard for its physical origin.

Nevertheless, it is meaningful and important to ask whether such a small value for λ_ϕ is in principle unnatural. Clearly, the answer depends on the particle physics model within which ϕ is embedded and on one's interpretation of naturalness. A small parameter λ is said to be "technically natural" if it is protected against large radiative corrections by a symmetry, *i.e.*, if setting $\lambda \rightarrow 0$ increases the symmetry of the system [5]. For example, in this way, low energy supersymmetry might protect the small ratio M_{weak}/M_{Pl}. However, in technically natural inflation models, the small coupling λ_ϕ, while stable against radiative corrections, is itself unexplained, and is generally postulated (*i.e.*, put in by hand) solely in order to generate successful inflation. Technical naturalness is a useful concept for low energy effective Lagrangians, like the electroweak theory and its supersymmetric extensions, but it points to a more fundamental level of theory for its origin. Since inflation takes place *relatively* close to the Planck scale, it would be preferable to find the inflaton in particle physics models which are "strongly natural", that is, which have no small numbers in the fundamental Lagrangian.

In a strongly natural gauge theory, all small dimensionless parameters ultimately arise dynamically, *e.g.*, from renormalization group (or instanton) factors like $\exp(-1/\alpha)$, where α is a gauge coupling. In particular, in an asymptotically free theory, the scale M_1, at which a logarithmically running coupling constant becomes unity, is $M_1 \sim M_2 e^{-1/\alpha}$, where M_2 is the fundamental mass scale in the theory. In some models, the inflaton coupling λ_ϕ arises from a ratio of mass scales, $\lambda_\phi \sim (M_1/M_2)^q$; for example, in the models to be discussed below, $q = 4$. As a result, in such models, λ_ϕ is naturally exponentially suppressed, $\lambda_\phi \sim e^{-q/\alpha}$.

An example of this kind, namely, a scalar field with naturally small self-coupling, is provided by the axion [6], a light pseudoscalar which arises in models introduced to solve the strong CP problem. In axion models, a global $U(1)$ symmetry is spontaneously broken at some large mass scale f, through the vacuum expectation value of a complex scalar field, $\langle\Phi\rangle = f\,\exp(ia/f)/\sqrt{2}$.

(In this case, Φ has the familiar Mexican-hat potential, and the vacuum is a circle of radius f.) At energies below the scale f, the only relevant degree of freedom is the massless axion field a, the angular Nambu-Goldstone mode around the bottom of the Φ potential. However, at a much lower energy scale, the symmetry is explicitly broken. For example, the QCD axion obtains a mass from non-perturbative gluon configurations (instantons) through the chiral anomaly. When QCD becomes strong at the scale $\Lambda_{QCD} \sim 100$ MeV, instanton effects give rise to a periodic potential of height $\sim \Lambda_{QCD}^4$ for the axion. In 'invisible' axion models [7] with canonical Peccei-Quinn scale $f_{PQ} \sim 10^{12}$ GeV, the resulting axion self-coupling is extremely small: $\lambda_a \sim (\Lambda_{QCD}/f_{PQ})^4 \sim 10^{-52}$. This small number simply reflects the hierarchy between the QCD and Peccei-Quinn scales, which arises from the slow logarithmic running of α_{QCD}.

Pseudo-Nambu-Goldstone bosons (PNGB's) are ubiquitous in particle physics models: they arise whenever an approximate global symmetry is spontaneously broken. We choose PNGB's as our candidates for the role of the inflaton. We assume a global symmetry is spontaneously broken at a scale f, with soft explicit symmetry breaking at a lower scale Λ. These two scales, f and Λ, completely characterize the model and will be specified by the requirements of successful inflation - namely, a sufficent number of e-folds of inflation, reheating to a high enough temperature to allow baryogenesis, and an acceptable amplitude and spectrum of density fluctuations. The resulting PNGB potential is generally of the form

$$V(\phi) = \Lambda^4[1 \pm \cos(N\phi/f)]\,. \tag{1.1}$$

We will take the positive sign in Eq.(1.1) (this choice has no effect on our results) and, unless otherwise noted, assume $N = 1$, so that the potential, of height $2\Lambda^4$, has a unique minimum at $\phi = \pi f$ (we assume the periodicity of ϕ is $2\pi f$). In a previous paper [8] (hereafter Paper I), three of us showed that, for $f \sim M_{Pl} \sim 10^{19}$ GeV and $\Lambda \sim M_{GUT} \sim 10^{15}$ GeV, the PNGB field ϕ can drive inflation; in this case, the effective quartic coupling is $\lambda_\phi \sim (\Lambda/f)^4 \sim 10^{-13}$, as required. In this paper, we study this class of models and their implications in greater depth.

We note that, in some cases, the potential of Eq.(1.1) is the lowest order approximation to a more complicated expression. For inflation, the important ingredients are the height ($\sim \Lambda^4$) and width ($\sim f$) of the potential, and the curvature in the vicinity of its extrema, which is determined by $m_\phi^2 = \Lambda^2/f$. Thus, while our treatment will focus on the specific form (1.1), our conclusions hold for more general forms of the PNGB potential which have the same overall shape (that is, same height, width, and curvature at the extrema; in addition, we assume $V(\phi)$ varies monotonically between $\phi = 0$ and πf, that is, we ignore higher order ripples, which might affect the perturbation spectrum over a small range of wavelengths).

In section II, we discuss the PNGB inflation scenario in the context of particle physics models. As noted above, a successful inflation scenario does not consist simply of a scalar field potential that does the trick; in addition, the parameters of the potential, in this case the requisite mass scales f and Λ, must have a natural origin in plausible particle physics models. PNGB potentials with these mass scales do arise naturally in particle physics models. For example, in the hidden sector of superstring (supergravity) theories, if a non-Abelian subgroup(s) remains unbroken, the running gauge coupling can become strong at the scale $\sim 10^{14} - 10^{15}$ GeV; indeed, it is hoped that the resulting gaugino condensation may play a role in determining the string coupling constant and possibly in breaking supersymmetry [9]. (We note that, in such models, the only fundamental scale is the Planck scale, $f \sim M_{Pl}$, and the lower scale Λ is generated dynamically.) In this case, as discussed in Section II, the role of the PNGB inflaton could be played by the "model-independent axion" (the imaginary part of the dilaton) [10].

In Section III, we provide a detailed analysis of the cosmological evolution of the PNGB inflaton field. By and large, the numerical results therein confirm the analytic treatment of paper I. In addition, we also discuss in detail constraints on the mass scales arising from the requirement of sufficient reheating, the density fluctuation amplitude, and the requirement that inflation be probable in the sense of initial (and final) conditions. We also discuss the issue of initial spatial gradients in the inflaton field and how they may be damped out prior to inflation.

In the standard lore of inflation, the adiabatic density fluctuations generated have a nearly scale-invariant Harrison-Zeldovich spectrum. This general statement can be violated, and an arbitrary perturbation spectrum 'designed', but, in most models, at the cost of fine-tuning several parameters of the inflaton potential (or adjusting coupling constants in models with multiple scalar fields) [11]. In the simplest natural inflation model with a potential given by Eq. (1.1), we have no freedom to introduce arbitrary features into the perturbation spectrum. Nevertheless, as discussed in sections III.C.2 and IV.A, the density fluctuations generated in this model can deviate significantly from a scale-invariant spectrum: for $f \lesssim 3M_{pl}/4$, the perturbation amplitude at horizon-crossing grows with mass scale M as $(\delta\rho/\rho)_{hor} \sim M^{m_{pl}^2/48\pi f^2}$. Thus, the primordial power spectrum for density fluctuations (at fixed time) is a power law, $\langle|\delta\rho(k)/\rho|^2\rangle \sim k^{n_s}$, with spectral index $n_s \simeq 1 - (M_{pl}^2/8\pi f^2)$. The extra power on large scales (compared to the scale-invariant $n_s = 1$ spectrum) can have important implications for large-scale structure, of particular interest since the scale-invariant spectrum with cold dark matter (CDM) appears to have too little power on large scales. Other inflation models can also give rise to non-scale-invariant power law spectra. Therefore, in section IV, we discuss tests of non-scale-invariant power law initial spectra with adiabatic perturbations and CDM, including the galaxy angular correlation function inferred from deep photometric surveys, the CMBR anisotropy detected by COBE, large-scale peculiar velocities, the power spectrum inferred from redshift surveys of IRAS galaxies, and the epoch of galaxy formation.

II. PARTICLE PHYSICS MODELS

There are a number of ways in which massive pseudo-Nambu-Goldstone bosons with the requisite mass scales discussed above may play a role in particle physics models. In this section, we schematically outline only a few of them. The basic idea is to build a model with a global symmetry spontaneously broken at a large mass scale $f \sim M_{Pl}$, which gives rise to one or more massless Nambu-Goldstone bosons. There are then several ways to introduce explicit breaking of (some or all of) the global symmetry at the scale $\Lambda \sim M_{GUT}$, resulting in potentials for the would-be Goldstone modes. Ideally, the lower scale emerges dynamically, so that no small parameters are introduced.

The most familiar example of a pseudo-Nambu-Goldstone boson in nature is the pion. Here, the global chiral symmetry is spontaneously broken by quark condensates at the QCD scale, $\langle\bar{q}q\rangle \simeq \Lambda_{QCD}^3 \simeq (100\ \mathrm{MeV})^3$, and explicitly broken by quark masses, $m_u \simeq m_d \simeq 10$ MeV. In the case of the pion, these two scales are close together (they differ by a factor of about ten), so the pion gains a mass comparable to the QCD scale, $m_\pi^2 \sim m_q\langle\bar{q}q\rangle/f_\pi^2 \sim (100\ \mathrm{MeV})^2$. By contrast, in invisible axion models [7], the scales of spontaneous and of explicit symmetry breaking are separated by many orders of magnitude: the spontaneous symmetry breaking scale f_{PQ} is elevated close to the GUT scale, while the explicit breaking scale is $\sim \Lambda_{QCD}$. The resulting hierarchy of scales yields a very light axion, $m_a^2 \sim m_q\langle\bar{q}q\rangle/f_{PQ}^2$; for example, $m_a \simeq 10^{-5}$ eV for $f_{PQ} \simeq 10^{12}$ GeV. For the PNGB inflaton, we will be interested in models with a relatively modest hierarchy between the spontaneous and explicit global symmetry breaking scales, $\Lambda/f \sim 10^{-4}$. Such a ratio of scales is intermediate between the case of the pion ($\Lambda/f \sim 0.1$) and the invisible QCD axion ($\Lambda/f \sim 10^{-13}$).

A. PNGBs from Condensates

In this section, we illustrate how such an intermediate mass hierarchy can arise. We consider an action that contains coupled scalar and fermion fields and exhibits a chiral U(1) symmetry. Spontaneous breaking of the chiral symmetry takes place at energy scale f (for inflation, $f \sim M_{pl}$); massless Nambu-Goldstone bosons arise at this scale. We illustrate an additional feature that may be attractive although not necessary to our model: if the scalar field couples non-minimally to

gravity, it may dynamically generate Newton's constant at this scale (induced gravity) [12]. Next, we discuss several ways in which the symmetry can be explicitly broken at a lower energy scale $\sim \Lambda$ (for inflation, $\Lambda \sim 10^{-4} M_{pl}$). At this scale, the Nambu-Goldstone boson acquires a mass, in a manner similar to the axion or schizon [13] (although at higher mass scale). We focus on axion-like scenarios, in which a gauge group becomes strong at the scale $\sim \Lambda$. We briefly discuss how this may arise in technicolor models and then, in somewhat more detail in Sec. IIB, in superstring models.

1) Spontaneous Symmetry Breaking

Taking our cue from the axion [14], we first describe a simple model which implements the mechanism described above. Consider the fundamental action for a complex scalar field Φ and fermion ψ, coupled to gravity:

$$S = \int d^4x\sqrt{-g}\left[g^{\mu\nu}\partial_\mu\Phi^*\partial_\nu\Phi - V(\Phi^*\Phi) - \xi\Phi^*\Phi R + i\bar{\psi}\gamma^\mu\partial_\mu\psi - (h\bar{\psi}_L\psi_R\Phi + h.c.)\right] \qquad (2.1)$$

where R is the Ricci scalar, and $\psi_{(R,L)}$ are respectively right- and left-handed projections of the fermion field, $\psi_{(R,L)} = (1 \pm \gamma^5)\psi/2$. This action is invariant under the global chiral $U(1)$ symmetry:

$$\psi_L \to e^{i\alpha/2}\psi_L\ , \quad \psi_R \to e^{-i\alpha/2}\psi_R\ , \quad \Phi \to e^{i\alpha}\Phi\ , \qquad (2.2)$$

analogous to the Peccei-Quinn symmetry in axion models.

We assume the global symmetry is spontaneously broken at the energy scale f in the usual way, *e.g.*, via a potential of the form

$$V(|\Phi|) = \lambda\left(\Phi^*\Phi - \frac{f^2}{2}\right)^2\ , \qquad (2.3)$$

where the scalar self-coupling λ can be of order unity. The resulting scalar field vacuum expectation value (vev) is $\langle\Phi\rangle = fe^{i\phi/f}/\sqrt{2}$.

In this model, spontaneous symmetry breaking dynamically generates Newton's constant for Einstein gravity [12]. At scales below f, the non-minimal coupling of the scalar field to the curvature induces the canonical Einstein Lagrangian, $\xi\langle\Phi^*\Phi\rangle R = (\xi f^2/2)R = R/16\pi G$, if the coupling ξ satisfies

$$\xi = \frac{1}{8\pi}\frac{M_{Pl}^2}{f^2}\ . \qquad (2.4)$$

Since inflation requires $f \sim M_{Pl}$, the above relation holds for ξ of order unity, a natural value for this dimensionless coupling. We note that generation of the Planck scale in this way is not a necessary ingredient of the models discussed below: since inflation takes place after Φ reaches its vev, we could simply replace the non-minimal coupling term in Eq.(2.1) with the usual Einstein Lagrangian. On the other hand, since the mass scale f must be comparable to M_{Pl} for successful inflation, it is natural and economical to tie it directly to the gravitational scale. Since the gravitational sector is canonical once the temperature of the universe drops below the scale f, we assume ordinary Einstein gravity from now on.

Below the scale f, we can neglect the superheavy radial mode of Φ ($m_{radial} = \lambda^{1/2}f \sim M_{Pl}$) since it is so massive that it is frozen out. The remaining light degree of freedom is the angular variable ϕ, the Goldstone boson of the spontaneously broken $U(1)$ (one can think of this as the angle around the bottom of the Mexican hat described by eqn. (2.3)). We thus study the effective chiral Lagrangian for ϕ:

$$\mathcal{L}_{eff} = \frac{1}{2}\partial_\mu\phi\partial^\mu\phi + i\bar{\psi}\gamma^\mu\partial_\mu\psi - (m_0\bar{\psi}_L\psi_R e^{i\phi/f} + h.c.)\ . \qquad (2.5)$$

Here the induced fermion mass $m_0 \equiv hf/\sqrt{2}$; for example, for values of the Yukawa coupling $10^{-3} \leq h \leq 1$, the fermion mass is in the range $M_{GUT} \leq m_0 \leq M_{pl}$. The global symmetry is now realized in the Goldstone mode: $\mathcal{L}_{eff}$ is invariant under

$$\psi_L \to e^{i\alpha/2}\psi_L \ , \quad \psi_R \to e^{-i\alpha/2}\psi_R \ , \quad \phi \to \phi + \alpha f \ . \tag{2.6}$$

At this stage, ϕ is massless because we have not yet explicitly broken the chiral symmetry.

2) Explicit Symmetry Breaking

Several options exist for explicitly breaking the global symmetry and generating a PNGB potential at a mass scale $\sim \Lambda$ several orders of magnitude below the spontaneous symmetry breaking scale f. In a class of Z_2-symmetric models studied by Hill and Ross[13], one adds a bare fermion mass term $m_1\bar{\psi}_L\psi_R$ to $\mathcal{L}_{eff}$, which presumably arises from another sector of the theory (just as quark masses in QCD are generated in the electroweak sector). The combination of terms involving m_0 and m_1 generates a 1-loop potential for ϕ of the form (1.1), with $\Lambda^2 \sim m_0 m_1$; a synopsis of these 'schizon' models is given in refs.[13,15].

For the rest of this discussion, we focus on the simplest mechanism for explicit symmetry breaking, by analogy with the QCD axion: dynamical chiral symmetry breaking through strongly coupled gauge fields. Suppose the gauge symmetry of the effective theory below the scale $f \sim M_{Pl}$ is a product group, $G_1 \times G_2$, where G_1 is a standard grand unified group (*e.g.*, E_6 or $SU(5)$) which spontaneously breaks down to the standard model at some scale M_{GUT}. In other words, G_1 describes the physics of ordinary quarks and leptons (and their heavier brethren) while G_2 might describe a 'hidden sector'. At the G_1 unification scale, the G_1 gauge coupling is small (perturbative unification). On the other hand, let G_2 be an asymptotically free non-abelian gauge theory which becomes strongly interacting at a scale κ comparable to the GUT scale. In addition, we assume that ψ transforms non-trivially under G_2 (ψ carries G_2-'color'). Starting with a perturbative G_2 gauge coupling at the Planck scale, $\alpha_2(M_{Pl}) = g_2^2(M_{Pl})/4\pi$ (which is, say, comparable to $\alpha_1(M_{Pl})$), the scale κ emerges from the renormalization group,

$$\kappa \simeq M_{Pl} \exp\left(\frac{-8\pi^2}{b_0 g_2^2(M_{Pl})}\right) \ , \tag{2.7}$$

where the renormalization group constant b_0 determines the lowest order term in the expansion of the β-function of G_2, $\beta_2(g) = -b_0 g_2^3/(4\pi)^2 - \ldots$. For example, for $G_2 = SU(N)$ and no light matter fields with G_2 charge, then $b_0 = 3N$; if there are N matter fields (one generation) with masses $m < \kappa$ in the fundamental representation of G_2, then $b_0 = 2N$. For reasonably large groups, and therefore large b_0, the gauge coupling can run sufficiently fast to generate $\kappa \sim M_{GUT}$. As examples, for $\alpha_2(M_{Pl}) = 1/30$ and $G_2 = SU(5)$ we find $\kappa \sim 3 \times 10^{14}$ GeV if there are no light ($m \lesssim M_{Pl}$) fermions transforming under G_2; on the other hand, with N light fermions, the same value of κ arises for the larger group $G_2 = SU(9)$.

Since ψ is charged under G_2, we expect chiral dynamics to induce a fermion condensate, $\langle\bar{\psi}\psi\rangle \sim \kappa^3$. (We assume the condensate can be rotated to be real; the extra phase it involves is irrelevant for our discussion). From eqn.(2.5), the condensate explicitly breaks the global symmetry, giving rise to a potential for the angular PNGB field ϕ,

$$V(\phi) = \mathrm{Re}[m_0\langle\bar{\psi}_L\psi_R\rangle e^{i\phi/f}] = m_0\kappa^3\cos(\phi/f) \ . \tag{2.8}$$

This has the form of eqn.(1.1), with $\Lambda^4 = m_0\kappa^3 = hf\kappa^3/\sqrt{2}$. For inflation, we require $\Lambda \sim M_{GUT}$. Such an energy scale can arise in at least two ways: (i) $m_0 \sim \kappa \sim M_{GUT}$; this requires the Yukawa coupling $h \sim 10^{-4}$, or (ii) $m_0 \sim M_{Pl}$, $h = O(1)$, and κ is slightly below the GUT scale, $\kappa \sim 10^{-1} M_{GUT}$. We indicated above that the running of the coupling constant for group G_2

may indeed provide such a value for κ. For this second choice of parameters, we do not need to introduce any small coupling constants in the fundamental Lagrangian near the Planck scale: the small ratio Λ/f emerges dynamically and is "strongly natural".

Although this model may be cosmologically appealing, we do not want to propose a new strongly interacting gauge sector in particle physics solely to generate an inflaton potential. Happily, there is well-founded particle physics motivation for an additional gauge group which becomes strong at the GUT scale, and this idea has a distinguished history in the particle physics literature.

One possibility is that G_2 is a technicolor group, and that ψ carries both G_1 and G_2 charge. [In this case, ϕ can couple through a $\psi - \psi - \psi$-triangle diagram to ordinary particles (*e.g.*, gluons and photons); this may be advantageous in that it leads to reheating of the 'ordinary' sector of quarks and leptons. We thank S. Dimopoulos for making this point to us.] Then, one must introduce a source for spontaneous breaking of the standard G_1 GUT group. Here, one may contemplate two possibilities: If the $\langle\bar{\psi}\psi\rangle$ condensate is a G_1 singlet (this may happen even though ψ carries G_1 charge), then G_1 must be broken by the usual Higgs mechanism or some equivalent. Alternatively, if the condensate $\langle\bar{\psi}\psi\rangle$ is G_1-non-singlet, it can spontaneously break G_1 at a scale $\kappa \sim M_{GUT}$, by analogy with technicolor models. If it can be implemented, the latter choice would be most economical: a single mechanism would give rise to both GUT symmetry breaking and inflation, and the only fundamental scalar (Φ) in the theory has Planck mass. This value of the mass for a scalar is natural, and in principle no small parameters would need to be introduced in the theory.

B. A Superstring Model: "Supernatural" Inflation

A second motivation for a gauge group which becomes strongly interacting at the GUT scale comes from superstring theory[16]. In these models, the gauge symmetry of the effective supergravity theory below the Planck scale is again a product group, $G_1 \times G_2$, where $G_1 = G_{GUT}$ contains the standard model and G_2 describes the hidden sector; for example, in the original heterotic string model, $G_1 \times G_2 = E_8 \times E_8'$.

In the effective field theory arising from superstrings, an important role is played by the complex scalar field S. The real part of this field, ReS, is the dilaton; the imaginary part ImS is the 'model-independent axion'. In string theory, the value of the dilaton determines the string coupling constant g_s through the relation[17] $\langle Re(S)\rangle = 1/g_s^2$. Since g_s is related by factors of $\mathcal{O}(1)$ to the gauge couplings $g_a(M_{pl})$ of the effective field theory at the Planck scale (a labels the gauge group G_a), the dilaton expectation value determines gauge couplings as well. In particular, a value for the dilaton in the range $\langle \mathrm{Re}S\rangle \equiv \mathrm{Re}S_0 \simeq 1.5 - 2.5$ yields a phenomenologically viable G_1 gauge coupling at the GUT scale, $\alpha_1(M_{GUT}) \sim 1/45$. If this theory is to have predictive power and time-independent constants of nature, one would expect that the dilaton potential $V(\mathrm{Re}S)$ has a minimum in this range. In perturbation theory, the dilaton (and axion) potential $V(S)$ is protected by supersymmetry: if supersymmetry is unbroken at tree level, then $V(S)$ vanishes to all finite orders in perturbation theory, leaving the gauge couplings indeterminate [18]. However, if the hidden sector G_2 is an asymptotically free non-abelian group, it will become strongly interacting, leading to condensation of gauginos (fermion supersymmetric partners of the gauge bosons) at a scale $\langle\lambda\lambda\rangle \sim M_{pl}^3 e^{-8\pi^2/b_0 g_2^2(M_{pl})}$. Through the relation between ReS and the string coupling constant above, this corresponds to a non-perturbative potential for the dilaton of the form $V(S) \propto e^{-cS}$. As a consequence, the imaginary part of the field, the axion partner of the dilaton, obtains a potential of the form (1.1), $V(\mathrm{Im}S) \propto \cos(\mathrm{Im}S)$. Our interest in this scenario derives from the fact that the 'model-independent' axion could in principle play the role of the inflaton in natural inflation [19].

Although nonperturbative effects in the hidden sector can generate a potential for the dilaton, an exponentially falling potential clearly will not by itself stabilize the dilaton in the desired range noted above: instead ReS runs away to infinity, yielding a free string theory. Additional physics is needed to help pin the dilaton at the appropriate minimum; we describe this further below. Here,

we mention that a second important role in particle physics of hidden sector gaugino condensation is that it might break supersymmetry (SUSY) [9]. If the condensate breaks supersymmetry in the hidden sector at the scale $\langle\lambda\lambda\rangle \sim M_{GUT} \sim 10^{14}$ GeV, then SUSY is broken in the observable sector at the scale $M_{SUSY} \sim M_{GUT}^3/M_{pl}^2 \sim$ TeV. SUSY breaking at this scale would protect the small Higgs mass and alleviate the heirarchy problem. Thus, the factor e^{-1/g^2} in the scale of gaugino condensation might lead to a large gauge hierarchy. (It is also possible that SUSY breaking arises from some other mechanism.)

The first attempts to implement these ideas in the $G_1 \times G_2 = E_8 \times E_8'$ heterotic string theory relied on the hidden E_8' sector becoming strongly interacting, and generating gaugino condensation, at a scale comparable to the GUT scale [9]. As noted above, in this case the gaugino condensation-generated potential for ReS decays exponentially for large values of the dilaton field. Attempts were made [9] to stabilize the dilaton by combining gaugino condensation with a term arising from the expectation value of the antisymmetric tensor field $\langle H_{\mu\nu\lambda}\rangle$. However, quantization conditions on the vacuum expectation value of this field [20] require it to be of order unity in Planck units, implying that the resulting potential $V(S)$ only has a minimum where ReS is small (well below the desired range above), *i.e.*, where g_s is large. As a result, the string theory would be strongly coupled, and the whole framework of perturbative calculations in the effective field theory would be unreliable [21].

Recently, this problem has been reconsidered by Krasnikov [22], Casas, *et al.* [23], and Kaplunovsky, Dixon, Louis, and Peskin (hereafter KDLP) [24], in the context of string models where the hidden sector G_2 is itself a product of two or more gauge groups. They found that the combined effect of gaugino condensates in multiple hidden groups can generate a dilaton potential with a weak-coupling (small perturbative g_s) minimum. In some cases, supersymmetry also appears to be broken at the requisite scale (L. Dixon, private communication; Kaplunovsky, unpublished). Here we will briefly study the axion potential generated in these multiple gaugino condensate models and explore its suitability for inflation.

The effective Lagrangian for the dilaton S can be written

$$\mathcal{L}_S = \frac{M_{Pl}^2}{8\pi(S+S^*)^2}\partial^\mu S \partial_\mu S^* - V(S,S^*) \tag{2.9}$$

where V is the effective potential generated by gaugino condensation. In string theory, the Planck scale is derived from the fundamental string tension α' via $M_{Pl}^2 = 16\pi/g_s^2\alpha'$. At tree level, the gauge coupling of group G_a is $g_a = g_s/\sqrt{k_a}$, where k_a is the level of the Lie algebra of G_a (a small integer). Thus, at tree level, we have $\langle \mathrm{Re}S\rangle \equiv \mathrm{Re}S_0 = [4\pi k_a \alpha_{GUT}(M_{Pl})]^{-1}$; assuming G_1 (G_{GUT}), which contains the standard model, is at level one ($k_1 = 1$), the phenomenologically acceptable value of the GUT gauge coupling, $\alpha_{GUT}(M_{Pl}) \simeq 1/20 - 1/30$, requires that the dilaton VEV be in the range $\mathrm{Re}S_0 = 1.5 - 2.5$, as noted above. As KDLP show, this large a value of the dilaton expectation value can be obtained with a hidden group structure $G_2 = SU(N_1) \times SU(N_2)$, provided that the expression $[(k_1/N_1) - (k_2/N_2)]^{-1}$ is large; *e.g.*, for their 'best case', $k_1 = k_2 = 1$ and $N_1 = 9$, $N_2 = 10$ (see below). In what follows, for simplicity, we shall follow KDLP in taking G_2 to be a product of two $SU(N)$ groups.

Following KDLP and ignoring gravitational and subleading $1/N$ corrections (that is, considering a global SUSY model with large hidden gauge groups), the effective dilaton potential is

$$V(S,S^*) = \frac{\pi}{2M_{Pl}^2}(S+S^*)^2 \Big|\sum_a k_a \langle\lambda\lambda\rangle_a\Big|^2 \tag{2.10}$$

where subscript $a = 1, 2$ now refers to the hidden gauge group G_{2_a}. When the coupling constant of group $G_{2_a} = SU(N_a)$ becomes strong, the resulting gaugino condensate is

$$\langle\lambda\lambda\rangle_a = N_a v M_{ren}^3 e^{i\theta_a} \exp\left[-\frac{24\pi^2 k_a S + \frac{3}{2}\Delta_a}{b_{0,a}}\right] \tag{2.11}$$

Here, the renormalization mass scale (at which the effective Lagrangian is defined) is taken to be

$$M_{ren}^2 = \frac{\rho^2}{\alpha'} \quad ; \quad \rho^2 = \frac{e^{1-\gamma}}{6\sqrt{3\pi}} = (0.216)^2 \ , \tag{2.12}$$

where γ is Euler's constant and $\alpha' = 8\pi(S+S^*)/M_{pl}^2$ is the inverse string tension; v is an N-independent constant of order unity; $\theta_a = 2\pi m/N_a$, with m integer, is an arbitrary discrete phase reflecting the N_a-fold degeneracy of the vacuum states of the theory; $b_{0,a}$ is the renormalization group constant for group G_{2_a}; and Δ_a is the threshold renormalization factor of order N_a. Δ_a, which in general can be a function of the moduli fields T^i, enters the coupling constant to one-loop order via

$$\frac{1}{g_a^2(\mu)} = \frac{1}{2}k_a(S+S^*) - \frac{b_{0,a}}{16\pi^2}\log\frac{M_{ren}^2}{\mu^2} + \frac{\Delta_a}{16\pi^2}. \tag{2.13}$$

Decomposing the dilaton into real and imaginary parts, and assuming no charged fermions in the hidden groups (*i.e.*, taking $b_{0,a} = 3N_a$), we have

$$\begin{aligned} V(S) = 5\times 10^{-9}\frac{v^2 M_{Pl}^4}{\mathrm{Re}S}\Bigg[& k_1^2 N_1^2 e^{\left(-\frac{16\pi^2 k_1 \mathrm{Re}S + \Delta_1}{N_1}\right)} + k_2^2 N_2^2 e^{\left(-\frac{16\pi^2 k_2 \mathrm{Re}S + \Delta_2}{N_2}\right)} \\ & + 2k_1k_2N_1N_2 e^{\left(-8\pi^2\left(\frac{k_1}{N_1}+\frac{k_2}{N_2}\right)\mathrm{Re}S - \frac{1}{2}\left(\frac{\Delta_1}{N_1}+\frac{\Delta_2}{N_2}\right)\right)}\cos\left(8\pi^2\left(\frac{k_1}{N_1}-\frac{k_2}{N_2}\right)\mathrm{Im}S + \delta\theta\right)\Bigg] \end{aligned} \tag{2.14}$$

where $\delta\theta = \theta_2 - \theta_1$.

To study inflation, it is preferable to work with scalar fields that have canonical kinetic terms in the Lagrangian. From eqn.(2.9), the kinetic Lagrangian for the real and imaginary components of the dilaton is not of this form, since

$$\mathcal{L}_{kin} = \frac{M_{Pl}^2}{32\pi(\mathrm{Re}S)^2}(\partial_\mu \mathrm{Re}S\partial^\mu \mathrm{Re}S + \partial_\mu \mathrm{Im}S\partial^\mu \mathrm{Im}S) \tag{2.15}$$

Thus the canonically normalized real component is taken to be [19] $\phi_R = -M_{Pl}\ln(\mathrm{Re}S)/\sqrt{16\pi}$. In general, the real and imaginary parts of S are interdependent, and one should follow the coupled evolution in the two-dimensional field space. For simplicity, to focus on the imaginary component, the model-independent axion, we shall assume the real component reaches its VEV, $\langle \mathrm{Re}S\rangle = \mathrm{Re}S_0$, well before the imaginary part does; in a chaotic scenario in which the field is initially randomly distributed, this will always be true in some regions of space. (Note that, near the Planck time, S will drop out of thermal equilibrium and its potential will be dynamically negligible; under these conditions, we expect no special initial value for S to be preferred.) In that case, we can define the canonical axion field,

$$\phi_a = M_{Pl}\mathrm{Im}S/\sqrt{16\pi}\mathrm{Re}S_0 \tag{2.16}.$$

However, from eqns. (1.1) and (2.14), we have $\phi_a/f = 8\pi^2\mathrm{Im}S[(k_1/N_1) - (k_2/N_2)]$. Combining these two expressions, we find the equivalent global symmetry breaking scale

$$f = \frac{M_{Pl}}{8\pi^2\sqrt{16\pi}\mathrm{Re}S_0}\left(\frac{k_1}{N_1}-\frac{k_2}{N_2}\right)^{-1} \tag{2.17}.$$

As we will see in Sections III and IV, the phenomenologically acceptable range for f is $f \gtrsim 0.3M_{Pl}$. From eqn.(2.14), the potential for the real part of the dilaton is minimized at

$$\mathrm{Re}S_0 = \frac{1}{8\pi^2}\left(\frac{k_1}{N_1}-\frac{k_2}{N_2}\right)^{-1}\left[\ln\left(\frac{k_1}{k_2}\right) + \ln\left(\frac{N_1}{N_2}\right) + \frac{1}{2}\delta_\Delta\right] \tag{2.18}$$

where

$$\delta_\Delta = \frac{\Delta_2}{N_2} - \frac{\Delta_1}{N_1} \tag{2.19}$$

is the difference in threshold renormalization factors. We thus find

$$f = \frac{M_{Pl}}{\sqrt{16\pi}} \left[\ln\left(\frac{k_1}{k_2}\right) + \ln\left(\frac{N_1}{N_2}\right) + \frac{1}{2}\delta_\Delta \right]^{-1} \tag{2.20}$$

In order to achieve an acceptably large value for $\mathrm{Re}S_0$, KDLP choose, *e.g.*, $N_1 = 9$, $N_2 = 10$, with $k_1 = k_2 = 1$; larger values of N_a are excluded because the size of the hidden sector is constrained by the total Virasoro central charge available. With this choice, to obtain $\mathrm{Re}S_0 > 1.5$ requires $\delta_\Delta \gtrsim 2.8$, which implies $f/M_{Pl} =\lesssim 0.11 \simeq 1/\sqrt{24\pi}$. If this upper limit is saturated, a sufficiently long epoch of slow-rollover inflation can occur (see section III), but the reheat temperature is unacceptably low and the density perturbation spectrum has too much power on large scales. On the other hand, for $\delta_\Delta = 1$, we would have $f/M_{Pl} \simeq 0.36$, which yields a viable inflationary model with an interesting fluctuation spectrum. However, as eqn.(2.18) shows, this value of δ_Δ would require larger groups, *e.g.*, $N_1, N_2 = 16, 17$, to achieve $\mathrm{Re}S_0 > 1.5$, and this violates the central charge limit (however, see comment below).

For these models, we can read off the effective scale Λ, defined in eqn.(1.1), from eqns.(2.14) and (2.18); Λ is determined up to a constant of order unity (the factor v) by the values of k_a, N_a, and Δ_a. For the $SU(9) \times SU(10)$ example, taking $\delta_\Delta = 2.8$, $\Delta_1/N_1 = -\Delta_2/N_2 = -1.4$, which corresponds to $\mathrm{Re}S_0 = 1.5$ and $f = 0.11 M_{Pl} \simeq M_{Pl}/\sqrt{24\pi}$, we find $\Lambda = 6 \times 10^{-5} v^{1/2} M_{Pl} = 8 \times 10^{14} v^{1/2}$ GeV, in the right vicinity for generating an acceptable density fluctuation amplitude (even though, as noted above, this value of f leads to an unacceptable fluctuation *spectrum*–see section IV). This is a pleasing feature of these models: the same physics which sets the condensate scale to be of order M_{GUT} ($\sim M_{Pl}\exp[-8\pi^2/g^2 b_0]$) fixes Λ to approximately the same scale.

From our perspective, the interesting result here is that a string model designed to yield a phenomenologically plausible particle physics scenario, in particular a large gauge hierarchy and possibly supersymmetry breaking near the weak scale, implies values for the PNGB parameters f and Λ for the model-independent axion which are quite close to those needed for successful inflation. Furthermore, as suggested in [23,24], with the inclusion of charged matter fields in one of the hidden groups, it is possible that the value of δ_Δ required to fix $\mathrm{Re}S_0$ could be reduced from ~ 3 to ~ 1, generating a sufficiently large value of f for inflation.

We end this subsection with several caveats about the treatment given here. First, as mentioned above, we have reduced a two-dimensional problem to a one-dimensional one by assuming the dilaton is already pegged to its expectation value during the evolution of the axion. Although this will be accurate for some region of parameter space, and for chaotic initial conditions in some regions of the universe, in general one should treat the full two-dimensional problem. In particular, the possibility of inflation in the dilaton direction deserves study (the potential for the canonical dilaton contains terms of the form $\exp[-ae^{-b\phi_R}]$). Second, due to 2-loop running of the gauge coupling, the prefactor of the exponential in eqn.(2.11) actually contains an additional factor of S [24]. This gives rise to an overall multiplicative factor of SS^* on the right side of eqn. (2.14), modifying the dependence of the potential on the axion field from a pure cosine. This could have interesting consequences for the cosmological evolution of the model-independent axion. Third, in this discussion we have assumed that the dominant non-perturbative effects in string theory arise at the level of the effective supergravity Lagrangian. It has been suggested [25] that some inherently stringy non-perturbative effects at the Planck scale are only suppressed by a factor $\exp(-2\pi/g)$ as opposed to the field theory factor $\exp(-8\pi^2/g^2)$. If such stringy effects contribute to the effective dilaton potential, they could substantially modify this effective field theory analysis.

C. Alternatives

In the preceding subsections, we have outlined two particle physics models which incorporate a PNGB with the requisite parameters for inflation. Clearly there are further possibilities [13,15]. For example, one can imagine doing away with fundamental scalars altogether, and having the PNGB arise as an effective field. One choice would be a composite PNGB built from a fermion condensate, in analogy with composite axion models [14] and the pion. A second possibility, recently discussed by Ovrut and Thomas [26], builds on the existence of instantons in the theory of an antisymmetric tensor field $B_{\mu\nu}$ (recall that such a tensor field arises, *e.g.*, in superstring theory.) Defining the field strength

$$H^{\mu\nu\lambda} = \partial^\mu B^{\mu\lambda} + \partial^\lambda B^{\mu\nu} + \partial^\nu B^{\lambda\mu} \ , \tag{2.21}$$

the action for this theory is

$$S = \frac{1}{6e^2} \int d^4x H_{\mu\nu\lambda} H^{\mu\nu\lambda} \ , \tag{2.22}$$

with the resulting equation of motion $\partial_\mu H^{\mu\nu\lambda} = 0$. As Ovrut and Thomas note, the theory (2.22) has pointlike, singular instanton solutions, analogous to Dirac monopoles in electromagnetism; evaluating their contribution to the partition function, one finds that the resulting effective action can be expressed in terms of an effective mean scalar field ϕ as

$$S_{eff} = \int d^4x \left[\frac{1}{4} e^2 \partial_\mu \phi \partial^\mu \phi - 2^9 \pi^2 e^{-(\alpha/e^4)^{1/3}} \left(\alpha^2 e^4\right)^{1/3} f^4 \left(1 \pm \cos\left(\frac{\phi}{f}\right)\right)\right] \ , \tag{2.23}$$

where α is a number, and f is a mass scale characterizing the instanton solutions. Clearly this is of the form (1.1) and, for $f \sim M_{Pl}$, (2.23) is another potential candidate model for natural inflation. In a variant of these models, the tensor field can be coupled to a fundamental real scalar field u with the symmetry-breaking potential $V(u) = (\lambda/4!)(u^2 - 6m^2/\lambda)^2$. This also leads to a potential of the form (1.1) for the associated scalar mean field theory; for $f \sim m \sim M_{Pl}$ and $\lambda \sim 10^{-4}$, one finds [26] $\Lambda \sim 10^{16}$ GeV, as desired for successful inflation. In both of these models, as in the string model of the previous subsection, the effective scale Λ is small compared to f due to the exponential (instanton) suppression factor. This is the origin of the hierarchy required for the generation of acceptably small density fluctuations in inflation. The advantage of these models is that this hierarchy does not need to be put in by hand.

D. Other Issues

Before leaving this survey of model-building, we note recent work drawing attention to the fact that global symmetries may be explicitly broken by quantum gravity effects [27,28] (*e.g.*, wormholes and black holes). If such effects are characterized by the Planck scale, they may induce non-renormalizable higher-dimension terms in the low-energy effective Lagrangian for Φ (see eqn.2.3), of the form

$$V_{eff}(\Phi) = g_{mn} \frac{|\Phi|^{2m} \Phi^n}{M_{Pl}^{2m+n-4}} \ . \tag{2.24}$$

The coefficients g_{mn} introduced here should not be confused with the gauge and string couplings discussed above. Terms with $n \neq 0$ explicitly break the global $U(1)$ symmetry of eqn.(2.2). Taking $g_{mn} = |g_{mn}| \exp(i\delta_{mn})$, the induced PNGB potential is a sum of terms of the form

$$V_{eff}(\phi) = |g_{mn}| \left(\frac{f}{M_{Pl}}\right)^{2m+n} M_{Pl}^4 \cos\left(\frac{n\phi}{f} + \delta_{mn}\right) \ . \tag{2.25}$$

Therefore, for $n \neq 0$, the effective explicit symmetry breaking scale is

$$\Lambda_{eff} = |g_{mn}|^{1/4} M_{Pl} \left(\frac{f}{M_{Pl}}\right)^{\frac{2m+n}{4}} , \tag{2.26}$$

where non-renormalizable terms have dimension $2m + n \geq 5$. Since PNGB inflation requires $f \gtrsim 0.3 M_{Pl}$ and $\Lambda \sim M_{GUT}$, the coefficients g_{mn} of these terms must be relatively small; for example, for the dimension 5 term, $g \lesssim 10^{-14}$ is required. (The upper limit on g_{mn} is relaxed for higher dimension terms.)

Naively, this effect appears to lead us back to the same difficulties this inflation model was meant to solve, namely, a small dimensionless constant of order 10^{-14} appearing in the Lagrangian. However, it is worth making several remarks about this problem. First, a caveat: in the discussion above (and in refs.(28)), it was implicitly assumed that the coefficients g_{mn} are 'naturally' of order unity. However, in the absence of a solvable quantum theory of gravity, these coefficients cannot be reliably calculated. In model wormhole calculations, one must introduce a cutoff scale $\mu \ll M_{Pl}$, in which case such effective operators are proportional to the tunneling factor $\sim \exp(-M_{Pl}^2/\mu^2)$. Thus, in the regime in which one can calculate, the coefficients g_{mn} are highly suppressed; the assumption that they are not at all suppressed depends on an uncertain extrapolation of the cutoff scale to the Planck scale. In addition, there may be other effects which enter to suppress these terms. In particular, in the axion model studied in more depth in ref.[27], wormhole effects are effectively cut off at the symmetry breaking scale f, leading to an exponential suppression $\sim \exp(-M_{Pl}/f)$ in the wormhole induced axion potential. Second, even supposing such terms are in principle unsuppressed (all g_{mn} of order unity), there are ways in which they could be evaded. For example, for a large gauge group (as contemplated above), a global symmetry may automatically be present, due to the gauge symmetry and field content of the theory, preventing terms up to some relatively large value of $2m + n$; in the present case, this would require that all terms up to $2m + n \sim 25$ be forbidden. Alternatively, if the field ϕ is an effective field which arises below the Planck scale, as suggested above, such explicit symmetry breaking terms can be forbidden by a local symmetry of the underlying theory, as in the superstring example of the previous subsection. Alternatively, as in the antisymmetric tensor model of section C above, the ϕ field may be unrelated to a global symmetry. Therefore, while the arguments of [28] are provocative, there are certainly examples of particle physics models which give rise to potentials of the form (1.1), with the requisite mass scales for inflation, which evade these difficulties.

III. COSMIC EVOLUTION OF THE INFLATON FIELD

With these models as theoretical inspiration, we turn now to the cosmological dynamics of an effective scalar field theory with a potential of the form (1.1) below the scale f. For example, in the model of Sec. II.A, f is the global spontaneous symmetry breaking scale, and ϕ describes the phase degree of freedom around the bottom of the Mexican hat potential (2.3); in other models, however, the picture may differ. To successfully solve the cosmological puzzles of the standard cosmology, an inflationary model must satisfy a variety of constraints, including sufficient inflation (greater than 60 e-folds of accelerated expansion) for a reasonable range of initial conditions; sufficiently high reheat temperature to generate a baryon asymmetry after inflation; and an acceptable amplitude and spectrum of density fluctuations. In this section we explore these constraints analytically and numerically for potentials of the form (1.1).

The ϕ interaction cross-sections with other fields are generally of order $\sigma \sim 1/f^2$, so its interaction rate is of order $\tau^{-1} \sim T^3/f^2$. Comparing this with the expansion rate $H \sim T^2/M_{Pl}$, we see that the scalar inflaton field thermally decouples at a temperature $T \sim f^2/M_{Pl} \sim f$. We therefore assume ϕ is initially laid down at random between 0 and $2\pi f$ in different causally connected regions. (This is the simplest but by no means only possible initial condition.) Within

each Hubble volume, (*i.e.*, ignoring spatial gradients–see below) the evolution of the field is then described by the classical equation of motion for a homogeneous field $\phi(t)$,

$$\ddot{\phi} + 3H\dot{\phi} + \Gamma\dot{\phi} + V'(\phi) = 0 \ , \tag{3.1}$$

where Γ is the decay width of the inflaton, and the expansion rate $H = \dot{a}/a$ is determined by the Einstein equation,

$$H^2 = \frac{8\pi}{3M_{Pl}^2}\left[V(\phi) + \frac{1}{2}\dot{\phi}^2\right] . \tag{3.2}$$

For completeness, it is also useful to have the second order Friedmann equation,

$$\frac{\ddot{a}}{a} = -\frac{8\pi}{3M_{Pl}^2}\left[\dot{\phi}^2 - V(\phi)\right] . \tag{3.3}$$

In Eqns.(3.2-3), we have assumed that the scalar field dominates the stress energy of the universe; this will hold starting near the onset of inflation.

In the temperature range $\Lambda \lesssim T \lesssim f$, the potential $V(\phi)$ is dynamically irrelevant, because the forcing term $V'(\phi)$ in Eq.(3.1) is negligible compared to the Hubble-damping term. (In addition, for axion-like models in which $V(\phi)$ is generated by non-perturbative gauge effects, $\Lambda \to 0$ as $T/\Lambda \to \infty$ due to the high-temperature suppression of instantons [14].) Thus, in this temperature range, aside from the smoothing of spatial gradients in ϕ (see below), the field does not evolve. Finally, for $T \lesssim \Lambda$, in regions of the universe with ϕ initially near the top of the potential, the field starts to roll slowly down the hill toward the minimum. In those regions, the energy density of the universe is quickly dominated by the vacuum contribution ($V(\phi) \simeq 2\Lambda^4 \gtrsim \rho_{rad} \sim T^4$), and the universe expands exponentially. Since the initial conditions for ϕ are random, our model is closest in spirit to the chaotic inflationary scenario [29]. In succeeding subsections, we study this evolution in more detail.

A. Standard Slow-Rollover Analysis

In this subsection, we recapitulate the analytic treatment of PNGB inflation given in Paper I. A sufficient, but not necessary, condition for inflation is that the field be slowly rolling (SR) in its potential. Therefore, by analyzing the conditions for, and number of e-foldings of, inflation in the SR regime, we should be at worst underestimating the true number of inflation e-folds. The field is said to be slowly rolling when its motion is overdamped, *i.e.*, $\ddot{\phi} \ll 3H\dot{\phi}$, so that the $\ddot{\phi}$ term can be dropped in Eq. (3.1) (*n.b.*, we assume $\Gamma \ll H$ during this phase). It is easy to show that in general this SR condition is a *sufficient* condition for inflation. First, from the scalar equation of motion (3.1), the defining SR condition implies that $\dot{\phi}^2 \ll 2V(\phi)$. On the other hand, the universe is inflating if the Robertson-Walker scale factor $a(t)$ is accelerating, $\ddot{a} > 0$; from Eqn. (3.3), this requires $\dot{\phi}^2 < V$. Thus, if the SR condition is well satisfied, we are guaranteed to be in an inflationary epoch. The converse is not necessarily true: inflation can occur even when the field is not slowly rolling. However, we will see in subsequent sections that, for this potential, if f is larger than about $M_{Pl}/\sqrt{24\pi}$, the SR epoch is roughly coincident with the inflationary epoch.

Hereon, for the purposes of numerical estimates, we shall assume inflation begins at a field value $0 < \phi_i/f < \pi$; since the potential is symmetric about its minimum, we could just as easily consider the case $\pi < \phi_i/f < 2\pi$. For the potential (1.1), the SR condition implies that two conditions are satisfied:

$$|V''(\phi)| \lesssim 9H^2 \ , \text{ i.e., } \quad \sqrt{\frac{2\,|\cos(\phi/f)|}{1+\cos(\phi/f)}} \lesssim \frac{\sqrt{48\pi}f}{M_{Pl}} \tag{3.4a}$$

and

$$\left|\frac{V'(\phi)M_{Pl}}{V(\phi)}\right| \lesssim \sqrt{48\pi}\ ,\ \text{i.e.,}\quad \frac{\sin(\phi/f)}{1+\cos(\phi/f)} \lesssim \frac{\sqrt{48\pi}f}{M_{Pl}}\ . \tag{3.4b}$$

From Eqns. (3.4), the existence of a broad SR regime requires $f \geq M_{Pl}/\sqrt{48\pi}$ (required below for other reasons). The SR epoch ends when ϕ reaches a value ϕ_2, at which one of the inequalities (3.4) is violated. In Fig.1, we show ϕ_2/f as a function of f/M_{Pl}; as f grows, ϕ_2/f approaches the potential minimum at π. For example, for $f = M_{Pl}$, $\phi_2/f = 2.98$, while for $f = M_{Pl}/\sqrt{24\pi}$, $\phi_2/f = 1.9$. For $f \gtrsim 0.3M_{Pl}$ which, as we shall see below, is the mass range of greatest interest, the two inequalities (3.4a) and (3.4b) give very similar estimates for ϕ_2. For simplicity, we can then use (3.4b) to obtain

$$\frac{\phi_2}{f} \simeq 2\arctan\left(\frac{\sqrt{48\pi}f}{M_{Pl}}\right) \qquad (f \gtrsim 0.3M_{Pl})\ . \tag{3.5}$$

Once ϕ grows beyond ϕ_2, the field evolution is more appropriately described in terms of oscillations about the potential minimum, and reheating takes place, as described below. We note that the expansion of the universe (the $3H\dot{\phi}$ term in Eq. 3.1) acts as a strong enough source of friction that the field is not able to roll through the minimum at πf and back up the other side sufficiently far to have any further inflationary period.

To solve the standard cosmological puzzles, we demand that the scale factor of the universe inflates by at least 60 e-foldings during the SR regime,

$$\begin{aligned} N(\phi_1,\phi_2,f) \equiv \ln(a_2/a_1) &= \int_{t_1}^{t_2} H dt = \frac{-8\pi}{{M_{Pl}}^2}\int_{\phi_1}^{\phi_2}\frac{V(\phi)}{V'(\phi)}d\phi \\ &= \frac{16\pi f^2}{{M_{Pl}}^2}\ln\left[\frac{\sin(\phi_2/2f)}{\sin(\phi_1/2f)}\right] \geq 60\ . \end{aligned} \tag{3.6}$$

Using Eqns. (3.4,5) to determine ϕ_2 as a function of f, the constraint (3.6) determines the maximum initial value (ϕ_1^{max}) of ϕ_1 consistent with sufficient inflation, $N_e(\phi_1^{max},\phi_2,f) = 60$. For $f \gtrsim 0.3M_{Pl}$,

$$\sin(\phi_1^{max}/2f) \simeq \left[1+\frac{{M_{Pl}}^2}{48\pi f^2}\right]^{-1/2}\exp\left(-\frac{15{M_{Pl}}^2}{4\pi f^2}\right)\ . \tag{3.7}$$

The fraction of the universe with $\phi_1 \in [0,\phi_1^{max}]$ will inflate sufficiently. If we assume that ϕ_1 is randomly distributed between 0 and πf from one Hubble volume to another, the *a priori* probability of being in such a region is $P = \phi_1^{max}/\pi f$. For example, for $f = 3M_{Pl}$, M_{Pl}, $M_{pl}/2$, and $M_{Pl}/\sqrt{24\pi}$, the probability $P = 0.7$, 0.2, 3×10^{-3}, and 3×10^{-41}. The initial fraction of the universe that inflates sufficiently drops precipitously with decreasing f, but is large for f near M_{Pl}. This is shown in Fig. 1, which displays $\log(\phi_1^{max}/f) = 0.5 + \log P$ and ϕ_2/f. These considerations show that for values of f sufficiently near M_{Pl}, sufficient inflation takes place for a broad range of initial values of the field ϕ. We note that these constraints do not determine the second mass scale Λ.

According to some inflationists, the discussion above of the probability of sufficient inflation is overly conservative, since it did not take into account the extra relative growth of the regions of the universe that inflate. After inflation, those initial Hubble volumes of the universe that did inflate end up occupying a *much* larger volume than those that did not. Hence, below we will also compute the *a posteriori* probability of inflation, that is, the fraction of the *final* volume of the universe that inflated.

B. Numerical Evolution of the Scalar Field

In this section, we expand upon the results of the preceding subsection by numerically integrating the equations of motion. This yields a more accurate estimate of the time (or field value) when inflation ends and the amount of inflation that takes place, as a function of the mass scale f and the initial value of the field ϕ_1.

First we rewrite Eq. (3.1) in terms of more useful variables. As a dimensionless time variable, we use the number of e-foldings of the scale factor,

$$dn = H dt, \tag{3.8}$$

and hence $d/dn = H^{-1} d/dt$. We also define the dimensionless field value, field 'velocity', and mass ratio

$$y \equiv \phi/f \quad ; \quad v = dy/dn \quad ; \quad \gamma \equiv 3M_{Pl}^2/8\pi f^2 \ . \tag{3.9}$$

Then we can write Eqs. (3.1) and (3.2) as

$$\frac{dv}{dn} = \Big[\gamma \tan(y/2) - 3v\Big] \Big[1 - v^2/2\gamma\Big] - \omega v \Big[1 - v^2/2\gamma\Big]^{3/2} \gamma^{1/2} \big[1 + \cos y\big]^{-1/2}, \tag{3.10}$$

where $\omega = \Gamma f/\Lambda^2$ contains the effects of dissipation. For the purpose of numerically calculating the evolution of the field, we will assume as in the previous section that this dissipation term is negligible. In this approximation, Eq. (3.10) depends only on the shape of the potential and on γ, *i.e.*, on the ratio f/M_{Pl}, and not explicitly on Λ.

In order to solve Eq. (3.10), we must specify two initial conditions: the initial values of the field and its time derivative. We allow the initial field value $y_1 = \phi_1/f$ to range over the interval 0 to π, and take the initial velocity to be $v_1 \equiv \dot{\phi}_1/Hf = 0$. The assumption of zero initial velocity is the one usually made in discussions of inflationary models. However, in the course of smoothing out gradients or due to randomness in the initial conditions, we expect the field to acquire an initial 'Kibble' [30] velocity at the temperature $T \sim \Lambda$ such that its kinetic energy is comparable to the potential energy $\sim \Lambda^4$. Naively, this velocity effect could delay or even prevent the onset of inflation. This problem has been studied previously in the context of new and chaotic inflationary models and has been shown to be potentially problematic for new inflation [31]. Initial velocities in the context of the present model have been studied numerically by Knox and Olinto [32]. They find that, due to the periodic nature of the potential, the effect of initial velocities is merely to shift, but not change the size of, the phase space of initial field values which lead to at least 60 e-folds of inflation. That is, as $\dot{\phi}_1$ is increased from zero, the value of ϕ_1 at which inflation begins is shifted, but the fraction of initial field space which inflates is approximately invariant. Therefore, for models of the form (1.1), we lose no generality by assuming $\dot{\phi}_1 = 0$. Given these initial conditions, we solve the equation of motion (3.10) numerically. The resulting solution $y(n, y_1)$ provides the value of the ϕ-field after n e-foldings of the scale factor.

As noted above, in an inflationary phase the scale factor accelerates in time, $\ddot{a} > 0$. The end of the inflationary epoch thus occurs at the transition from $\ddot{a} > 0$ to $\ddot{a} < 0$. We denote the field value at the end of inflation by ϕ_{end}. We find that the value of ϕ_{end} is virtually insensitive to where the field started rolling on the potential, ϕ_1. In Paper I and Sect. IIIA, we used ϕ_2, the value of the field at the end of the SR epoch, as an estimate of the end of inflation. Comparing the correct value ϕ_{end} with the approximate value ϕ_2, we find that the error is only 1% for $f \simeq M_{Pl}$, 10% for $f = 0.1 M_{Pl}$, and rapidly gets large for smaller values of f. In particular, no slow rollover regime exists for $f \leq M_{Pl}/\sqrt{48\pi}$, and yet for small enough values of ϕ_1, significant inflation can still occur. In practice, however, the small difference between ϕ_2 and the exact result ϕ_{end} shown in Figure 1 is irrelevant, since, as we show below, values of f smaller than $0.3 M_{Pl}$ are excluded for other reasons.

For a given initial value of the field ϕ_1 (or y_1), the solution to Eq. (3.10) tells us the total number of inflation e-foldings of the scale factor, $N(\phi_1)$ (where the end of inflation is defined by the condition $\ddot{a} = 0$). Figure 2 shows the number $N(\phi_1, f)$ of e-foldings as a function of the initial value of the field ϕ_1 for different choices of the mass scale f. One can see that, for $\phi_1/f < 1$, the dependence is almost exactly logarithmic,

$$N(\phi_1) = A - B\ln(\phi_1/f). \tag{3.11}$$

In the limit of small ϕ_1/f, the analytic SR estimate of Eq. (3.6) implies this same functional dependence and provides values for the constants A and B; in particular, $B_{sr} = 16\pi f^2/M_{Pl}^2$. The numerical values obtained for A and B by solving (3.10) are virtually the same as the SR estimates if f is near M_{Pl} and start to differ as f decreases. From Fig. 2, one can read off values for $y_1^{max} = \phi_1^{max}/f$, the largest initial value of the field that can give rise to $N(\phi_1^{max}) = 60$ e-foldings of inflation. Again, the numerical results for ϕ_1^{max} are nearly identical to the SR estimates (shown in Fig. 1) for values of f near M_{Pl}; they differ by $\sim 10\%$ for $f = M_{Pl}/10$, and deviate significantly as f approaches $M_{Pl}/\sqrt{24\pi}$ from above.

1) Analytic Solution: Small-angle approximation

The simple logarithmic behavior of the number of e-foldings $N(\phi_1)$ indicates that an analytic approximation can be found, one which differs from the SR approximation and which is more useful for smaller values of f/M_{Pl}. In this region of parameter space, the conditions

$$y \ll 1 \qquad \text{and} \qquad v \ll 1, \tag{3.12}$$

always apply during the inflationary epoch, and the equation of motion (3.10) can be approximated by

$$\frac{dv}{dn} = \frac{\gamma}{2}y - 3v\ , \tag{3.13}$$

where we have made the "small angle" (SA) approximation for the trigonometric functions and have neglected higher order terms in y and v. Eqn. (3.13) has solutions of the form

$$y(n) = y_1\, e^{\alpha n}\ , \tag{3.14a}$$

that is,

$$\phi = \phi_1 e^{\alpha \int H dt}\ , \tag{3.14b}$$

where the constant α is given by

$$\alpha = \frac{1}{2}\left[9 + 2\gamma\right]^{1/2} - \frac{3}{2} = \frac{3}{2}\left(\left[1 + \frac{M_{Pl}^2}{12\pi f^2}\right]^{1/2} - 1\right)\ . \tag{3.15}$$

Thus, the total number N of e-foldings can be written as

$$N = \frac{1}{\alpha}\ln(\phi_2/f) - \frac{1}{\alpha}\ln(\phi_1/f)\ , \tag{3.16}$$

where ϕ_2 is the value of the field at the end of inflation. Eqn. (3.16) provides us with an analytic solution of the same form as Eqn.(3.11); note that, here, the constant B of Eqn. (3.11) is given by $B_{sa} = 1/\alpha$, which differs in general from the value B_{sr} predicted by the slow rollover approximation. However, for large values of f, such that $f \gg M_{Pl}/\sqrt{12\pi}$, the two approximations agree, $B_{sa} \to B_{sr} = 16\pi f^2/M_{Pl}^2$. Comparison with Fig. 2 shows that, unlike the SR approximation,

the small angle approximation is also in excellent agreement with the numerical results for *small* values of f.

C. Constraints: Density Fluctuations, Reheating, Sufficient Inflation

Having studied the evolution of the homogeneous mode $\phi(t)$ of the scalar field and delineated the regions of initial field space for sufficient inflation, we now address other constraints the model must satisfy for successful inflation, including density fluctuations and reheating. In particular, these phenomena place tighter constraints on the range of allowed scales f and also limit the second mass scale Λ. Since, in Sec. IIIB, we showed that the SR approximation is accurate for the parameter range of interest, we shall rely on it throughout this discussion.

1) Density Fluctuation Amplitude

Quantum fluctuations of the inflaton field as it rolls down its potential generate adiabatic density perturbations that may lay the groundwork for large-scale structure and leave their imprint on the microwave background anisotropy [33-36]. In this context, a convenient measure of the perturbation amplitude is given by the gauge-invariant variable ζ, first studied in ref.[36]. We follow ref.[11] in defining the power in ζ,

$$P_\zeta^{1/2}(k) = \frac{15}{2}\left(\frac{\delta\rho}{\rho}\right)_{HOR} = \frac{3}{2\pi}\frac{H^2}{\dot{\phi}}. \tag{3.17}$$

Here, $(\delta\rho/\rho)_{HOR}$ denotes the perturbation amplitude (in uniform Hubble constant gauge) when a given wavelength enters the Hubble radius in the radiation- or matter-dominated era, and the last expression is to be evaluated when the same comoving wavelength crosses outside the Hubble radius during inflation. For scale-invariant perturbations, the amplitude at Hubble-radius-crossing is independent of perturbation wavelength.

To normalize the amplitude of the perturbation spectrum, we assume that the underlying density perturbations P_ρ at a given time are traced by the galaxy number density fluctuations P_{gal} up to an overall bias factor b_g, that is, $P_\rho^{1/2} = P_{gal}^{1/2}/b_g$. As inferred from redshift surveys, the variance σ_{gal}^2 in galaxy counts in spheres of radius 8 h^{-1} Mpc is about unity (where the Hubble parameter $H_0 = 100h$ km/sec/Mpc). For a scale-invariant spectrum of primordial fluctuations with cold dark matter (CDM), this implies [11]

$$P_\zeta^{1/2} \simeq \frac{10^{-4}}{b_g}. \tag{3.18}$$

As we shall see below, we will be interested in cases where the primordial spectrum may deviate significantly from scale-invariant, and these cases will be discussed in detail in Sec. IV; here, we will use the scale-invariant normalization to get an approximate fix on the scale Λ. (For values of f close to M_{Pl}, this approximation is very accurate.) For the scale-invariant CDM model, the recent COBE observation of the microwave background anisotropy [37] roughly implies $7.7 \times 10^{-5} < P_\zeta^{1/2} < 1.4 \times 10^{-4}$, or, using eqn. (3.18), $0.7 < b_g < 1.3$.

Using the analytic estimates of Sec. IIIA, the largest amplitude perturbations on observable scales are produced 60 e-foldings before the end of inflation, where $\phi = \phi_1^{max}$, and have amplitude

$$P_\zeta^{1/2} \simeq \frac{\Lambda^2 f}{M_{Pl}^3}\frac{9}{2\pi}\left(\frac{8\pi}{3}\right)^{3/2}\frac{[1+\cos(\phi_1^{max}/f)]^{3/2}}{\sin(\phi_1^{max}/f)}. \tag{3.19}$$

Applying the COBE constraint above to Eq.(3.19), we find Λ as a function of f; this is plotted in Fig. 1. For example,

$$\Lambda = 8.8 \times 10^{15} - 1.2 \times 10^{16}\,\mathrm{GeV} \text{ for } f = M_{Pl} \tag{3.20a}$$

$$\Lambda = 1.4 \times 10^{15} - 2 \times 10^{15}\,\mathrm{GeV} \text{ for } f = M_{Pl}/2\ . \tag{3.20b}$$

Thus, to generate the fluctuations responsible for large-scale structure, Λ should be comparable to the GUT scale, and the inflaton mass $m_\phi = \Lambda^2/f \sim 10^{11} - 10^{13}$ GeV.

We can obtain an analytic estimate of Λ as a function of f when $f \lesssim (3/4)M_{Pl}$; in this case, it is a good approximation to take $\phi_1^{max}/\pi f \ll 1$. As a result, in Eqn.(3.19), we have approximately

$$P_\zeta^{1/2} \approx \frac{1.4\Lambda^2 f}{M_{Pl}^3}\left(\frac{16\pi}{3}\right)^{3/2}\left(\frac{f}{\phi_1^{max}}\right)\ . \tag{3.21}$$

Now the last term in this expression is obtained by using Eqn. (3.6) with $N(\phi_1^{max}, \phi_2, f) = 60$:

$$\frac{\phi_1^{max}}{f} \simeq 2\sin\left(\frac{\phi_2}{2f}\right)\exp\left[-\frac{15M_{pl}^2}{4\pi f^2}\right]\ . \tag{3.22}$$

Substituting (3.22) on the RHS of (3.21) and using Eqn.(3.18) we find the value of $\Lambda(f)$ in terms of the bias parameter:

$$\Lambda(f) = \frac{1.7 \times 10^{16}}{b_g^{1/2}}\,\mathrm{GeV}\left[\frac{M_{pl}}{f}\sin\left(\frac{\phi_2}{2f}\right)\right]^{1/2}\exp\left(-\frac{15M_{pl}^2}{8\pi f^2}\right)\ . \tag{3.23}$$

Here, the quantity $\sin(\phi_2/2f)$ is determined by the slow-rollover conditions, Eqns. (3.4-3.5) and is generally of order unity. The dominant factor in (3.23) is the exponential dependence on f^2, which is responsible for the rapid downturn as f begins to drop significantly below M_{Pl} in the curve for $\Lambda(f)$ in Fig.1 [Note that Fig. 1 is valid for all f, even outside the regime of validity of the above analytic estimates.] For completeness, we note that the value in Eqn.(3.23) is strictly only an upper bound on the scale Λ, since the perturbations responsible for large-scale structure could be formed by some other (non-inflationary) mechanism.

2) Density Fluctuation Spectrum

Using the approximations above, we can investigate the wavelength dependence of the perturbation amplitude at Hubble-radius-crossing and in particular study how it deviates from the scale-invariant spectrum usually associated with inflation. Here we give a quick derivation of the spectrum, and defer a fuller discussion to Sec. IV.

Let k denote the comoving wavenumber of a fluctuation. The comoving lengthscale of the fluctuation, k^{-1}, crosses outside the comoving Hubble radius $[Ha]^{-1}$ during inflation at the time when the rolling scalar field has the value ϕ_k. This occurs $N_I(k) \equiv N(\phi_k, \phi_2, f)$ e-folds before the end of inflation, where $N(\phi_k, \phi_2, f)$ is given by Eqn.(3.6) with ϕ_1 replaced by ϕ_k. The corresponding comoving lengthscale (expressed in current units) is

$$k^{-1} \simeq (3000h^{-1}\mathrm{Mpc})\exp(N_I(k) - 60)\ , \tag{3.24}$$

where the horizon size today is $\simeq 3000h^{-1}$Mpc. For scales of physical interest for large-scale structure, $N_I(k) \gtrsim 50$; for $f \lesssim (3/4)M_{Pl}$, these scales satisfy $\phi_k/f \ll 1$. In this limit, comparing two different field values ϕ_{k_1} and ϕ_{k_2}, from Eqn.(3.6) we have

$$\phi_{k_2} \simeq \phi_{k_1}\exp\left(-\frac{\Delta N_I M_{Pl}^2}{16\pi f^2}\right)\ , \tag{3.25}$$

where $\Delta N_I = N_I(k_2) - N_I(k_1)$. Thus, using Eqns.(3.19) and (3.21), we can compare the perturbation amplitude at the two field values,

$$\frac{(P_\zeta^{1/2})_{k_1}}{(P_\zeta^{1/2})_{k_2}} \simeq \frac{\phi_{k_2}}{\phi_{k_1}} \simeq \exp\left(-\frac{\Delta N_I M_{Pl}^2}{16\pi f^2}\right) . \tag{3.26}$$

Now, from Eqn.(3.24), we have the relation $\Delta N_I = \ln(k_1/k_2)$ (here we have approximated $H_{k_1} \simeq H_{k_2}$; more precisely, $\Delta N_I = \ln(k_1 H_{k_2}/k_2 H_{k_1})$). Substituting this relation into (3.26), we find how the perturbation amplitude at Hubble radius crossing scales with comoving wavelength,

$$\left(\frac{\delta\rho}{\rho}\right)_{HOR,k} \sim (P_\zeta^{1/2})_k \sim k^{-M_{Pl}^2/16\pi f^2} \tag{3.27}$$

By comparison, for a scale-invariant spectrum, the Hubble radius amplitude would be independent of the perturbation lengthscale k^{-1}; the positive exponent in Eqn.(3.27) indicates that the PNGB models with $f \lesssim M_{Pl}$ have more relative power on large scales than do scale-invariant fluctuations.

It is useful to transcribe this result in terms of the power spectrum of the primordial perturbations at fixed time (rather than at Hubble-radius crossing). Defining the Fourier transform δ_k of the density field, from Eqn.(3.27) the power spectrum is a power law in the wavenumber k, $P_\rho = \langle|\delta_k|^2\rangle \sim k^{n_s}$, where the index n_s is given by

$$n_s = 1 - \frac{M_{Pl}^2}{8\pi f^2} \quad (f \lesssim 3M_{Pl}/4) . \tag{3.28}$$

For comparison, the scale-invariant Harrison-Zel'dovich-Peebles-Yu spectrum corresponds to $n_s = 1$. For values of f close to M_{Pl}, the spectrum is close to scale-invariant, as expected; however, as f decreases, the spectrum deviates significantly from scale-invariance–*e.g.*, for $f = M_{Pl}/\sqrt{8\pi} = 0.2M_{Pl}$, the perturbations have a white noise spectrum, $n_s = 0$. In sec. IV, we explore the implications of models with power law primordial spectra in depth.

3) Quantum Fluctuations

For the semi-classical treatment of the scalar field used so far to be valid, the initial value of the field should be larger than the characteristic amplitude of quantum fluctuations in ϕ, *i.e.*, $\phi_1 \geq \Delta\phi = H/2\pi$. In particular, requiring that quantum fluctuations do not reduce the number of inflation e-folds below 60 implies that the condition $\phi_1^{max} > H/2\pi$ must be satisfied. Using the SR approximation and Eqn.(3.22), we find

$$\frac{H/2\pi}{\phi_1^{max}} \simeq \frac{1}{3\pi} P_\zeta^{1/2} \left(\frac{M_{Pl}}{f}\right)^2 = \frac{10^{-5}}{b_g}\left(\frac{M_{Pl}}{f}\right)^2 . \tag{3.29}$$

Since this ratio is very small over the parameter range of interest, this constraint places no significant restrictions on the model. For example, this constraint requires that $\phi_1/f > 10^{-7}$ for $f = M_{Pl}$ and $\phi_1/f > 6 \times 10^{-9}$ for $f = M_{Pl}/2$, while the corresponding values of ϕ_1^{max}/f are 0.63 and 9.4×10^{-3}. Even if ϕ_1 is at some stage smaller than this constraint, we expect that quantum fluctuations would eventually bring the field into the semiclassical regime, so inflation would begin, if the field was sufficiently spatially coherent.

4) Probability of Sufficient Inflation

Armed with the numerical and analytic results above, we now calculate the *a posteriori* probability of sufficient inflation. We consider the universe at the end of inflation, and calculate

the fraction $\mathcal{P}$ of the volume of the universe at that time which had inflated by at least 60 e-foldings:

$$\mathcal{P} = 1 - \frac{\int_{\phi_1^{max}}^{\pi f} d\phi_1 \exp[3N(\phi_1)]}{\int_{H/2\pi}^{\pi f} d\phi_1 \exp[3N(\phi_1)]}. \tag{3.30}$$

Here, the lower limit of integration in the denominator is the limit of validity of the semiclassical treatment of the scalar field; the initial value of ϕ must exceed its quantum fluctuations, $\phi_1 \geq \Delta\phi = H/2\pi$. We will use the form for $N(\phi_1)$ given by Eq. (3.11) to evaluate the integrals appearing in Eq. (3.30). As shown previously, this approximate form for $N(\phi_1)$ is only valid for $\phi_1/f < 1$. However, we will assume that it holds over the entire range of integration; in the Appendix, we show that the resulting errors are small. Our basic result is that the *a posteriori* probability for inflation is essentially unity for f larger than the critical value $f_c \simeq 0.06 M_{Pl}$. As f drops below this value, the probability given by Eq. (3.30) rapidly approaches 0. To illustrate this result, we evaluate the integrals in (3.30); both are of the form

$$\begin{aligned} I &= \int_\epsilon^\pi dy_1 e^{3A} e^{-3B \ln y_1} \\ &= \frac{e^{3A}}{3B-1}\left\{\left(\frac{1}{\epsilon}\right)^{3B-1} - \left(\frac{1}{\pi}\right)^{3B-1}\right\}, \end{aligned} \tag{3.31}$$

where ϵ is a small number, $\epsilon = H/2\pi f$ or y_1^{max}, and B is the f-dependent coefficient appearing in Eqn.(3.11). If $3B > 1$, the integral I is dominated by the lower end of the range of integration and only the first term in Eq. (3.31) is significant. In this case, the probability $\mathcal{P}$ is given by

$$\mathcal{P} = 1 - \left(\frac{H}{2\pi\phi_1^{max}}\right)^{3B-1}, \tag{3.32}$$

where $3B - 1$ is positive. The probability of sufficient inflation is close to unity as long as the ratio in brackets $H/2\pi\phi_1^{max}$ is small; however, this is guaranteed by Eqn.(3.29). Combining Eqs. (3.29) and (3.32) yields the probability:

$$\mathcal{P} \geq 1 - \left[\frac{10^{-5}}{b_g}\left(\frac{M_{Pl}}{f}\right)^2\right]^{3B-1}. \tag{3.33}$$

This expression is valid provided that $3B - 1$ is positive and not extremely close to 0.

As the value of $3B$ decreases toward unity, the probability $\mathcal{P}$ decreases and the approximation leading to (3.32) begins to break down. As a reference point, consider the special case $3B = 1$; then the integral $I = e^{3A}\ln(\pi/\epsilon)$ and the probability $\mathcal{P} \approx 0.05$. As B decreases further, the integral in Eq. (3.31) obtains most of its contribution from the upper end of the range of integration and hence both integrals appearing in Eq. (3.30) have nearly the same value. As a result, the probability $\mathcal{P}$ rapidly approaches 0.

To summarize, we find that the probability $\mathcal{P}$ of sufficient inflation depends primarily on the value of the coefficient B appearing in Eq. (3.11), which in turn determines the number of e-foldings of the universe as a function of the initial value ϕ_1 of the field. For $B > 1/3$, the probability $\mathcal{P}$ is nearly unity; for $B < 1/3$, the probability $\mathcal{P}$ quickly approaches 0. In the SR approximation, $B \approx 16\pi f^2/M_{Pl}^2$, which would imply a critical value $f_c^{sr} = f(B = 1/3) = 1/\sqrt{48\pi}$. On the other hand, the numerical calculations yield the critical value of the mass scale $f_c = 0.058$. This discrepancy is traced to the fact that the SR approximation is invalid for such small values of f. In this case, the "small angle" approximation discussed in Sec. III.B is more appropriate; using Eqn.(3.15), we can analytically determine the critical value of f for which $B_{sa} \equiv 1/\alpha = 1/3$,

$$f_c^{sa} = \frac{M_{Pl}}{\sqrt{96\pi}}. \tag{3.34}$$

This is in excellent agreement with the value found numerically.

5) Reheating

At the end of the slow-rolling regime, the field ϕ oscillates about the minimum of the potential, and gives rise to particle and entropy production. The decay of ϕ into fermions and gauge bosons reheats the universe to a temperature $T_{RH} = (45/4\pi^3 g_*)^{1/4}\sqrt{\Gamma M_{Pl}}$, where g_* is the number of relativistic degrees of freedom. On dimensional grounds, the decay rate is $\Gamma \simeq g^2 m_\phi{}^3/f^2 = g^2\Lambda^6/f^5$, where g is an effective coupling constant. (For example, in the axion model [6,7], $g \propto \alpha_{EM}$ for two-photon decay, and $g^2 \propto (m_\psi/m_\phi)^2$ for decays to light fermions ψ.) Thus, the reheat temperature is

$$T_{RH} = \left(\frac{45}{4\pi^3 g_*}\right)^{1/4} \frac{g\Lambda^3}{f^2}\left(\frac{M_{Pl}}{f}\right)^{1/2} \tag{3.35}$$

For example, for $f = M_{Pl}$, using (3.20a) for Λ, and taking $g_* = 10^3$, we find $T_{RH} \simeq 10^8 g$ GeV, too low for conventional GUT baryogenesis, but high enough if baryogenesis takes place through sphaleron-mediated processes at the electroweak scale. Alternatively, the baryon asymmetry can be produced directly during reheating through baryon-violating decays of ϕ or its decay products. The resulting baryon-to-entropy ratio is $n_B/s \simeq \epsilon T_{RH}/m_\phi \sim \epsilon g\Lambda/f \sim 10^{-4}\epsilon g$, where ϵ is the CP-violating parameter; provided $\epsilon g \gtrsim 10^{-6}$, the observed asymmetry can be generated in this way.

We saw above that the amplitude of density perturbations produced during inflation yields a bound on the scale Λ as a function of the fundamental scale f, eqn.(3.23). We can use this to express T_{RH} as a function of f (which depends only weakly on g and g_*); requiring that this be sufficiently high for some form of baryogenesis leads to an important *lower* bound on the scale f, which as we shall see below, is more restrictive than the *a posteriori* bound above and comparably restrictive with the microwave anisotropy bound on the perturbation spectrum to be discussed in Sec. IV. Since we will be interested in a lower bound on f, we consider the case $f \leq (3/4)M_{Pl}$ so that eqn.(3.23) applies. Substituting (3.23) into (3.35), we find the reheat temperature

$$T_{RH} = \frac{10^{10}\ \text{GeV}}{b_g^{3/2}} g\left(\frac{100}{g_*}\right)^{1/4}\left(\frac{M_{Pl}}{f}\right)^4 \sin^{3/2}\left(\frac{\phi_2}{2f}\right)\exp\left[-\frac{45M_{pl}^2}{8\pi f^2}\right] . \tag{3.36}$$

The important point here is that the reheat temperature drops exponentially as f drops well below M_{Pl}. For baryogenesis to take place after inflation, at a minimum we should require $T_{RH} > 100$ GeV, the electroweak scale. From eqn.(3.36), this leads to the lower bound

$$\frac{f}{M_{Pl}} \geq 0.28 . \tag{3.37}$$

(Here, we have set $g = 1$ and $g_* = 100$, but this limit depends only logarithmically on g and g_*.) In terms of the density perturbation spectrum given in Eqn.(3.28), *if* inflation produces the dominant fluctuations on all scales, then this reheating constraint implies $n_s \geq 0.5$.

One additional point concerning reheating in these models deserves mention. In the string models of §II, the axion couples predominantly to the hidden sector; in such inflation models, one might then worry that reheating would take place more efficiently in the hidden as opposed to the ordinary sector. (This would not be a concern in models without a hidden sector, such as those patterned after technicolor.) In practice, this is not an insurmountable obstacle for these models, because gravitational interactions lead to an effective coupling between the hidden sector inflaton and the ordinary sector particles. Furthermore, for $f \sim M_{Pl}$, the gravitationally induced decay rate to ordinary particles, $\Gamma \sim m_\phi^3/M_{Pl}^2$, is comparable to the axion's decay rate to the hidden sector. Thus, we would expect the two sectors to reheat to comparable temperatures. It

is then easy to imagine a subsequent entropy-producing ordinary particle decay which heats the ordinary sector relative to the hidden sector, so that the contribution of the hidden sector to the total energy density at the time of big bang nucleosynthesis is negligible.

6) Initial Spatial Gradients

In the previous discussion, we have focussed on the evolution of a nearly homogeneous scalar field $\phi(t)$. However, since we expect the field initially to be laid down at random on scales larger than the Hubble radius, spatial 'Kibble' [30] gradients will be present on these scales. For inflation to occur, it is necessary that the stress energy tensor averaged over a Hubble volume be dominated by the potential $V(\phi)$, not by gradient terms ($(\partial_i\phi)^2$). (This is of course a concern for *all* models of inflation, not just those considered here.) In paper I, we addressed this issue at some length, and argued that, when the universe has cooled to the temperature $T \sim \Lambda$ at which inflation would otherwise begin, the energy density contributed by field gradients would be at most comparable to that in the potential. (During the prior radiation-dominated epoch, the gradient energy density scales like radiation, $\rho_{grad} \sim (\partial_i\phi)^2 \sim f^2/t^2 \sim T^4$, where the last equality assumes $f \sim M_{Pl}$; thus, at $T \sim \Lambda$, we expect $\rho_{grad} \sim \Lambda^4 \sim V(\phi)$.) Since these gradients rapidly redshift away with the subsequent expansion, they would typically delay only slightly the onset of inflation.

Here, we point out that the canonical PNGB model has an additional automatic feature which can ensure that spatial gradients in the PNGB field are negligible at the onset of natural inflation. Namely, if ϕ is the angular component of a complex field Φ, as in the model of Eqn.(2.3), then the heavier, radial component of Φ can generate an earlier period of inflation as it rolls down its potential. If the later angular inflation leads to more than 60 e-folds of growth in the scale factor (as we have been assuming), then the only important effect of the earlier inflation epoch would be to rapidly stretch out spatial gradients in the angular ϕ field. (This point was stressed to us by A. Linde, private communication.) Furthermore, as we show below, the earlier inflation period does not require another small coupling constant. In particular, for the model of Eqn.(2.3), for a broad range of initial conditions, radial inflation takes place even if the complex scalar self-coupling λ is of order unity. In addition, only a small number of radial inflation e-folds is required to efficiently damp spatial gradients in ϕ.

In the usual way, we can decompose the complex field Φ into two real radial and angular components η and ϕ,

$$\Phi = e^{i\phi/f}\frac{\eta}{\sqrt{2}} \ . \tag{3.38}$$

Consider the evolution of the radial mode η in the potential (2.3), $V(\eta) = (\lambda/4)(\eta^2 - f^2)^2$ (in general the radial and angular motions are coupled; however, since the radial mode is much heavier, its evolution can be approximately decoupled). Analyzing this motion in a manner analagous to §III.A, and using the fact that f is comparable to M_{Pl}, we see that some amount of radial inflation is expected provided the initial value of η is sufficiently far from its minimum $\langle\eta\rangle = f$. In fact, this initial period of inflation will be generic as long as gradient terms in the η energy density do not dominate over the potential $V(\eta)$ near the Planck scale and the initial value of η is not very close to f. For example, for $f = M_{Pl}$, if the initial value η_1 of the radial field is greater than $2M_{Pl}$, then in rolling to its minimum it will generate at least 5 e-foldings of 'chaotic' inflation, and angular gradients would be stretched by a large factor. Alternatively, if $\eta_1 \leq 0.3M_{Pl}$, the universe would experience about the same number of e-foldings of 'new' inflation as the field rolls from near the local maximum of the Mexican hat at the origin. We note that, for a potential of the form (2.3), for f near M_{Pl} the SR condition holds over some range of η, independent of the value of the coupling λ (just as Eqn.(3.6) does not depend on Λ). Therefore, radial inflation takes place even if λ is large. The density fluctuations produced during this phase are on unobservably large scales if the subsequent angular inflation lasts for at least 65 e-folds of expansion, so there are no strong constraints on λ arising from density fluctuations and the microwave anisotropy. One should, however, require $\sqrt{\lambda}/\xi \lesssim 1$ to avoid fluctuations of order unity on the Hubble radius, since these would pinch off into black holes.

IV. POWER LAW SPECTRA AND LARGE-SCALE STRUCTURE

Recent observations of large scale galaxy clustering and flows suggest that there is more power on large scales than given by an $n_s = 1$ scale invariant spectrum in 'standard' cold dark matter dominated universes (CDM models). In this section, we consider a primordial power spectrum $|\delta_k|^2 \sim k^{n_s}$; we show the degree to which varying the index n_s, while keeping all other features of the CDM model fixed, helps solve this large scale structure dilemma. We have shown that natural inflation will generate such a power law perturbation spectrum with $n_s \leq 1$ over a wide range of wavenumbers, in particular over the waveband directly probed by observations of large scale galaxy clustering and microwave background anisotropies. We demonstrate this in more detail in Sec. IV.A below, where we also discuss other inflation models (such as those with exponential potentials and many versions of extended inflation) which also predict power law spectra with $n_s \neq 1$.

In Sec. IV.B, we show that current data on microwave anisotropies and large-scale flows, and the requirement that structure forms sufficiently early, constrain n_s to be $\gtrsim 0.6$ for CDM models, whereas values $\lesssim 0.6$ are needed to explain the large scale clustering of galaxies. The reason we put the CDM model under such scrutiny rather than other inflation-inspired models, apart from its having dominated the theoretical scene for the past decade, is that it is a minimal model, in the sense that it requires a small number of ingredients to specify it. For the 'standard' CDM model, one assumes a flat geometry for the Universe with $\Omega \approx 1$ in non-relativistic particles and takes h≈ 0.5, where h is the Hubble constant H_0 in units of 100 km s^{-1}Mpc^{-1}. (For values of h larger than this, if $\Omega = 1$ the Universe would be younger than the inferred ages of globular cluster stars.) In the following, we assume a negligible baryon abundance, $\Omega_B \ll \Omega$, since a value of $\Omega_B \lesssim 0.07$ is indicated by primordial nucleosynthesis constraints. The rest of the non-relativistic matter is in cold dark matter relics, $\Omega_{cdm} = \Omega - \Omega_B$. Since the large scale structure dilemma has been with us in one guise or another since the early 1980s, a major line of research over the past decade has been to invent models with scale invariant primordial spectra that have more power than the $n_s = 1$ CDM model does on large scales. These 'nonstandard' $n_s = 1$ models include scenarios with a non-zero cosmological constant, a larger baryon density Ω_B than that inferred from standard nucleosynthesis, and mixtures of hot and cold dark matter, to name just a few. Often somewhat baroque from the particle physics prespective, such alterations would all result in more stringent constraints on n_s if we allow it to vary than the ones we derive for the standard CDM model. (Indeed there are models that require the effective n_s to be $\gg 1$, such as the isocurvature baryon model, but this is certainly not an outcome of natural inflation.)

A. Inflation Models and Power Law Spectra

Before turning to the data, we first show explicitly how tiny the deviations from a power law form are for natural inflation, and that Eqn.(3.28) for n_s is highly accurate. We also discuss the form that n_s takes for other popular models of inflation such as power law, extended, and chaotic inflation. Since we are dealing with spectra that can change somewhat with wavenumber, we define a 'local' (*i.e.*, k-dependent) spectral index $n_s(k)$ by

$$n_s(k) \equiv 1 + d\ln P_\zeta(k)/d\ln k \ , \tag{4.1}$$

where the ζ-power spectrum $P_\zeta(k)$ introduced in Sec. III provides a better measure of the post-inflation spectrum than does the density power spectrum. The quantity ζ, the variation of the 3-space volume on uniform Hubble parameter hypersurfaces, is gauge- and hypersurface-invariant, whereas the density is neither.

1) Natural Inflation

For natural inflation this local index is

$$n_s(k) \approx 1 - \frac{{M_{Pl}}^2}{(8\pi f^2)} \left[\frac{1 + [1 + ({M_{Pl}}^2/48\pi f^2)]^{-1} \exp[-\frac{{M_{Pl}}^2}{8\pi f^2} N_I(k)]}{1 - [1 + ({M_{Pl}}^2/48\pi f^2)]^{-1}[1 + ({M_{Pl}}^2/16\pi f^2)] \exp[-\frac{{M_{Pl}}^2}{8\pi f^2} N_I(k)]} \right] . \quad (4.2)$$

Here $N_I(k)$ is the number of e-foldings between the time when the inverse wavenumber k^{-1} first exceeded the comoving Hubble length (the first 'horizon crossing') and the end of inflation. For waves on scales of observable interest, $N_I(k) \sim 50 - 60$, so the factor in large brackets is always very close to unity over the entire range of values of f we are considering.

The derivation of (4.2) is very similar to that given in Sec. III, so we just sketch the steps here. From Eqns.(3.17) and (4.1), we must evaluate $n_s - 1 = 2d\ln((3/2\pi)H^2/|\dot{\phi}|)/d\ln Ha$ (since $k = Ha$ at horizon crossing). If we use the slow roll approximation for $\dot{\phi}$ and H, we have

$$n_s(k) \approx 1 - \frac{{M_{Pl}}^2}{8\pi f^2} \left[\frac{1 + \sin^2(\phi_k/2f)}{1 - \sin^2(\phi_k/2f)[1 + ({M_{Pl}}^2/16\pi f^2)]} \right] . \quad (4.3)$$

Here ϕ_k is the value of the scalar field at which $k = Ha$, and we have taken the positive sign for the potential (1.1), as in Sec. III. The scalar field reaches the value ϕ_k roughly $N_I(k) \equiv N(\phi_k, \phi_2, f)$ e-folds before the end of inflation, where $N(\phi_k, \phi_2, f)$ is given by Eq.(3.6) with ϕ_1 replaced by ϕ_k. As a result [Cf. Eq.(3.7)], we find

$$\sin^2(\phi_k/2f) = \left[1 + \left(\frac{{M_{Pl}}^2}{48\pi f^2}\right)\right]^{-1} \exp\left[-\frac{{M_{Pl}}^2}{8\pi f^2} N_I(k)\right] .$$

When this expression is substituted into Eq.(4.3), Eq.(4.2) is obtained. (Here, we have approximated the 'end of inflation' as the end of the slow-roll epoch, as in Eq.(3.5). If we instead took the end of inflation to be the time when the scalar field kinetic energy grows to the value $\dot{\phi}^2 = V$ and approximated $\dot{\phi}$ by the slow roll result, the factors of $\sqrt{48\pi}$ above would become $\sqrt{24\pi}$; since this factor is multiplied by the exponential suppression factor $\exp[-(M_{Pl}^2/8\pi f^2)N_I(k)]$ in Eq.(4.2), this difference is negligible.)

Defining k_{end} to be the wavenumber that equals $(Ha)_{end}$ at the end of inflation, and using the fact that $N_I(k) = \ln(H(\phi_k)k_{end}/H(\phi_{end})k)$, we find that the relation between $N_I(k)$ and k is given by

$$\ln\left(\frac{k}{k_{end}}\right) = -N_I(k) + \frac{1}{2}\ln\left(1 + \left(\frac{{M_{Pl}}^2}{48\pi f^2}\right)^{-1} \left(1 - \exp\left[-\frac{{M_{Pl}}^2}{8\pi f^2} N_I(k)\right]\right)\right) .$$

Thus between the current Hubble length $k^{-1} \sim 3000\,\mathrm{h}^{-1}\mathrm{Mpc}$ and the galactic structure length scale, $k^{-1} \sim 0.5\,\mathrm{h}^{-1}\mathrm{Mpc}$, the range which encompasses all of the large scale structure observations, $N_I(k)$ only changes by about 10. Since $N_I(k)$ only enters the exponentially suppressed terms in Eq.(4.2), the index n_s is quite constant at $1 - ({M_{Pl}}^2/8\pi f^2)$ over observable scales.

2) Exponential Potential Inflation

Although we view natural inflation as the best motivated model for obtaining power law indices below unity, other possibilities for getting $n_s(k)$ significantly different from unity have been widely discussed in the literature. Power law inflation [38,39] (in which the scale factor grows as a large power p of the time, $a \propto t^p$, instead of quasi-exponentially) is the simplest

example of a model which predicts power law spectra. It is realized with an exponential potential of form $V = V_0 \exp[-\sqrt{16\pi/p}\ \phi/M_{Pl}]$, and has

$$n_s = 1 - \frac{2}{p-1}\ . \tag{4.4}$$

The deceleration parameter of the universe, $q = -a\ddot{a}/\dot{a}^2$ is $q = -(1-p^{-1})$ for power law inflation. In order to have a viable model of inflation, the universe must pass from acceleration, $q < 0$, to deceleration, $q > 0$, so that it can reheat; hence it is essential that p evolves, with inflation ending when p falls below unity. Thus, although power law inflation models are instructive since they are analytically simple, the exponential part of the potential can only be valid over a limited range of the evolution. Indeed, it is often convenient to characterize potentials that are not exponentials by an index p defined by $\sqrt{4\pi p} = HM_{Pl}/|\dot{\phi}|$, which reduces to the p in the exponential potential for that case. However, in these models, structure on observable scales may be generated in a regime where p varies with k rather than being constant. Even so, power law approximations are often locally valid, even when rather drastic potential surfaces are adopted to 'design' spectra. Some examples of cases where n_s changes considerably over the observable window of large scale structure are given, for example, in [40,11].

3) Extended Inflation

Extended inflation also leads to a power law form over a wide band in k-space [41]. In extended inflation, a Brans-Dicke field, whose inverse is an effective Newton gravitational 'constant', is introduced as well as an inflaton. The analysis of [41] showed that the power law index can be simply expressed in terms of the Brans-Dicke parameter ω (the coefficient of the kinetic term of the Brans-Dicke field),

$$n_s = 1 - \frac{8}{2\omega - 1}\ , \qquad p = \frac{2\omega + 3}{4}\ . \tag{4.5}$$

As far as density fluctuations are concerned, the model just mimics a power law inflation one described in Section IV.A.2 above. Indeed, the fluctuation spectrum is most easily computed in a conformally-transformed reference frame, where a new field defined as the log of the Brans-Dicke field experiences an exponential potential with p as given in Eq.(4.5) [41]; using Eq. (4.4), one then obtains n_s as given in Eq. (4.5). In most versions of the theory, a value of $\omega \lesssim 18 - 25$ is needed to avoid an excessive CMBR anisotropy due to large bubbles; thus, the spectrum deviates from scale invariant, with $n_s \lesssim 0.77 - 0.84$. At the same time, it is also necessary that the effective value of ω must have evolved to a high number (> 500) by now in order to satisfy solar system tests. This can be arranged by, *e.g.*, giving the Brans-Dicke field a mass or by other means, but at the cost of complicating the model.

4) Chaotic Inflation

References [40] and [11] probed the question of how much deviation from scale-invariance could be produced in various models in the waveband that corresponds to observable large-scale structure; their main conclusion was that the deviations must be small. We illustrate the level of breaking of scale invariance expected for the popular chaotic inflation models. We assume power law potentials of the form $V(\phi) = \lambda_e M_{Pl}{}^4 (\phi/M_{Pl})^{2\nu}/(2\nu)$, where the power ν is usually taken to be 1 or 2. A characteristic of such potentials is that the range of values of ϕ which correspond to all of the large scale structure that we observe is actually remarkably small. For example, for $\nu = 2$, the region of the potential curve that corresponds to all of the structure between the scale of galaxies and the scales up to our current Hubble length is just $4M_{Pl} \lesssim \phi \lesssim 4.4M_{Pl}$ [11]. Consequently, the Hubble parameter does not evolve by a large factor over the large scale structure region and we therefore expect near scale invariance. Although this is usually quoted

in the form of a logarithmic correction to the ζ-spectrum, a power law approximation is quite accurate. Following exactly the same prescription used to evaluate Eq.(4.2), we have

$$n_s(k) \approx 1 - \frac{\nu+1}{N_I(k) - \frac{\nu}{6}} \ . \tag{4.6}$$

For waves the size of our current Hubble length we have the familiar $N_I(k) \sim 60$, hence $n_s \approx 0.95$ for $\nu = 2$ and $n_s \approx 0.97$ for $\nu = 1$ (massive scalar field case). The relation between $N_I(k)$ and k is given by

$$\ln\left(\frac{k}{k_{end}}\right) = -N_I(k) + \left(\frac{\nu}{2}\right) \ln\left(1 + \frac{3N_I(k)}{\nu}\right) \ , \tag{4.7}$$

where k_{end} is the wavenumber that equals Ha at the end of inflation. Thus, over the range from our Hubble radius down to the galaxy scale, n_s decreases by only about 0.01.

B. Implications for Large-Scale Structure

We have discussed various inflationary models (natural, power law, extended, and chaotic), which give rise to density perturbation spectra of the form $|\delta_k|^2 \sim k^{n_s}$, where $n_s \leq 1$. We now turn to their implications for large scale structure.

1) Galaxy and Cluster Clustering

Ideally, if one knew the precise specifications of the inflaton potential, then the amplitude of density perturbations generated during inflation would be fixed. In the absence of this knowledge, one normalizes the amplitude to observations of large-scale structure today. In this way, one can use the observations to restrict the parameters in the potential and thus in the underlying particle physics. We normalize the amplitude of the density perturbation spectra by setting the *rms* fluctuation in the mass distribution within spheres of radius $8\,h^{-1}$Mpc, $\sigma_{\rho,8} \equiv \langle(\delta M/M)^2\rangle^{1/2}_{R=8h^{-1}\mathrm{Mpc}}$, to be σ_8. The *rms* fluctuation in galaxy counts on this scale in the CfA survey is unity. The quantity $b_8 \equiv \sigma_8^{-1}$ is sometimes called the 'biasing' factor, as discussed below. Roughly, if $b_8 \approx 1$, galaxies would be clustered like the mass distribution, while if $b_8 > 1$, galaxies would be more strongly clustered than the mass. For standard CDM models with $n_s = 1$, σ_8 was thought to lie in the range $0.4 - 1.2$ before the recent COBE measurement.

In Fig.3a, we show the evolved power spectra of the linear CDM density fluctuations. To obtain Fig.3a, we have taken a primordial density spectrum in the mass density of the form $|\delta_k(t_i)|^2 \propto k^{n_s}$, with n_s in the range -1 to 1, and evolved it forward in time to the present day using a transfer function $T(k)$, $|\delta_k(t_0)|^2 = T^2(k)|\delta_k(t_i)|^2$. For the CDM transfer function, we use the fitting formula given in Appendix G of BBKS [42]; this formula is highly accurate in the $\Omega_B \to 0$ limit, but should be somewhat modified for the $\Omega_B \sim 0.05$ values more appropriate from nucleosynthesis. The actual quantity plotted in the Figure is $d\sigma_\rho^2/d\ln k = k^3\langle|\delta_k(t_0)|^2\rangle/2\pi^2$ $= P_\rho k^3/2\pi^2$ in units of σ_8, as a function of wavenumber k. The spectra are plotted in this way to provide a measure of the contribution of a band around the given wavenumber to the overall *rms* density fluctuations. The ordinate is approximately equal to $(1 + z_{nl}(k))/\sigma_8$, where $z_{nl}(k)$ is the redshift at which the *rms* fluctuations in the band become nonlinear. Notice that there is a peak in the CDM spectrum for $n_s < 1$. This indicates that there is a characteristic scale, roughly at the peak of the spectrum, associated with the first objects that form [43]. A potential problem with these models is immediately apparent from Fig.3(a): the redshift of galaxy formation is an increasing function of n_s. Thus, for n_s much smaller than the scale invariant value $n_s = 1$, the model may encounter grave difficulties in explaining why there are quasars at $z \sim 5$. We discuss this point more fully below.

To relate such perturbations in the mass density in the linear regime of growth to the actual clustering of galaxies, one must generally do N-body simulations. However, on large scales, the

waves evolve in an essentially linear fashion; there is an excellent approximation which relates the power spectrum in the mass density to the power spectra of galaxies and galaxy clusters (if they arise from any function of the Gaussian process through which perturbations arose). This relation is an extension [44] of the theory which identifies galaxies and clusters with appropriately selected peaks of the initial density field [42, 45]. For scales large compared with the local processes that define these objects and large enough that the waves are evolving in the linear regime, the power spectra for galaxies and clusters are linearly proportional to the mass density power spectrum; the proportionality constants define 'biasing factors', b_g for galaxies and b_c for clusters (Cf. Sec. III.C.1):

$$P_g(k) = b_g^2 P_\rho(k), P_c(k) = b_c^2 P_\rho(k),$$

or, equivalently,

$$\frac{d\sigma_g^2}{d\ln k} = b_g^2 \frac{d\sigma_\rho^2}{d\ln k}\ , \ \frac{d\sigma_c^2}{d\ln k} = b_c^2 \frac{d\sigma_\rho^2}{d\ln k}\ . \tag{4.8}$$

In Figure 3b, we show a blow-up of a portion of Fig.3a; 3b focuses on the region of k-space in 3a probed by large scale structure observations. [Note that in Fig.3b the ordinate has been relabeled in terms of galaxy power spectra using Eq.(4.8); thus, the spectrum is in units of $b_g\sigma_8$.] This figure compares the theoretical galaxy spectra described in the previous paragraph with large scale clustering data from the QDOT and UC Berkeley IRAS surveys and the APM survey. In the conventional BBKS peaks approach to biasing [42], we would have $b_g = 1/\sigma_8$, which is why σ_8^{-1}, the inverse of an amplitude measure, is often referred to as a biasing factor (*e.g.*, in Sec. III). In general, b_g will differ from galaxy type to galaxy type and there is no clear reason why we should suppose that $b_g = \sigma_8^{-1}$; nonetheless, it is rather remarkable that this assumption appears to give the correct amplitude for galaxy clustering. However, we note that the slight differences in the power spectrum levels for the 3 surveys could be simply explained with slightly differing b_g's. To compare with the data in the nonlinear regime of the spectrum, $k^{-1} \lesssim 5\sigma_8\ \mathrm{h^{-1}Mpc}$, N-body computations are needed. However, just from the linear regime it would appear that spectral indices n_s in the range 0–0.6 are much preferred over the scale invariant value of unity. (This point would appear even more dramatic had we forced the models to agree with the data at the 8 h^{-1} Mpc normalization scale.)

Probably the most reliable indication of excess large scale power is the angular correlation function of galaxies, $w_{gg}(\theta)$, inferred from deep photometric surveys. Figure 4 compares theoretical predictions of $w_{gg}(\theta)$ for various primordial power law spectra with observations from the APM survey. Although the angular correlation function suffers from having only two- rather than three-dimensional information, it gains enormously since angular surveys currently involve a few million galaxies, while three-dimensional (redshift) surveys are still limited to samples of several thousand galaxies. Two groups have now independently catalogued the galaxies of the Southern Sky and have derived $w_{gg}(\theta)$'s in agreement with each other. A Northern Sky survey is also in basic agreement. To compare with these data, Bond and Couchman [44] showed that the theoretically predicted angular correlation function at large angles can be evaluated using the linear power spectrum for galaxies, although nonlinear effects substantially modify the estimates at small angles; they also showed how to evaluate the angular correlation function directly from the power spectrum. We applied these techniques to the power spectra of Figure 3b to compare $w_{gg}(\theta)$ as we vary n_s with the APM results in Figure 4. The dots denote the APM data for various magnitude intervals, scaled back to the depth of the Lick survey [46]. The spread of points is considered to provide a rough indicator of the error level. Although there is a certain amount of vertical freedom in fitting the theory to the data, from the overall scale $b_g\sigma_8$, it is clear that $0 \lesssim n_s \lesssim 0.4$ is required if we are to take the spread of dots as an error estimate. It was this graph that led to the conclusion given in Bond [47] that this was the allowed range. However, estimates for various corrections to the APM catalogue such as those from plate errors and variable absorption by Galactic dust may revise $w_{gg}(\theta)$ downward slightly, and the hatched region is now expected to be allowed by the data [46]. Thus, for this paper, we consider the allowed range to be $0 \lesssim n_s \lesssim 0.6$. We note that this fit has been done with a CDM spectrum with h=0.5 and

$\Omega_B \approx 0$. If we can contemplate h as low as 0.4 or Ω_B as large as 0.1, then $n_s \approx 0.7$ is feasible as well.

The high degree of clustering of clusters has been a puzzle since the early 1980's. Observations [48] indicated that the correlation function of rich clusters was enhanced by a factor of about 11-16 over the correlation function of galaxies, if one assumed the same power law behavior for both correlation functions. The sample from which most of the estimates of clustering were derived was the Abell catalogue, which has been criticized on a number of grounds. The main problem seems to be the projection effect: clusters at different redshifts superimpose upon one another and lead to the impression that the clusters are more massive than they truly are. Recently two redshift surveys of clusters identified using the Southern Sky galaxy surveys estimate correlations about half as large as the original values; these surveys have shown that they are not as subject to contamination by projection effects. [The possibility also exists that these new surveys are probing clusters less rich than the older observations.] These new values are roughly compatible with what is expected if one uses the power spectra suggested by the galaxy clustering data [49] as shown above. Provided we are in the linear regime, Eq.(4.8) shows that the ratio of the cluster-cluster correlation function to the galaxy-galaxy correlation function should be given by $(b_c/b_g)^2$. A rough estimate for this enhancement factor can be obtained using the methods of [45] for a peak model of clusters; just from the abundance of clusters, one can determine that the combination $(b_c - 1)\sigma_8 \simeq 2.1$. Since $(b_c/b_g)^2 \sim (2.1 + \sigma_8)^2/(b_g\sigma_8)^2$, and taking $b_g = \sigma_8^{-1}$, we find that the enhancement factor ranges from 6 to 10 as σ_8 ranges from 0.5 to 1. Thus, if the new cluster correlation functions prove to be valid, they can also be explained with the same range of n_s as the w_{gg} data indicates.

2) Constraints from Microwave Background Anisotropies

We now determine the range of σ_8 as a function of n_s allowed by the COBE observations of microwave background anisotropy with the Differential Microwave Radiometer experiment [37]. The DMR team have presented data for: a) $\sigma_T(10^o)$, the *rms* fluctuations on the scale of 10^o; b) $\sigma^2_{T,\ell=2}$, the sum of the squares of the components of the quadrupole moment tensor; and c) estimates of the correlation function with the dipole and quadrupole contributions removed. Here, we divide their results by the background temperature of 2.736K in order to obtain dimensionless quantities in units of $\Delta T/T$.

The *fwhm* of the DMR beam (7^o) is sufficiently large that it is quite accurate to assume for the adiabatic fluctuations of interest here that the microwave background anisotropies arise from curvature fluctuations experienced by the photons as they travel out of the gravitational potential wells at the surface of last scattering to the present (the Sachs-Wolfe effect). If we assume that the universe is matter dominated from photon decoupling to the present, the variance C_ℓ of the multipole coefficient $a_{\ell m}$ in the spherical harmonic expansion of the radiation pattern (see *e.g.*, ref. [50]), is given by

$$C_\ell = \langle |a_{\ell m}|^2 \rangle = \frac{4\pi}{9} \int_0^\infty d\ln k \, \frac{d\sigma_\Phi^2}{d\ln k} \, j_\ell^2(k\tau_0) \; , \tag{4.9a}$$

where j_ℓ is a spherical Bessel function and τ_0 is the comoving distance to the last scattering surface, $\tau_0 \simeq 2H_0^{-1} \approx 6000\,\mathrm{h}^{-1}\mathrm{Mpc}$. The comoving wavenumber k is referred to current length units. The gravitational potential power spectrum is related to that for the density by

$$d\sigma_\Phi^2/d\ln k = ((3/2)H_0^2 k^{-2})^2 d\sigma_\rho^2/d\ln k \; . \tag{4.9b}$$

Although we used Eq.(4.9a) directly to evaluate the temperature power spectrum C_ℓ, for power law spectra on the large scales that COBE probes, there is a simple expression in terms of Gamma functions [50] and the quadrupole power C_2:

$$C_\ell = C_2 \frac{\Gamma[\ell + \frac{(n_s-1)}{2}]\Gamma[\frac{(9-n_s)}{2}]}{\Gamma[\ell + \frac{(5-n_s)}{2}]\Gamma[\frac{(3+n_s)}{2}]} \; , \tag{4.10}$$

for $\ell \geq 2$. In terms of C_ℓ, the *rms* value expected in each multipole for COBE is

$$\sigma_{T\ell}^2 = \frac{2\ell+1}{4\pi} C_\ell \, \mathcal{F}_\ell^2 \ , \tag{4.11}$$

where $\mathcal{F}_\ell$ is a filter appropriate to their beam, and is approximated by a Gaussian

$$\mathcal{F}_\ell = \exp[-0.5(\ell+0.5)^2/(\ell_{dmr}+0.5)^2] \ , \qquad \ell_{dmr} \approx 19 \ ,$$

where ℓ_{dmr} corresponds to 7° *fwhm*.

a) The strongest result to use for estimating the amplitude σ_8 is provided by $\sigma_T(10^\circ)$, which the COBE team determined by evaluating the intrinsic sky dispersion after further smoothing their data with a 7° *fwhm* Gaussian filter. To compare with this, we calculate the average value that our theoretical model predicts for this,

$$\sigma_T^2(10^\circ) = \sum_\ell \mathcal{F}_\ell^2 \sigma_{T\ell}^2 \ . \tag{4.12}$$

The extra filtering by $\mathcal{F}_\ell^2$ brings the total smoothing up to a total of 10°. Since the realization of the Universe that we observe involves a specific set of multipole coefficients drawn from (Gaussian) distributions with variance C_ℓ, there will be a theoretical dispersion in the values of $\sigma_T^2(10^\circ)$, what the COBE team refers to as 'cosmic variance'. For $\sigma_T^2(10^\circ)$, we have

$$\langle [\Delta\sigma_T^2(10^\circ)]^2 \rangle = 2 \sum_\ell \frac{1}{2\ell+1} \left[\mathcal{F}_\ell^2 \sigma_{T\ell}^2 \right]^2 \ . \tag{4.13}$$

An excellent fit to our calculation of Eqs.(4.12,4.13) (using 4.9a, 4.9b, and 4.11) is

$$\sigma_T(10^\circ) = 0.93 \times 10^{-5} \, \sigma_8 \, e^{2.63(1-n_s)} \, [1 \pm 0.1 e^{0.42(1-n_s)}] \ . \tag{4.14}$$

(Since the error in Eq. (4.13) is for the square, $\sigma_T^2(10^\circ)$, there is actually a slight asymmetry between the upper and lower error bars for $\sigma_T(10^\circ)$; we have included this asymmetry in Figure 5.) Eq.(4.14) is to be compared with the DMR result, with its '1 sigma' error,

$$[\sigma_T(10^\circ)]_{dmr} = 1.085 \times 10^{-5} \, [1 \pm 0.169] \ . \tag{4.15}$$

(These errors should be slightly enhanced since the detected large scale anisotropy can lead to bigger fluctuations in $\sigma_T(10^\circ)$ than one would get solely using single pixel errors, as the DMR team did. This appears to be a sufficiently small correction that it can be ignored.) The combined theoretical and experimental error is therefore about 20% for $n_s = 1$, rising slightly for lower values, hence

$$\sigma_8 = 1.17 e^{-2.63(1-n_s)} \, [1 \pm 0.2] \ . \tag{4.16}$$

The central value for σ_8 as a function of n_s with error bars is shown by the solid lines in Figure 5. In particular, for $n_s \lesssim 0.6$, the DMR result requires $\sigma_8 \lesssim 0.5$ (or a biasing factor $b_8 \gtrsim 2$). However, we caution that this value is for the $\Omega_B = 0$ limit. With the value $\Omega_B \sim 0.06$ favoured by primordial nucleosynthesis, the theoretical prediction for $\sigma_T(10^\circ)$ rises by about 15% and the value of σ_8 obtained by comparison with COBE data drops by this amount.

b) The quadrupole determination by the DMR team is not nearly as restrictive, because the cosmic variance as well as the DMR error bars are quite large. Integrating Eq.(4.9a) over all $k > 10^{-4} \, \mathrm{h^{-1}Mpc}$ for C_2, we obtain

$$\sigma_{T,\ell=2} = 0.46 \times 10^{-5} \, \sigma_8 \, e^{2.94(1-n_s)} \, [1 \pm 0.3] \ , \tag{4.17}$$

to be compared with

$$[\sigma_{T,\ell=2}]_{dmr} = 0.475 \times 10^{-5}\ [1 \pm 0.31]\ ; \tag{4.18}$$

hence

$$\sigma_8 \approx 1.02 e^{-2.94(1-n_s)}\ [1 \pm 0.46] \tag{4.19}$$

(again, we have ignored the asymmetry on the cosmic variance errors). As for $\sigma_T(10^o)$, small values of σ_8 are required for $n_s \lesssim 0.6$. We find that Eq. (4.16) is more restrictive than Eq. (4.19).

c) One can also use the correlation function data for given n_s to determine the allowed range for σ_8. The correlation function (with quadrupole removed) and its cosmic variance are given by [50]

$$C(\theta) = \sum_{\ell>2} P_\ell(\cos\theta)\ \sigma_{T\ell}^2\ . \tag{4.20a}$$

and

$$\langle [\Delta C(\theta)]^2 \rangle = 2 \sum_{\ell>2} \frac{1}{2\ell+1} \left[P_\ell(\cos\theta)\ \sigma_{T\ell}^2 \right]^2\ . \tag{4.20b}$$

There are also correlations from angle to angle, so a matrix is more appropriate. As well, one should restrict the region of correlation function estimation to that actually used by the DMR team, which involved a cut in Galactic lattitude. This will increase the theoretical variance. In Figure 6, we compare our theoretical correlation functions, including their errors derived from Eq.(4.20), for the $n_s = 1$ (Fig. 6a) and $n_s = 0.4$ (Fig. 6b) cases with the DMR correlation function given in ref. [37]. We have fixed the amplitude of the theory curves by requiring that they give the DMR $\sigma_T(10^o) = 1.09 \times 10^{-5}$. If we vary this amplitude for fixed n_s, then the theory will cease to agree with the data. Using the error bars that the DMR team give, and calculating χ^2 for the model fits to the data assuming the errors are independent and Gaussian (which they are not), we have constructed an allowed range for σ_8 which basically agrees with that derived from $\sigma_T(10^o)$, but with slightly larger errors. A more precise treatment that takes into account the correlation in the variances of the theory $C(\theta)$ and the influence of the extra correlation over pixel noise on the data $C(\theta)$ error bars is needed to precisely pin down the allowed range. However, we are encouraged by the general agreement between limits derived from $\sigma_T(10^o)$, $C(\theta)$ and the quadrupole. The DMR team derive the constraint $n_s = 1.1 \pm 0.5$ from the correlation function data. Although it can be seen from Figure 6 that there is a slight preference for the $n_s = 1$ case compared with the $n_s = 0.4$ case, we do not consider that the $n_s = 0.4$ case can be ruled out by these data alone.

3) Large-scale Streaming Velocities

There is another type of data that directly probes the amplitude of the mass density fluctuations as opposed to the fluctuations in galaxy or cluster number densities, namely large scale streaming velocities. From optical surveys, Bertschinger *et al.* [51] estimated the three-dimensional velocity dispersions of galaxies within spheres of radius $40\,h^{-1}$Mpc and $60\,h^{-1}$Mpc after the data had been smoothed with a Gaussian filter of $12\,h^{-1}$Mpc,

$$\sigma_v(40) = 388\ [1 \pm 0.17]\ \text{km s}^{-1}\ \ ;\ \ \sigma_v(60) = 327\ [1 \pm 0.25]\ \text{km s}^{-1}\ . \tag{4.21}$$

These data should be compared with the *rms* 3D velocity dispersions for power law CDM models (with errors calculated from the variance $\langle [\Delta\sigma_v^2(40)]^2 \rangle$):

$$\sigma_v(40) = 300\,\sigma_8\, e^{1.06(1-n_s)}\ [1^{+.35}_{-.57}]\ \text{km s}^{-1}\ \ ;\ \ \sigma_v(60) = 238\,\sigma_8 e^{1.19(1-n_s)}\ [1^{+.35}_{-.57}]\ \text{km s}^{-1}\ . \tag{4.22}$$

The fits are good for $0 \lesssim n_s \lesssim 1$. Although we do not regard these bulk flow estimates to be on as firm a foundation as the DMR measurement of $\sigma_T(10^o)$, it is interesting to note that the range suggested for σ_8 by the velocity data is similar,

$$\sigma_8 \approx 1.29 e^{-1.06(1-n_s)}\ [1^{+.38}_{-.65}]\ , \tag{4.23}$$

provided n_s is not very far from unity. Eq.(4.23) can be combined with Eq.(4.16) from $\sigma_T(10^o)$ to yield a preferred value for n_s of 1.07 (and $\sigma_8 = 1.4$!), and a '2 sigma' lower bound of $n_s = 0.72$. Using the $60\,h^{-1}$Mpc σ_v–estimate gives a similar result. This constraint is so restrictive because the dramatic decrease in σ_8 with decreasing n_s from $\sigma_T(10^o)$ more than offsets the increased velocity due to the enhanced large scale power.

4) The Epoch of Structure Formation and Other Tests

Given σ_8 and the spectral index n_s we can consider when structures of various types formed in the Universe. In Figure 7, we plot the range in linear *rms* density fluctuations $\sigma_\rho(M) = \langle(\Delta M/M)^2\rangle$ as a function of mass scale M allowed by Eq.(4.16). We actually calculate the *rms* fluctuations smoothed on a 'top hat' filtering scale R_{TH} which is related to the mass by $M \approx 10^{12.4}(R_{TH}/\,h^{-1}\mathrm{Mpc})^3$. The range in R_{TH} around $R_g = 0.5\,h^{-1}$Mpc corresponds to the filtering appropriate for galaxy formation (top hat mass $10^{11.5}M_\odot$). The $\sigma_\rho(M)$ shown are evaluated at the current epoch if one extrapolates their growth by linear theory. This means that the *rms* fluctuations on the scale R_g reach nonlinearity at a redshift somewhat above

$$1 + z_{nl}(R_g) = \sigma_\rho(R_g) \approx 6.2\sigma_8\, e^{-(1-n_s)} \approx 7.2e^{-3.63(1-n_s)}\,[1 \pm 0.2]\,, \qquad (4.24)$$

where we have used Eq.(4.16) for σ_8. Galaxies represent a much smaller fraction of space than that in typical fluctuations, but there is a lag between nonlinearity and complete collapse. These effects tend to cancel each other so Eq.(4.24) gives a first reasonable, although somewhat low, estimate of the redshift of galaxy formation.

A better estimate of the redshift of galaxy formation is obtained in the following way. We take the observed luminosity function for galaxies [52] and assign an average mass-to-light ratio $\overline{(M/L)}$ for galaxies with luminosities above L. We then have, approximately, for the mass fraction in objects with luminosity greater than L,

$$\Omega(>L) \approx 0.035\exp(-L/L_*)[\overline{(M/L)}/(50\mathrm{h})]\Omega\,,$$

where L_* is a fitting parameter that gives the typical luminosity for a bright galaxy. The corresponding mass is $M = 6 \times 10^{11}\mathrm{h}^{-1}[(M/L)/(50\mathrm{h})]\; L/L_*$. Therefore, the fraction of the mass in L_* galaxies for the models we are considering is about a percent. Now consider the fraction of the mass in the Universe in collapsed objects with mass above $3 \times 10^{11}M_\odot$; if we choose 50h for (M/L) and $\overline{(M/L)}$, this corresponds to the mass above $L_*/4$, and the expression for $\Omega(>L)$ above indicates that 2.7% of the mass should be in such objects. We thus determine the redshift at which the Press-Schechter mass function [53] for these models would predict that 2.7% of the mass in the Universe is in collapsed objects with mass above $3 \times 10^{11}M_\odot$. The corresponding value for this redshift is just 30% higher than Eq.(4.24) and provides a better estimate of when pervasive galaxy formation would have occurred,

$$(1 + z_{gf})_{PS} = 8.1\sigma_8\, e^{-(1-n_s)} \approx 9.5e^{-3.63(1-n_s)}\,[1 \pm 0.2]\,. \qquad (4.25)$$

The power 3.63 is so large that even if we err on the conservative side by using Eq.(4.25) rather than Eq.(4.24) and take the upper limit, we obtain relatively strong limits on n_s:

$$n_s \gtrsim 0.63\,,\ \text{if } z_{gf} > 2\,;\quad n_s \gtrsim 0.71\,,\ \text{if } z_{gf} > 3\,. \qquad (4.26)$$

A more careful analysis of star formation history would be required to improve upon these limits, but they illustrate that the amplitude factors allowed by the DMR data lead to strong limits on the spectral index to have galaxy formation occur early enough. Note that these bounds on n_s are similar to those derived from the streaming velocities.

A more powerful analysis of when objects of various masses form is provided by the hierarchical peaks method [54, 55], which identifies virialized potential wells with patches of the Universe centred on peaks of the density field that have undergone collapse, but solves the 'cloud-in-cloud problem' inherent in the original BBKS peak method [42] by merging small scale peak substructures into the dominant peaks that contain them. A mass function for dark matter halos at redshift z, $n(M,z)dM$, as well as detailed information about the spatial distribution of the halos, can be calculated. The objects found with this method have been shown to agree well with groups found in N-body calculations. Curiously, the mass function agrees reasonably well with that derived using the Press-Schechter approach [53], especially at the high mass end. This gives us some confidence in the validity of the Eq.(4.26), $n_s > 0.63$, constraint. However, the Press-Schechter mass function has no strong theoretical justification [56] and cannot deal with the spatial distribution of objects.

Since the total dark matter mass in galaxies is not directly measured, the mass function $n(M)$ is of limited diagnostic use. On the other hand, the depth of galaxy and cluster potential wells can be inferred from their internal velocity dispersion v. Therefore, in Figure 8 we show the number density of objects with velocity dispersion in excess of v, $n(>v,z)$, for a variety of redshifts. The $n_s = 1$ CDM model with $\sigma_8 = 0.7$ has roughly the right number of $v = 200\,\mathrm{km\ s^{-1}}$ halos at $z > 3$ to be a viable model of galaxy formation, and the number of clusters with 3D virial velocity above 1500 $\mathrm{km\ s^{-1}}$ roughly corresponds to the number of rich Abell clusters. Increasing σ_8 for this model, as is suggested by the DMR data, might result in an excess of clusters with high velocity dispersions and thus high X-ray temperatures that may already be excluded by the X-ray data [55]. However, current indications from gravitational lensing observations in clusters [57] are that clusters exist with velocities in excess of $v = 2000\,\mathrm{km\ s^{-1}}$ at $z \gtrsim 0.2$, and a $z \sim 0.2$ cluster observed with the X-ray satellite Ginga has an X-ray temperature of 13 keV [58], which translates into a $v \sim 2500\,\mathrm{km\ s^{-1}}$ dispersion. It is also possible that cluster X-ray temperatures are below the values one would infer from the dark matter potential. Thus it may turn out that $\sigma_8 \sim 1$ will be preferred over 0.7 as the data improves. On the other hand, it is evident that cluster velocity dispersion estimates are easily contaminated by projection effects that always give overestimates [59], so the lack of $v \sim 1500\,\mathrm{km\ s^{-1}}$ clusters in the $\sigma_8 = 0.5$, $n_s = 0.6$ model cannot at present be used to exclude it. Thus, although it is universally agreed that the abundance of rich clusters as a function of velocity dispersion will be one of the most powerful measures of σ_8, better data and extensive theoretical comparisons with the X-ray and optical data are required to test how strongly n_s is constrained. The basic conclusion of the more complete analysis of ref.[55] is that, while one may argue that low amplitude models are not excluded by the velocity or temperature data, it seems quite unlikely that the errors in the X-ray flux and luminosity data, both for nearby and distant ($z \sim 0.2$) clusters, are so large as to allow these models to survive; explicitly, the $n_s = 0.6$ CDM model with $\sigma_8 \leq 0.5$ is ruled out [55].

What even more strongly rules out the $n_s = 0.6$ model, in agreement with the analytic argument constraining n_s using z_{gf} given above, is the lack of high redshift activity, in particular the paucity of halos with dispersion in excess of $200\,\mathrm{km\ s^{-1}}$ even as late as $z = 2$. These are the sites of bright galaxy formation. There are some interesting differences that appear at high z even with the modest change in slope from $n_s = 1$ to 0.8, with σ_8 fixed: *e.g.*, there would be an order of magnitude more $v = 100\,\mathrm{km\ s^{-1}}$ 'dwarf' galaxies at $z = 10$ in the $n_s = 1$ model than in the case of $n_s = 0.8$. It has been argued [60] that only those dwarf galaxies with velocities above this number will survive the supernova explosions that occur when galaxies assemble themselves. Having some old cores of stable objects is probably a good thing rather than a bad thing, since they could be the birthplaces of quasars, but because of uncertainties in modelling the gas dynamical behaviour of forming galaxies and of the intergalactic medium one cannot be sufficiently definitive about the high z consequences of a theory to select one model over the other at this stage.

Another test which has been used to argue that $\sigma_8 \lesssim 0.6$ and which therefore favours $n_s < 1$ models is the velocity dispersion of pairs of galaxies over separations of order a Mpc [61]. In the early N-body simulations of $n_s = 1$, $\sigma_8 = 1$ CDM models, the pair velocity dispersion of dark

matter halos on these scales was found to be much higher than the velocities of galaxies inferred from redshift surveys. However, Carlberg and Couchman [62] computed an $n_s = 1$ CDM model in which the relative velocity of galaxies was much less than that for the dark matter, an effect termed 'velocity bias'. Coincidently, they chose $\sigma_8 = 1.17$, the value suggested by DMR. Although how effective this velocity biasing can have been at lowering the pair velocities is a matter of much debate, smaller n_s will obviously help to ease the problem.

Experimental upper limits on small and intermediate angle anisotropies in the microwave background can also be used to constrain the index n_s, but require detailed computations along the lines of those given in ref. [50] and we shall not undertake them here. We note however that the pre-COBE limits on anisotropy were already strong enough to place constraints of $n_s \gtrsim 0.6$ for $\sigma_8 = 1$ and $n_s \gtrsim 0.3$ for $\sigma_8 = 0.5$ [47] at the 90% confidence level, and the constraints from an earlier DMR limit [63] also gave similar values. (For other previous discussions of power law CDM spectra, see [38,39,67].)

5) The Role of Gravitational Wave Modes

Stimulated by the DMR results, other groups have been independently considering inflation-inspired power law spectra [68, 69]. Davis *et al.* [69] have pointed out that, although gravitational wave (GW) modes are generally small for nearly scale invariant spectra [70], for $n_s \ll 1$ these modes can be important. The work of these authors amplifies upon the work of Abbott and Wise [71]. Whenever the GW mode power spectrum is comparable to the scalar density fluctuation spectrum computed above, the constraints on the allowed spectral index from COBE become even more restrictive. As we will show, gravitational wave modes are negligible for the case of natural inflation, but are significant for power law and extended inflation models.

We first outline a calculation of the gravitational wave mode power spectrum, and compare it to the scalar density perturbation spectrum. During inflation, the same zero point quantum fluctuation phenomenon which leads to the inflaton density perturbations also leads to statistically independent gravitational wave perturbations. If h_+ and $h_\times$ are the two linear gravitational wave perturbations, then the gravitational modes $\varphi_i = M_{Pl} h_i / \sqrt{16\pi}$, where $i = +, \times$, behave just like single massless scalar field degrees of freedom as far as fluctuation generation is concerned. Each of the fields φ_i of comoving wavenumber k has a power spectrum $P_{\varphi_i}^{1/2}(k)$ equal to the Hawking temperature $H/(2\pi)$ when $k = Ha$, just as the inflaton fluctuations do, except that the gravitational perturbations are not amplified during subsequent evolution. With the factor given above, we therefore have for the total gravitational wave power, $P_{GW}^{1/2} \equiv [P_{h_+} + P_{h_\times}]^{1/2}$ $= \sqrt{32\pi} {M_{Pl}}^{-1} H/(2\pi)$. The ratio of the gravitational wave power spectrum to the adiabatic metric perturbation power spectrum P_ζ, at horizon crossing is therefore

$$\frac{P_{GW}^{1/2}}{P_\zeta^{1/2}} = \frac{\sqrt{2}\sqrt{16\pi}|\dot{\phi}|}{3 M_{Pl} H} ,$$

where the $\sqrt{2}$ comes from the 2 independent GW polarizations that can be generated. Using the WKB values at horizon crossing usually gives accurate estimates of final fluctuation amplitude [11].

For natural inflation, using the slow roll approximation, we have

$$\frac{P_{GW}^{1/2}}{P_\zeta^{1/2}} = \frac{2\sqrt{2}}{3} \left(\frac{{M_{Pl}}^2}{16\pi f^2}\right)^{1/2} \left[\left(1 + \frac{{M_{Pl}}^2}{48\pi f^2}\right) \exp\left[\frac{{M_{Pl}}^2}{8\pi f^2} N_I(k)\right] - 1\right]^{-1/2} . \qquad (4.27)$$

Thus the gravity waves are exponentially suppressed relative to the adiabatic scalar fluctuations of the inflaton over the observable large scale structure waveband. In particular, for $f \leq M_{Pl}$, this ratio is less than 0.04 for modes with wavelength equal to the current Hubble radius.

On the other hand, for power law inflation with an exponential potential, the ratio is

$$\frac{P_{GW}^{1/2}}{P_\zeta^{1/2}} = \frac{2\sqrt{2}}{3\sqrt{p}} = \frac{2\sqrt{2}}{3}\left[1+\frac{2}{1-n_s}\right]^{-1/2} . \tag{4.28}$$

Thus, for small n_s, the power in GW modes becomes almost comparable to the power in scalar density fluctuations.

The amplitude of gravitational wave modes decays by directional dispersion as the modes re-enter the horizon, just as waves in any relativistic collisionless matter do [43]; adiabatic fluctuations, on the other hand, maintain a constant gravitational potential. Before the gravitational wave structure disperses, however, it influences the microwave background through the Sachs-Wolfe effect. A number of authors have calculated the magnitude of this effect [70,71]. We denote the ratio of GW tensor to scalar contributions to the radiation field multipole moments a_{LM} by A_L. Abbott and Wise [71] show that this ratio is not very sensitive to the multipole moment L. Davis *et al.* [69] use the results of [70,71] to obtain the ratio A_2 for the quadrupole moment,

$$A_2 \equiv \frac{\sigma_{T\,\ell=2}^{GW}}{\sigma_{T\,\ell=2}^{adiab}} \simeq 3.9\,\frac{P_{GW}^{1/2}}{P_\zeta^{1/2}} . \tag{4.29}$$

To estimate the more restrictive constraints on the power law index when one includes the effects of GW modes for power law inflation, we shall assume $A_L \simeq A_2$ for all L; substituting Eq. (4.28) into Eq.(4.29), we find

$$A_2 \approx 3.7\left[1+\frac{2}{1-n_s}\right]^{-1/2} . \tag{4.30}$$

To include the effects of GW perturbations, the theoretical predictions for $\sigma_T(10^o)$ given in Eq.(4.14) should be multiplied by $[1+A_2^2]^{1/2}$. Thus, the allowed range of σ_8 as a function of n_s is lowered substantially. The new allowed range of parameter space is plotted in Fig. 5. For example, for $n_s = 0.6$, one can see that the maximum allowed value of σ_8 drops by a factor of 1.8. This makes the already strong constraints we have derived significantly stronger. The n_s-constraint we derived by requiring that galaxies form early enough in the theory, $n_s > 0.63$ for $z_{gf} > 2$, changes to $n_s > 0.76$ for power law inflation; similarly, the bound $n_s > 0.71$ from the requirement $z_{gf} > 3$ now becomes $n_s > 0.82$. Also, the '2 sigma' streaming velocity limit of $n_s > 0.72$ increases to $n_s > 0.89$.

For the chaotic inflation potentials used above, we have

$$\frac{P_{GW}^{1/2}}{P_\zeta^{1/2}} = \frac{2\sqrt{\nu}}{3}\left[N_I(k)+\frac{\nu}{3}\right]^{-1/2} , \qquad A_2 \approx 2.63\sqrt{\nu}\left[N_I(k)+\frac{\nu}{3}\right]^{-1/2} ; \tag{4.31}$$

hence gravity waves diminish σ_8 by only 11% for a ϕ^4 potential, and by 5.5% for a ϕ^2 potential. Slightly higher values for A_2 (and therefore lower values for σ_8) are obtained if we use a power law inflation formula with $n_s = 0.95$ and 0.97 for the ϕ^2 and ϕ^4 models, respectively. Motivated by COBE, various authors have been looking again at the gravitational wave contribution in these conventional inflation models [69,72].

It is clear from this discussion that if one could unearth the gravity wave component of anisotropy from the adiabatic component, it would allow a strong discrimination among models. In particular, natural inflation predicts only a negligible contribution from GW modes.

6) Discussion

Since our $n_s \gtrsim 0.6$ limit comes from a variety of arguments, we believe it is quite robust. Thus, unless the errors in the analysis of the large scale clustering observations (which require $n_s < 0.6$ with standard CDM, see Section IV.B.1) are larger than currently estimated, a fluctuation spectrum with broken scale invariance (*i.e.*, $n_s < 1$) that has a slowly changing spectral index over the range $k^{-1} \sim 10 - 10^4$ Mpc cannot be the sole solution to the extra power dilemma that the CDM model faces. However, the allowed values of $n_s \gtrsim 0.7$ can help to ease the requirements on some of the extra power fixes proposed in the literature (*e.g.*, [45]); for example, $n_s = 0.7$ with CDM and $h = 0.4$ or $\Omega_B = 0.1$ marginally fits the observations.

Motivated by the DMR results and the many prospects for broken scale invariance in inflation, Cen *et al.* [68] have very recently undertaken combined hydrodynamical and N-body calculations of CDM models with $n_s = 0.7$ and have independently come to a number of the conclusions we have about such models, namely that they help but do not fully solve the large scale structure dilemma. Some related pre-COBE results on the implications of power-law spectra with CDM were obtained by Vittorio, *et al.* [38] (in particular, on CMBR anisotropy and large-scale flows). In addition, independently of our work, Liddle, *et al.* [39] came to similar conclusions about constraints from the APM data on power-law models.

Finally, our limit on n_s can be translated into constraints on the parameters of inflation models that give rise to power law spectra. For example, it gives a very strong constraint on the effective value of ω, the Brans-Dicke parameter which arises in extended inflation models. When the effect of GW tensor waves is included, the $z_{gf} > 2$ constraint, $n_s \gtrsim 0.76$, becomes $\omega \gtrsim 17$; this lower limit comes close to reaching the largest allowed value of ω for successful extended inflation [73], $\omega \lesssim 25$, in most versions of this theory. Indeed, a closer examination [74] of the upper bound on ω, which arises from the requirement that large bubbles do not produce an excessive microwave anisotropy, suggests that in fact $\omega < 18$ is required if the dark matter is cold. Combined with our lower bound on ω, this limit would leave little room for most extended inflation scenarios. For natural inflation, from Eqn.(4.2), the constraint $n_s > 0.63$ translates into a lower bound for f of $0.33 M_{Pl}$. This is comparable to the constraint from reheating, Eq.(3.37).

V. CONCLUSIONS

We have studied an inflation scenario inspired by particle physics models with weakly self-coupled (pseudo-)scalars such as the axion. With the requisite mass scales, which can emerge dynamically for plausible choices of gauge groups, PNGB inflation appears to be robust in the sense that it arises in the simplest class of models, with a potential of the form (1.1). We have shown how these models can arise in a variety of theoretical settings, and indeed that superstring models already in the literature come very close to providing the desired mass parameters for natural inflation. Although the tendency of higher dimension operators on PNGBs arising from wormhole effects, for example, would be to increase Λ, we discussed quite plausible ways in which the upward movement can be exponentially suppressed, so our model retains its naturalness. We numerically and analytically studied the cosmological dynamics of the inflaton field, and derived several constraints on the two-dimensional parameter space (f, Λ). The allowed band of parameter space includes models which have more relative fluctuation power on large lengthscales than the standard scale-invariant spectrum.

We have studied in depth the consequences of power law initial fluctuation spectra for large-scale structure and the microwave background anisotropy. We find that the large-scale galaxy angular correlation function $w_{gg}(\theta)$ observed in the APM survey is consistent with power law initial spectra and standard CDM for $n_s \lesssim 0.6$; if $h = 0.4$ or $\Omega_B = 0.1$, then n_s as large as 0.7 would be acceptable. However, the COBE results require a rather small perturbation amplitude for these models, $\sigma_8 \lesssim 0.5$ ($b_8 \gtrsim 2$) for $n_s \lesssim 0.6$. For this range of n_s, this makes the epoch of galaxy formation uncomfortably recent and predicts large-scale flows of relatively

small amplitude. Turning this argument around, we have combined the COBE results with the requirement of sufficiently early galaxy formation ($z_{gf} > 2$) and large-scale flows of the inferred amplitude to find the constraint $n_s \gtrsim 0.6 - 0.7$. For natural inflation, this implies $f \gtrsim 0.3 M_{Pl}$, virtually the same bound as we get from the requirement of sufficient reheating and consonant with the requirement that the probability of sufficient inflation be $\mathcal{O}(1)$. We have also found that the effects of gravitational wave modes on the microwave anisotropy are negligible for natural inflation, but can be important for power law and extended inflation. For the latter models, inclusion of gravitational waves in the COBE signal yields an even tighter constraint on the spectral index, $n_s \gtrsim 0.76 - 0.89$. For many brands of extended inflation, the Brans-Dicke parameter is restricted to an extremely narrow range.

Although the simple expedient of reducing n_s does not, by itself, solve all the large scale structure dilemmas for the CDM model, it can be combined with other ways to explain the extra large scale power [45], for example, by introducing into the CDM model a neutrino with a mass of a few eV, a nonzero cosmological constant ($M_{Pl}{}^2 \Lambda / 8\pi \mathrm{h} = 0.2$ with CDM fits for $n_s = 1$), a smaller Hubble constant ($\mathrm{h} \sim 0.4$), a larger baryon abundance, or by simply supposing that galaxies are distributed on large scales somewhat differently than the mass so that the linear biasing assumption of Eq.(4.8) is invalid. We conclude that inflation with pseudo-Nambu-Goldstone bosons offers an attractive model for generating curvature fluctuations whose gravitational instability can lead to all of the cosmological structure we observe around us.

Acknowledgements

We acknowledge useful conversations with and comments from S. Dimopoulos, L. Dixon, M. K. Gaillard, C. T. Hill, S. Hsu, L. Knox, A. Liddle, A. Linde, S. Myers, S. J. Rey, and N. Vittorio and thank K. Fisher, M. Davis, and M. Strauss for providing the IRAS 1.2 Jansky power spectrum. We would like to thank R. Davis and P. Steinhardt for drawing our attention to the important role gravity waves would play in power law and extended inflation models. Four of us acknowledge the hospitality of the Institute for Theoretical Physics during its workshop on Cosmological Phase Transitions, where part of this work was completed. Three of us (K.F., J.F., and A.O.) also acknowledge the hospitality of the Aspen Center for Physics. JRB was supported by NSERC and a Canadian Institute for Advanced Research Fellowship. KF was supported in part by NSF grant NSF-PHY-92-96020, a Sloan Foundation fellowship, and a Presidential Young Investigator award. The research of JAF is supported in part by the DOE and by NASA grant NAGW-2381 at Fermilab. AVO acknowledges support from the NSF at the University of Chicago. FCA is supported in part by NASA Grant No. NAGW–2802 and in part by funds from the Physics Department at the University of Michigan.

APPENDIX: APPROXIMATION OF INTEGRALS

In this Appendix, we demonstrate the validity of the results presented in §III.C on the *a posteriori* probability of inflation. The main difficulty is that the simple logarithmic form (Eq. 3.11) for the number of e-foldings as a function of $y_1 = \phi_1/f$ does not hold for large y_1 (*i.e.*, for $y_1 \geq 1$). We should thus write the integral I (see Eq. 3.31) in the form

$$\begin{aligned} I &= \int_\epsilon^1 dy_1 e^{3A} e^{-3B \ln y_1} + \int_1^\pi dy_1 e^{3N(y_1)} \\ &= \frac{e^{3A}}{3B-1}\left\{\left(\frac{1}{\epsilon}\right)^{3B-1} - 1\right\} + \int_1^\pi dy_1 e^{3N(y_1)}. \end{aligned} \tag{A1}$$

In §III.C, we argued that when $3B > 1$, the integral can be approximated by the first term above,

$$I \approx \frac{e^{3A}}{3B-1}\left(\frac{1}{\epsilon}\right)^{3B-1}. \tag{A2}$$

We now calculate the relative error suffered in making this approximation. We first note that the number of e-foldings $N(y_1)$ is a strictly decreasing function of the starting value y_1. In particular,

$$N(y_1) \leq N(1) = A \qquad \forall y_1 \in [1, \pi]. \tag{A3}$$

8We thus obtain a bound on the second integral in Eq. [A1],

$$\int_1^\pi dy_1 e^{3N(y_1)} \leq e^{3A}(\pi - 1). \tag{A4}$$

This contribution to the error is always positive, whereas the other contribution [namely $-e^{3A}/(3B-1)$] is always negative. The total error E is therefore bounded from above by

$$E \leq e^{3A}\left[\pi - 1 - \frac{1}{3B-1}\right]. \tag{A5}$$

The total error is also bounded from below by the second (negative) term alone, so we obtain the relation

$$-1 \leq E(3B-1)e^{-3A} \leq 3B(\pi - 1) - \pi, \tag{A6}$$

and hence the relative error $\mathcal{E} = E/I$ is bounded by

$$\mathcal{E} \leq \epsilon^{3B-1} \times \max\{1,\, 3B(\pi - 1) - \pi\}. \tag{A7}$$

This error is always sufficiently small for the cases of interest. For example, for $f \approx M_{Pl}$, $3B \simeq 48\pi(f/M_{Pl})^2 \approx 48\pi$, then $\epsilon \leq y_1^{max} \simeq 0.6$, and hence $\mathcal{E} \leq 2 \times 10^{-31}$. For the other end of the mass range of interest (*i.e.*, for f near $f_c = 0.06 M_{Pl}$), let $3B - 1 = \delta$ where δ is a small positive number. In this regime $y_1^{max} \sim 10^{-60}$ and hence $\mathcal{E} \leq 10^{-60\delta}$. The error is thus completely negligible until δ becomes smaller than 1/60 or so, that is, until f is very close to f_c.

REFERENCES

[1] A. H. Guth, *Phys. Rev.* D **23**, 347 (1981).

[2] For a general review of inflation, see K. Olive, Phys. Repts. **190**, 307 (1990).

[3] A. D. Linde, *Phys. Lett.* **108 B**, 389 (1982); A. Albrecht and P. J. Steinhardt, *Phys. Rev. Lett.* **48**, 1220 (1982).

[4] F. C. Adams, K. Freese, and A. H. Guth, *Phys. Rev.* D**43**, 965 (1991).

[5] G. 't Hooft, in *Recent Developments in Gauge Theories*, eds. G. 't Hooft, *et al*, (Plenum Press, New York and London, 1979), p. 135.

[6] H. Quinn and R. Peccei, *Phys. Rev. Lett.* **38**, 1440 (1977); S. Weinberg, *Phys. Rev. Lett.* **40**, 223 (1978); F. Wilczek, *Phys. Rev. Lett.* **40**, 279 (1978).

[7] J. E. Kim, *Phys. Rev. Lett.* **43**, 103 (1979); M. Dine, W. Fischler, and M. Srednicki, *Phys. Lett.* **104 B**, 199 (1981); M. Wise, H. Georgi, and S. L. Glashow, *Phys. Rev. Lett.* **47**, 402 (1981).

[8] K. Freese, J. A. Frieman, and A. V. Olinto, *Phys. Rev. Lett.* **65**, 3233 (1990). See also J. A. Frieman, in *Trends in Astroparticle Physics*, eds. D. Cline and R. Peccei, (World Scientific, Singapore, 1992).

[9] J. P. Derendinger, L. E. Ibanez, H. P. Nilles, *Phys. Lett.* **155B**, 65 (1985); M. Dine, R. Rohm, N. Seiberg, and E. Witten, *Phys. Lett.* **156 B**, 55 (1985).

[10] E. Witten, *Phys. Lett.* **149B**, 351 (1984); K. Choi and J. E. Kim, *Phys. Lett.* **154B**, 393 (1985).

[11] See, *e.g.*, D. S. Salopek, J. R. Bond, and J. M. Bardeen, *Phys. Rev. D* **40**, 1753 (1989)

[12] A. Zee, *Phys. Rev. Lett.* **42**, 417 (1979);**44**, 703 (1980). L. Smolin, *Nucl. Phys.* **B160**, 253 (1979).

[13] C. T. Hill and G. G. Ross, *Phys. Lett.* **203 B**, 125 (1988); *Nucl. Phys.* **B 311**, 253 (1988). D. Chang, R. N. Mohapatra, and S. Nussinov, *Phys. Rev. Lett.* **55**, 2835 (1985).

[14] For a review, see J. E. Kim, *Phys. Rep.* **150**, 1 (1987).

[15] J. A. Frieman, C. T. Hill, and R. Watkins, Fermilab preprint Fermilab-Pub-91/324-A, to appear in *Phys. Rev.* D.

[16] For a review, see M. Green, J. Schwarz, and E. Witten, *Superstring Theory*, (Cambridge University Press, Cambridge, 1987).

[17] E. Witten, ref. 10.

[18] E. Martinec, *Phys. Lett.* **171B**, 189 (1986); M. Dine and N. Seiberg, *Phys. Rev. Lett.* **57**, 2625 (1986).

[19] P. Binetruy and M. K. Gaillard, *Phys. Rev.* D**34**, 3069 (1986) also considered this possibility in the context of the models of ref.9.

[20] R. Rohm and E. Witten, *Ann. Phys.* **170**, 454 (1986).

[21] M. Dine and N. Seiberg, *Phys. Lett.* **162B**, 299 (1985).

[22] N. V. Krasnikov, *Phys. Lett.* **193B**, 37 (1987).

[23] J. A. Casas, Z. Lalak, C. Munoz, and G. G. Ross, preprint OUTP-90-07P.

[24] V. Kaplunovsky, L. Dixon, J. Louis, and M. Peskin, unpublished; L. Dixon, in *Proc. of the 15th APS Div. of Particles and Fields General Meeting*, Houston, TX, Jan. 3-6, 1990. J. Louis, in *Proc. of the APS Div. of Particles and Fields General Meeting*, Vancouver, Canada,

Aug. 18-22, 1991.

[25] S. Shenker, Rutgers preprint RU-90-47 (1990).

[26] B. Ovrut and S. Thomas, *Phys. Lett.* **267B**, 227 (1991); preprint UPR-0455T.

[27] J. Kim and K. Lee, *Phys. Rev. Lett.* **63**, 20 (1989);

[28] M. Kamionkowski and J. March-Russell, preprint IASSNS-HEP-92-9 (1992); R. Holman, S. Hsu, E. Kolb, R. Watkins, and L. Widrow, preprint NSF-ITP-92-06. S. Barr and D. Seckel, Bartol preprint.

[29] A. D. Linde, *Phys. Lett.* **129 B**, 177 (1983).

[30] T. W. B. Kibble, *J. Phys.* **A 9**, 1387 (1976).

[31] D. Goldwirth, *Phys. Lett.* **243B**, 41 (1990).

[32] L. Knox and A. V. Olinto, unpublished.

[33] A. H. Guth and S.-Y. Pi, *Phys. Rev. Lett.* **49**, 1110 (1982).

[34] S. W. Hawking, *Phys. Lett.* **115B**, 295 (1982).

[35] A. A. Starobinskii, *Phys. Lett.* **117B**, 175 (1982).

[36] J. Bardeen, P. Steinhardt, and M. S. Turner, *Phys. Rev.* D **28**, 679 (1983).

[37] G. F. Smoot, C. L. Bennett, A. Kogut, E. L. Wright, J. Aymon, N. W. Boggess, E. S. Cheng, G. De Amici, S. Gulkis, M. G. Hauser, G. Hinshaw, C. Lineweaver, K. Loewenstein, P. D. Jackson, M. Jansen, E. Kaita, T. Kelsall, P. Keegstra, P. Lubin, J. Mather, S. S. Meyer, S. H. Moseley, T. Murdock, L. Tokke, R. F. Silverberg, L. Tenorio, R. Weiss and D. T. Wilkinson, *Ap. J. Lett.*, in press (1992).

[38] N. Vittorio, S. Mattarese, and F. Lucchin, *Ap. J.* **328**, 69 (1988).

[39] A. Liddle, D. H. Lyth, and W. Sutherland, *Phys. Lett.* **279B**, 244 (1992).

[40] L. A. Kofman and A. D. Linde, *Nucl. Phys.* **B282**, 555 (1987); L. A. Kofman and D. Yu. Pogosyan, *Phys. Lett.* **214B**, 508 (1988).

[41] E. W. Kolb, D. S. Salopek, and M. S. Turner, *Phys. Rev.* D**42**, 3925 (1990).

[42] J. M. Bardeen, J. R. Bond, N. Kaiser, and A. S. Szalay, *Ap. J.*, **304**, 15 (1986), BBKS.

[43] J. R. Bond and A. S. Szalay, *Ap. J.* **274**, 433 (1983).

[44] J. R. Bond and H. Couchman, in *General Relativity and Astrophysics*, Proc. Second Canadian Conference on General Relativity, p. 385 (1987); H. Couchman and J. R. Bond, in: Large Scale Structure and Motions in the Universe, eds. M. Mezzetti *et al.* (Dordrecht: Kluwer), p.335 (1989); J. R. Bond and H. Couchman, in preparation (1992).

[45] J. M. Bardeen, J. R. Bond, and G. Efstathiou, *Ap. J.*, **321**, 18 (1987).

[46] S. J. Maddox, G. Efstathiou, and W. J. Sutherland, *Mon. Not. R. astr. Soc.*, **246**, 433 (1990); and in preparation (1992).

[47] J. R. Bond, in *Highlights in Astronomy, volume 9*, Proceedings of IAU Joint Discussion IV, Buenos Aires General Assembly, ed. J. Bergeron, *Structure Constraints from Large Angle CMB Anisotropies* (1991).

[48] N. Bahcall and R. Soneira, *Ap. J.*, **270**, 70 (1983).

[49] G. B. Dalton, G. Efstathiou, S. J. Maddox and W. J. Sutherland, *Ap. J.*, in press (1992); R. C. Nichol, C. A. Collins, L. Guzzo, S. L. Lumsden, *Mon. Not. R. astr. Soc.*, **255**, 21P (1992).

[50] J. R. Bond and G. Efstathiou, *Mon. Not. R. astr. Soc.*, **226**, 655 (1987).

[51] E. Bertschinger, A. Dekel, S. M. Faber, A. Dressler and D. Burstein, *Ap. J.*, **364**, 370 (1990).

[52] G. Efstathiou, R. S. Ellis and B. A. Peterson, *Mon. Not. R. astr. Soc.* **232**, 431 (1988).

[53] W. H. Press and P. Schechter, *Ap. J.* **187**, 425 (1974).

[54] J. R. Bond, in *Frontiers in Physics — From Colliders to Cosmology*, Proc. Lake Louise Winter Institute, p. 182, ed. A. Astbury, B.A. Campbell, W. Israel, A.N. Kamal and F.C. Khanna, Singapore: World Scientific (1989).

[55] J. R. Bond and S. T. Myers, in *Trends in Astroparticle Physics*, eds. D. Cline & R. Peccei, World Scientific, Singapore, p262 (1992); in Proceedings of the Third Teton Summer School on *Evolution of Galaxies and Their Environment*, July 5–10, 1992, ed. M. Shull (1992).

[56] J. R. Bond, S. Cole, G. Efstathiou and N. Kaiser, *Ap. J.* **379**, 440 (1991).

[57] B. Fort, *et al.* preprint (1992).

[58] K. Arnaud, *et al.* preprint (1992).

[59] C. S. Frenk, S. D. M. White, G. Efstathiou and M. Davis, *Ap. J.*, **351**, 10 (1990).

[60] A. S. Dekel and J. Silk, *Ap. J.* **303**, 39 (1986).

[61] M. Davis, G. Efstathiou, C. S. Frenk, and S. D. M. White, *Ap.J.* **292** (1985).

[62] H. M. P. Couchman and R. G. Carlberg, *Ap. J.*, **389**, 453 (1992).

[63] G. Smoot, *et al. Ap. J. Lett.* **371**, 1 (1991).

[64] P. Meinhold and P. Lubin, Ap. J. Lett. 370, 11 (1991).

[65] N. Kaiser, G. Efstathiou, R. S. Ellis, C. S. Frenk, A. Lawrence, M. Rowan-Robinson and W. Saunders, *Mon. Not. R. astr. Soc.*, **252**, 1 (1991).

[66] K. B. Fisher, M. Davis, M. A. Strauss, A. Yahil and J. P. Huchra, *Ap. J.*, in press (1992); K. B. Fisher, Ph. D. thesis, U. C. Berkeley (1992).

[67] Y. Suto, N. Gouda, and N. Sugiyama, *Ap. J. Suppl.* **74**, 665 (1990).

[68] R. Cen, N. Y. Gnedin, L. A. Kofman and J. P. Ostriker, preprint (1992).

[69] R. L. Davis, H. Hodges, G. F. Smoot, P. J. Steinhardt and M. S. Turner, preprint (1992).

[70] A.V. Veryaskin, V.A. Rubakov and M. V. Sazhin, *Sov. Astron.* **27**, 16 (1983); A. A. Starobinsky, *Sov. Astron. Lett.* **11**, 133 (1985).

[71] L. Abbott and M. Wise, *Nucl. Phys.* **B244**, 541 (1984).

[72] A. Dolgov and J. Silk, preprint (1992); L. Krauss and M. White, preprint (1992); D. S. Salopek, preprint (1992).

[73] D. La and P. J. Steinhardt, *Phys. Rev. Lett.* **62**, 376 (1989); E. Weinberg, *Phys. Rev.* **D40**, 3950 (1989); D. La, P. J. Steinhardt and E. W. Bertschinger, *Phys. Lett.* **B231**, 231 (1989).

[74] A. R. Liddle and D. Wands, *Mon. Not. R. astr. Soc.* **253**, 637 (1991).

FIGURE CAPTIONS

Figure 1: Plot of various field values and parameters vs. f/M_{Pl}. The upper curves show that our estimate ϕ_2/f (eq.3.5) for the value of the field at the end of the SR epoch (dotted) is very close to our numerical result ϕ_{end}/f for when inflation ends (solid). The middle (dashed) curve shows $\log(\phi_1^{max}/f)$, the largest initial value of the field consistent with 60 e-folds of inflation. The lower (dotted) curve shows the density perturbation constraint (3.23) on the scale Λ [plotted as $\log(\Lambda/M_{Pl})$], assuming the bias parameter $b_g = 1$.

Figure 2: Results of the numerical integration of the scalar and gravitational equations of motion. The number of inflation e-folds $N(\phi_1)$ of the scale factor is shown as a function of the initial value of the scalar field, ϕ_1, for different values of the fundamental mass scale, $f/M_{Pl} = 0.05$, 0.07, 0.1, 0.2, and 0.5.

Figure 3(a): Theoretical power spectra $[d\sigma_\rho^2/d\ln k]^{1/2}/\sigma_8$ for CDM models with variable spectral indices n_s are plotted against comoving wavenumber k (in units appropriate to current length). The power spectra are derived assuming linear dynamics (appropriate for $k^{-1} \gtrsim 5\sigma_8\, h^{-1}$Mpc and large scale linear biasing). There is progressively more large scale power as n_s decreases through the values $n_s = 1$, 0.6, 0.4, 0, -0.4, and -1 shown in the figure. The lines under the labels (whose vertical placements are arbitrary) indicate approximate regions in k-space that various probes of structure are sensitive to: microwave background anisotropy experiments of large angles (COBE, [37]) and of intermediate angles (*e.g.*, SPole is a 1° experiment [64]); clustering observations for galaxies in the APM Galaxy Survey (w_{gg}, [46]), galaxies in the QDOT redshift survey [65], and clusters (ξ_{cc}) [48]; and large scale streaming velocities (LSSV) [51]. The hatched region denotes the range that the power spectrum must pass through to explain the APM angular galaxy correlation function data [46].

Figure 3(b): A blow-up of the portion of Fig. 3(a) that focuses on the range of wavelengths probed by observations of large-scale clustering. The ordinate has been relabelled so that the spectra are in units of $b_g\sigma_8$. The hatched region is the APM region of 3(a), while the points denote the power spectra estimated from the QDOT redshift survey [65] (triangular points) and the IRAS 1.2 Jansky survey [66] (square points). Different biasing factors for the (slightly) different types of galaxies probed by the APM, QDOT and 1.2 Jy surveys could explain the differences in these results. There are indications that $b_g = 0.8\sigma_8^{-1}$ is needed for the 1.2 Jy galaxies [66], while $b_g = \sigma_8^{-1}$ describes the APM survey well. This difference in b_g is enough to bring the required power spectra for the different observations into agreement; in particular, the $n_s = 0.2$–0.6 range is also preferred by the 1.2 Jy data if $b_g = 0.8\sigma_8^{-1}$, while the $n_s = 1$ curve falls below the data error bars.

Figure 4: The models of Fig. 3(b) (with n_s = 1, 0.8, 0.6, 0.4,..., -1) are compared with the angular correlation function $w_{gg}(\theta)$ determined from the APM Galaxy Survey [46] scaled to the depth of the Lick catalogue, at which 1° corresponds to a physical scale of $\sim 5h^{-1}$Mpc (dots). No nonlinear corrections were applied to the theoretical power spectra, but for angular scales above $\sim 1°$ and for amplitude factors $\sigma_8 \lesssim 1$, the linear approximation is accurate [44]. The theoretical curves are in units of $(b_g\sigma_8)^2$. The straight line gives the angular correlation that would result if the behavior of the spatial correlation function observed over distances $r \lesssim 10h^{-1}$ Mpc, $\xi \sim r^{-1.8}$, were extended to large separations. Vertical hatchmarks indicate the allowed region once corrections for systematic errors in the observations are included. The data therefore suggest $0 \lesssim n_s \lesssim 0.6$ is needed for the CDM model if biasing is linear on large scales.

Figure 5: Solid curves indicate the allowed range of the amplitude parameter σ_8 as a function of the power law slope n_s for a standard CDM model (in the limit that $\Omega_B = 0$); this is the range allowed by comparison of $\sigma_T(10°)$ (the *rms* fluctuations on 10°) in COBE's DMR experiment with

the theoretical predictions. The central curve indicates the best fit value, while the two adjacent lines give '1 sigma' error bars. Both the theoretical variance and the quoted experimental error are included in the error bars, which are in total about $\pm 20\%$. The values of σ_8 drop by a further $\sim 15\%$ when $\Omega_B \sim 0.06$ is used rather than the value zero used here. The correlation function data of Fig.6 give rise to similar constraints. The two horizontal solid lines (whose vertical placement is arbitrary) illustrate the range in n_s suggested by the APM angular correlation function data and the '1 sigma error bars' on n_s derived using the correlation function by the DMR team. The horizontal dotted lines encompass the range of values of σ_8 that have been advocated for the $n_s = 1$ CDM model by different workers, *e.g.*, $\sigma_8 = 0.4$, 0.55, 0.65, and 1.2 in [61,44,54,62] respectively. The dashed curves give the allowed range for $\sigma_8(n_s)$ when gravitational wave modes are included for power law (and extended) inflation. For natural inflation, the contribution of GW modes to the anisotropy is negligible, and the deviation from the solid curves is infinitesimal.

Figure 6: Comparison of the DMR $53A+B \times 90A+B$ cross correlation function $C(\theta)$ (where the quadrupole contribution has been removed) [37] with the theoretical predictions for (a) $n_s = 1$ and (b) $n_s = 0.4$ spectra. The theoretical curves have been normalized (*i.e.*, the amplitudes σ_8 set) by requiring the angular power spectrum to reproduce the *rms* fluctuations on 10^o. The central curves indicate the *rms* values predicted by theory, while the outer two curves indicate the 'cosmic' variance. Clearly, although the data is somewhat better fit by the $n_s = 1$ rather than the $n_s = 0.4$ model, one cannot strongly distinguish between the 2 models solely on the basis of the shape of $C(\theta)$; in particular, the spectral index $n_s = 0.4$ cannot be ruled out by these data alone.

Figure 7: The linear *rms* fluctuations $\sigma_\rho(M)$ averaged over spherical regions of radius R_{TH} are plotted as a function of mass scale $M \approx 10^{12.4}(R_{TH}/\mathrm{h^{-1}Mpc})^3\,\mathrm{M_\odot}$, for CDM models with $n_s =$ 0.4, 0.6, 0.8, and 1 (with n_s increasing as one moves vertically up the figure). The error bars show the 1 sigma range in spectrum normalization as a result of DMR and cosmic variance errors in $\sigma_T(10^o)$. Although Fig.3(a) shows that $n_s < 1$ spectra have more power on large scales and less on small scales than $n_s = 1$ models with the same σ_8, when $\sigma_8(n_s)$ determined from COBE is used, the amplitude for $n_s < 1$ is less on *all* mass scales. The extreme problems with the $n_s = 0.4$ model and the marginality of the $n_s = 0.6$ model in terms of both large-scale structure and a sufficiently early epoch of galaxy formation are evident from this graph alone.

Figure 8: In (a), we show the number density of collapsed objects with 3D virial velocity in excess of v for the CDM model with spectral index $n_s = 0.8$ and for the value of the amplitude parameter $\sigma_8 = 0.7$ (indicated by the DMR $\sigma_T(10^o)$ data for this model). The densities are shown as a function of redshift z, with z decreasing as one moves to the right in the figure. The velocities in the hierarchical peaks method [55] used for this computation could be larger by an amount given by the error bar labelled by 'v range'; these error bars are explicitly put on the $z = 0$ curve. The number densities shown should be compared with the abundances indicated by the horizontal lines and velocity dispersions indicated by the downward arrows: for 'bright' galaxies, $\sim 10^{-2}(\mathrm{h^{-1}Mpc})^{-3}$ with $v \sim 220\,\mathrm{km\ s^{-1}}$, for rich clusters, $\sim 6 \times 10^{-6}(\mathrm{h^{-1}Mpc})^{-3}$ with $v \sim 1500\,\mathrm{km\ s^{-1}}$, and for at least one object between us and redshift 2, $\sim 10^{-9}(\mathrm{h^{-1}Mpc})^{-3}$ with $v \sim 2500\,\mathrm{km\ s^{-1}}$, according to the Ginga X-ray satellite team [58]. In (b), we choose the DMR 1 sigma upper bound $\sigma_8 = 0.5$ for $n_s = 0.6$; even so, the number of 'bright galaxy' halos is too small by $z = 2$. In (c), we plot the densities for $n_s = 1$, using the DMR 2 sigma lower bound $\sigma_8 = 0.7$ for the amplitude, to facilitate comparison with (a). The number densities of model (c) accord reasonably well with the hierarchy of objects in the Universe. There is little to distinguish between the $n_s = 1$ and $n_s = 0.8$ models with the same σ_8. To explicitly show this, we also plot with light solid curves the tails of the $z = 0$ abundances for cases (a) and (b). The third light curve, also for $z = 0$ (the highest curve at large v), shows the effect of increasing σ_8 to 1 for the $n_s = 1$ model, closer to the number indicated by DMR. Although this may lead to too many clusters with higher X-ray temperatures than observed [55], $\sigma_8 = 1$ does help to explain the Ginga event.

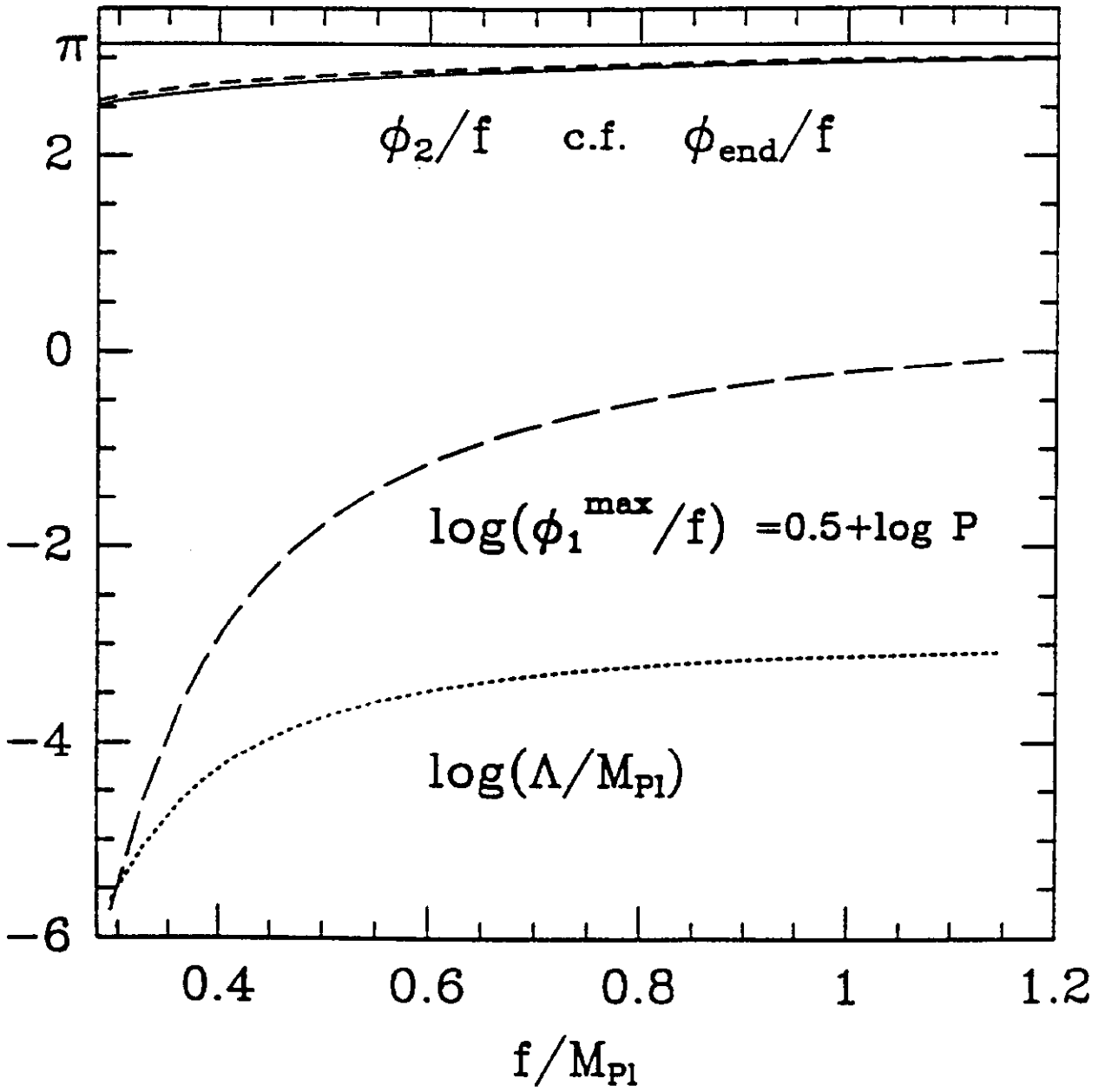
π
2
0
−2
−4
−6
ϕ_2/f c.f. ϕ_{end}/f
$\log(\phi_1^{max}/f)$ =0.5+log P
$\log(\Lambda/M_{Pl})$
0.4
0.6
0.8
1
1.2
f/M_{Pl}

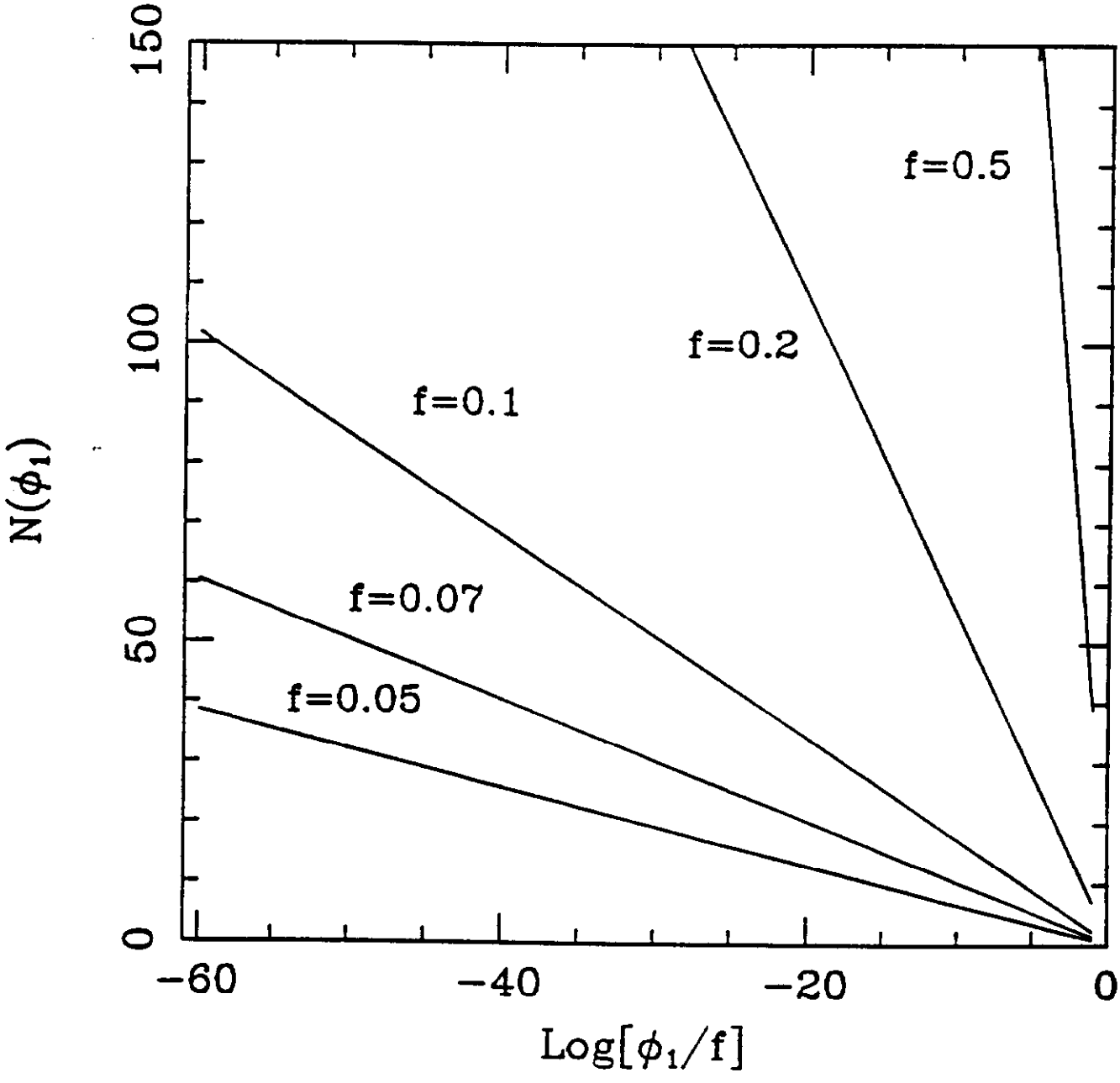
150
100
50
0
N(φ1)
f=0.5
f=0.2
f=0.1
f=0.07
f=0.05
−60
−40
−20
0
Log[φ1/f]

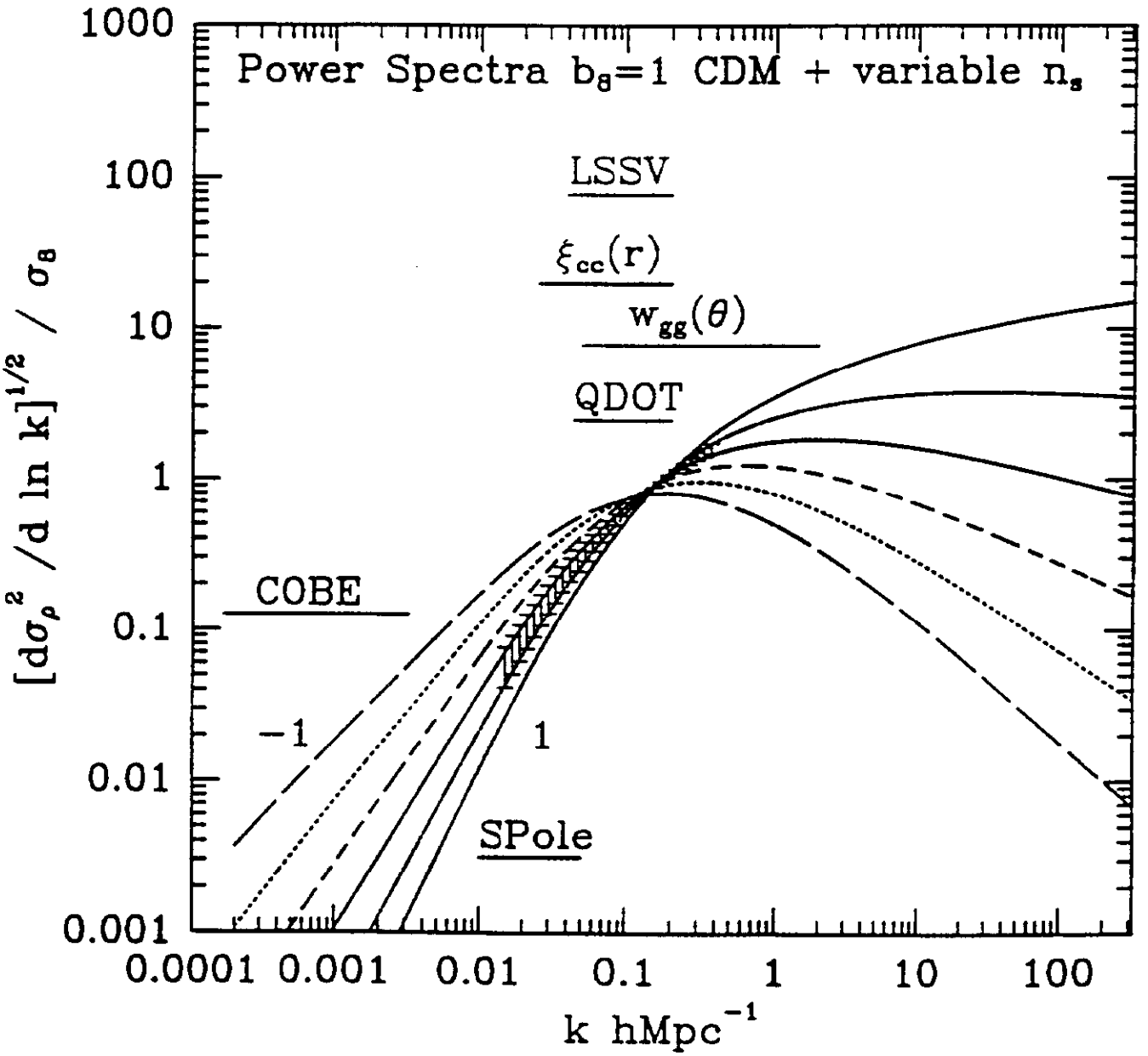
Power Spectra b_g=1 CDM + variable n_s
LSSV
$\xi_{cc}(r)$
$w_{gg}(\theta)$
QDOT
COBE
−1
1
SPole
$[d\sigma_\rho^2 / d \ln k]^{1/2} / \sigma_8$
k hMpc^{-1}
1000
100
10
1
0.1
0.01
0.001
0.0001
0.001
0.01
0.1
1
10
100

F-3(a)

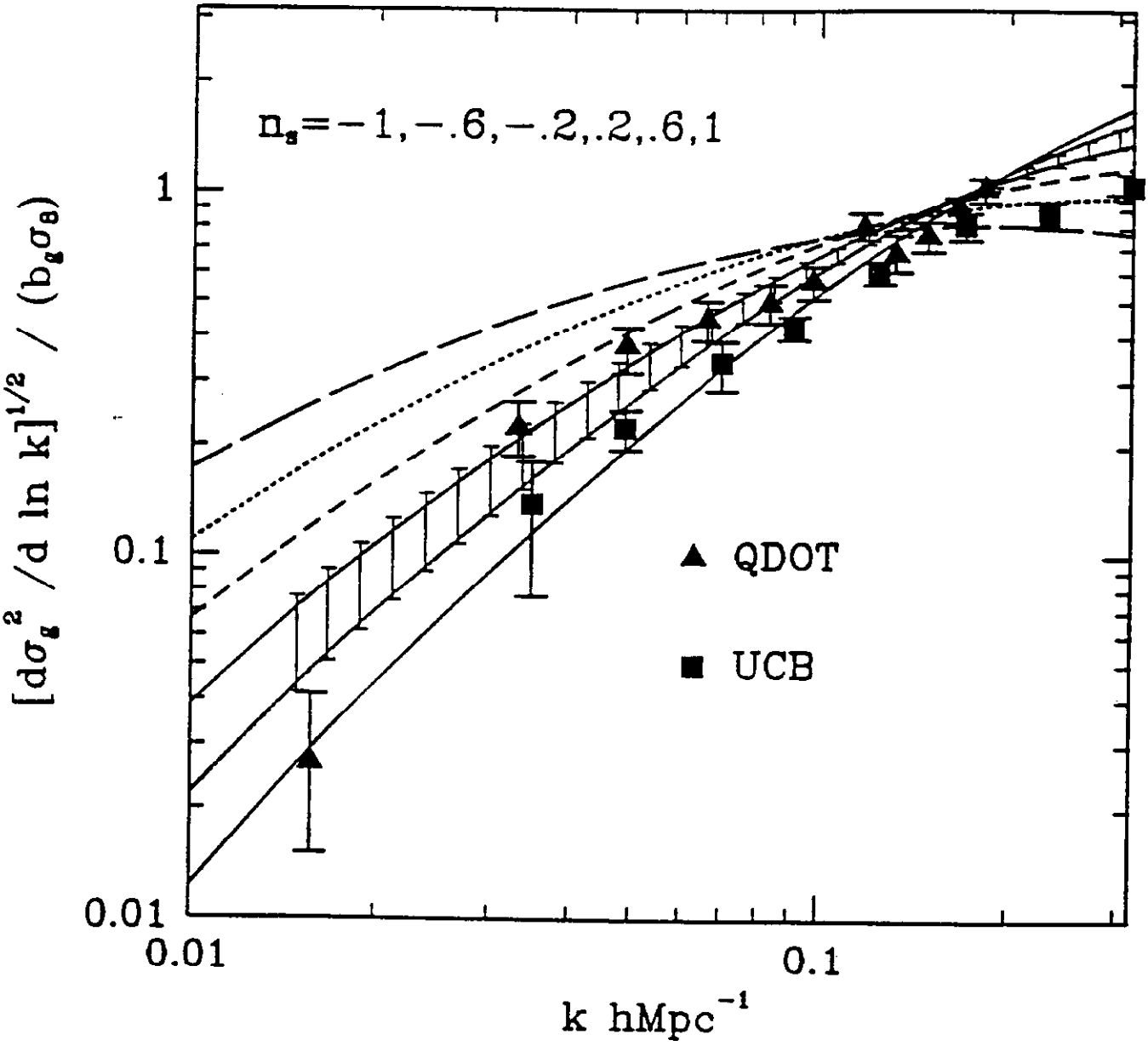
$n_s = -1, -.6, -.2, .2, .6, 1$
1
0.1
0.01
0.01
0.1
$[d\sigma_g^2 / d \ln k]^{1/2} / (b_g \sigma_8)$
k hMpc^{-1}
QDOT
UCB

F 3(b)

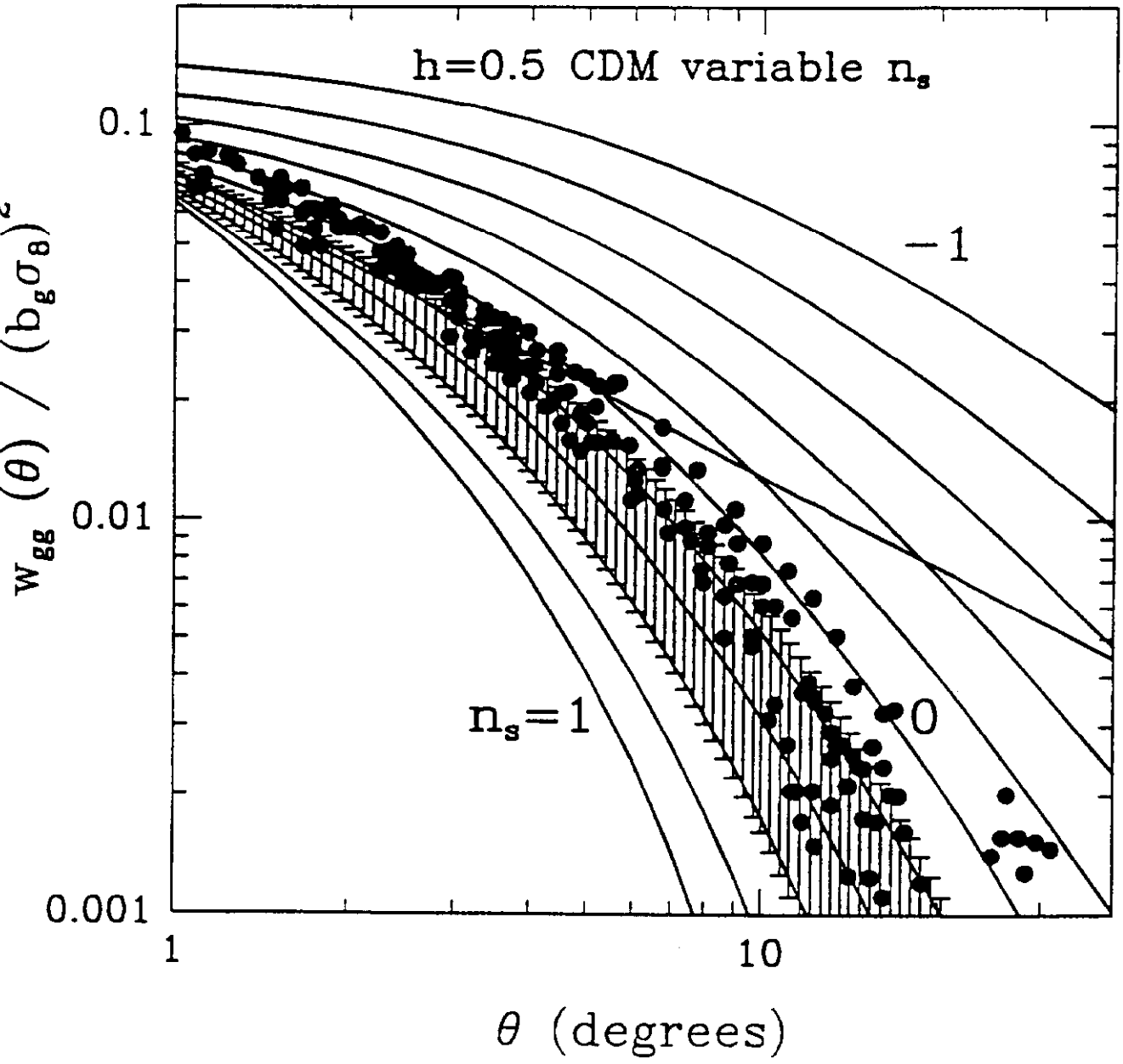
h=0.5 CDM variable n_s
0.1
0.01
0.001
1
10
$w_{gg}(\theta) / (b_g\sigma_8)^2$
θ (degrees)
$n_s=1$
0
−1

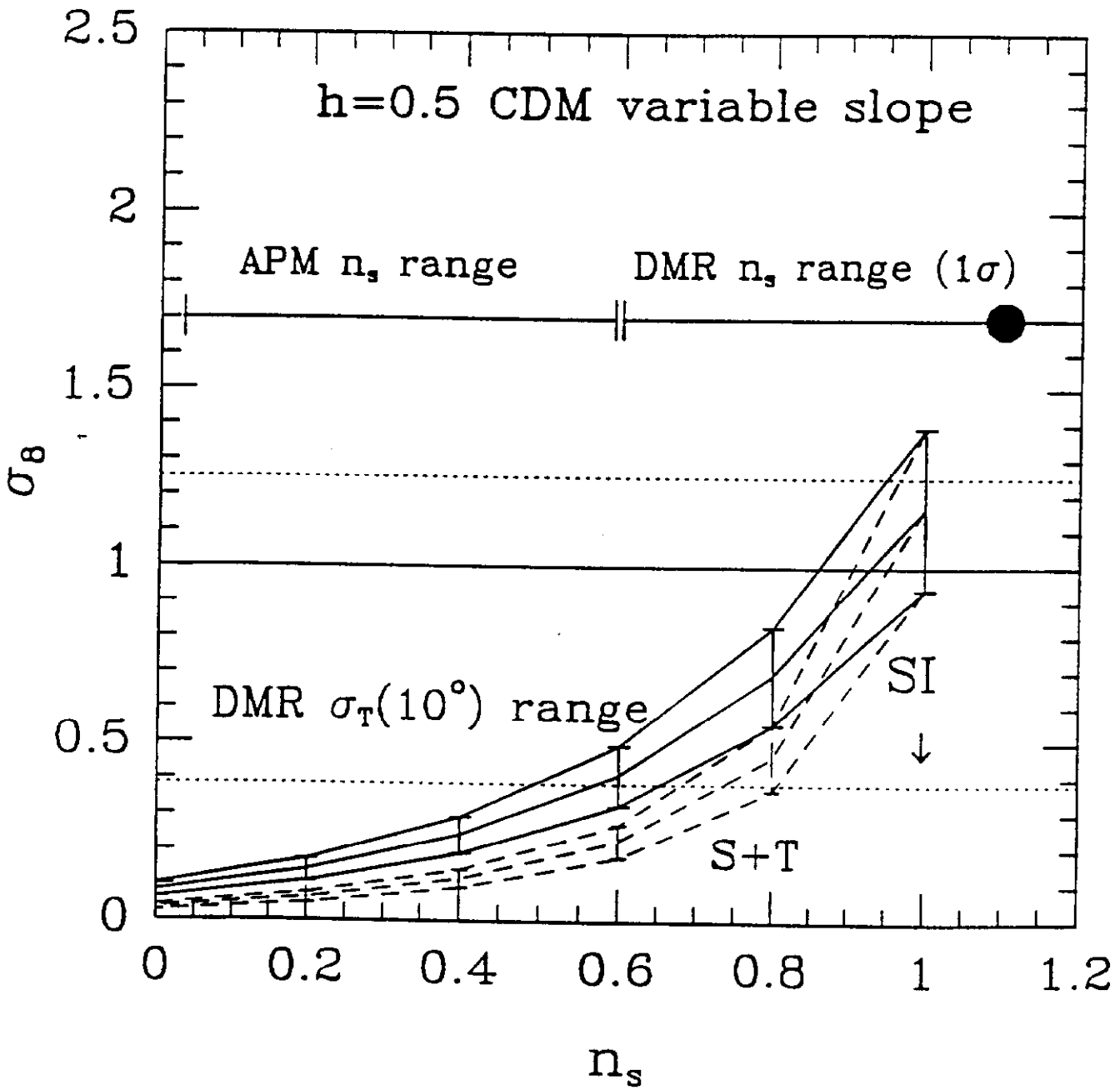
h=0.5 CDM variable slope
APM n_s range
DMR n_s range (1σ)
DMR $\sigma_T(10^\circ)$ range
SI
S+T
σ_8
n_s
2.5
2
1.5
1
0.5
0
0
0.2
0.4
0.6
0.8
1
1.2

F. 5

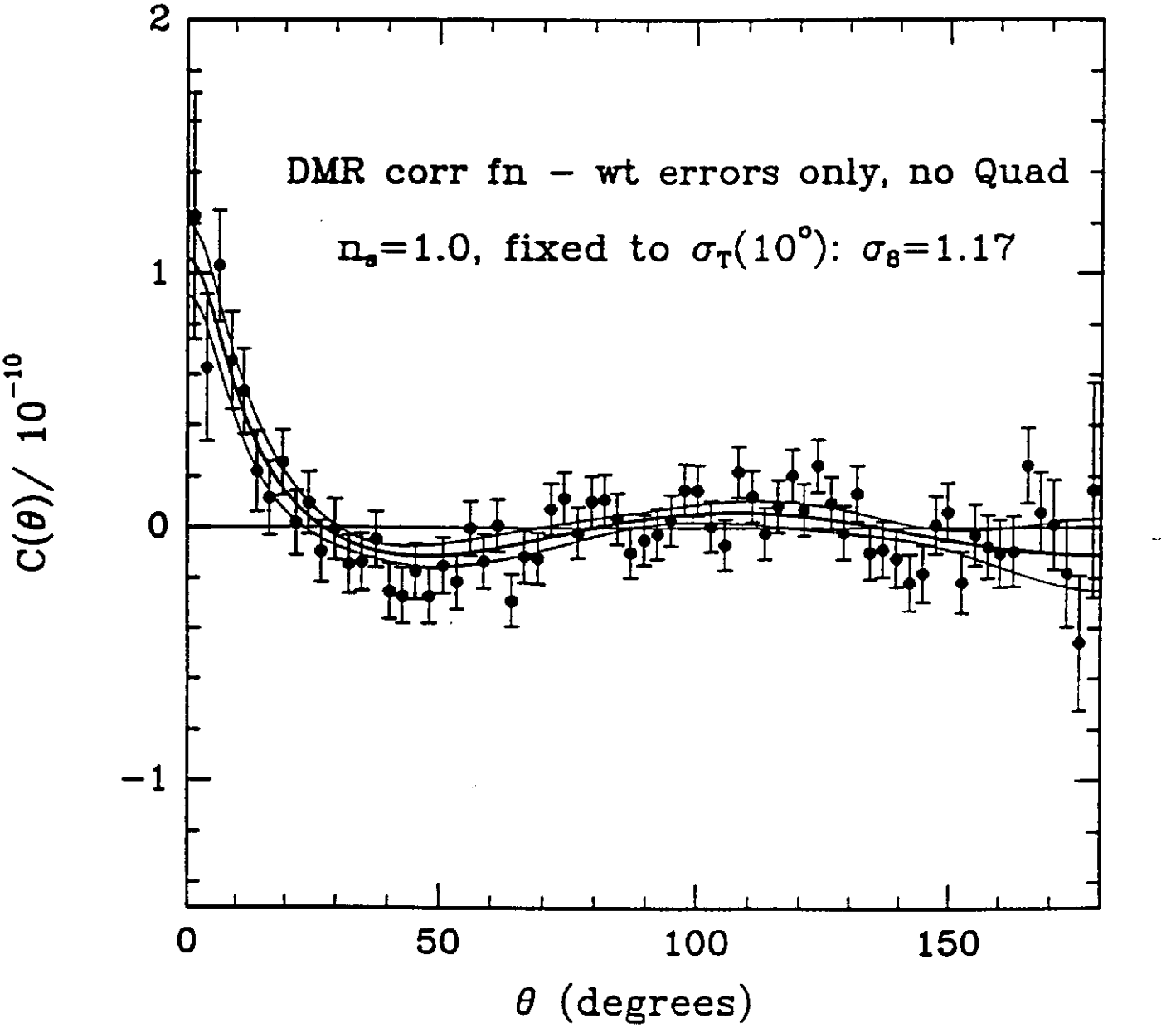
DMR corr fn – wt errors only, no Quad
n_s=1.0, fixed to $\sigma_T(10^\circ)$: σ_8=1.17
$C(\theta)/\ 10^{-10}$
θ (degrees)
2
1
0
−1
0
50
100
150

F. 6(a)

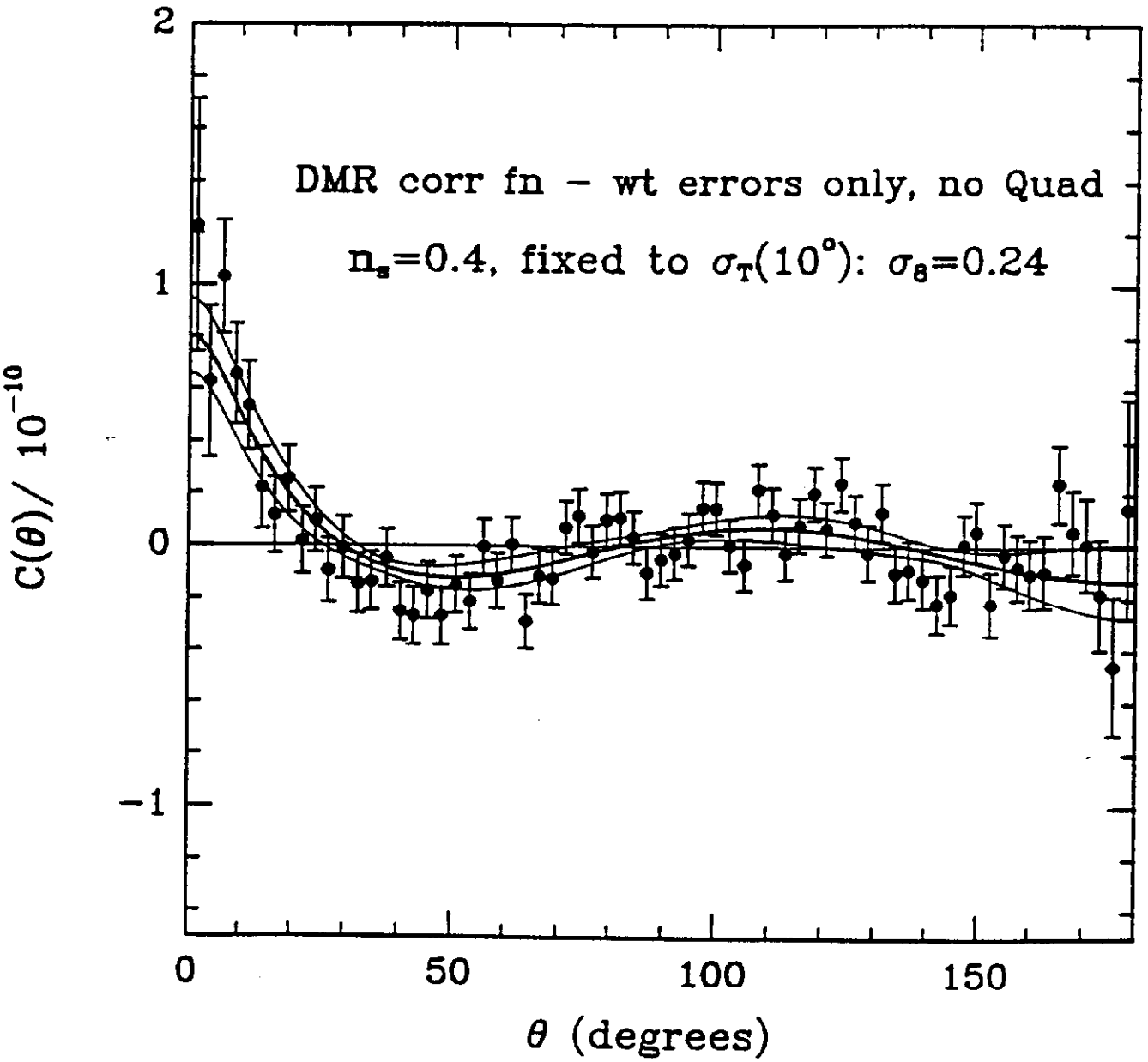
DMR corr fn – wt errors only, no Quad
n_s=0.4, fixed to $\sigma_T(10^\circ)$: σ_8=0.24
$C(\theta)/\ 10^{-10}$
θ (degrees)
2
1
0
−1
0
50
100
150

F. 6(b)

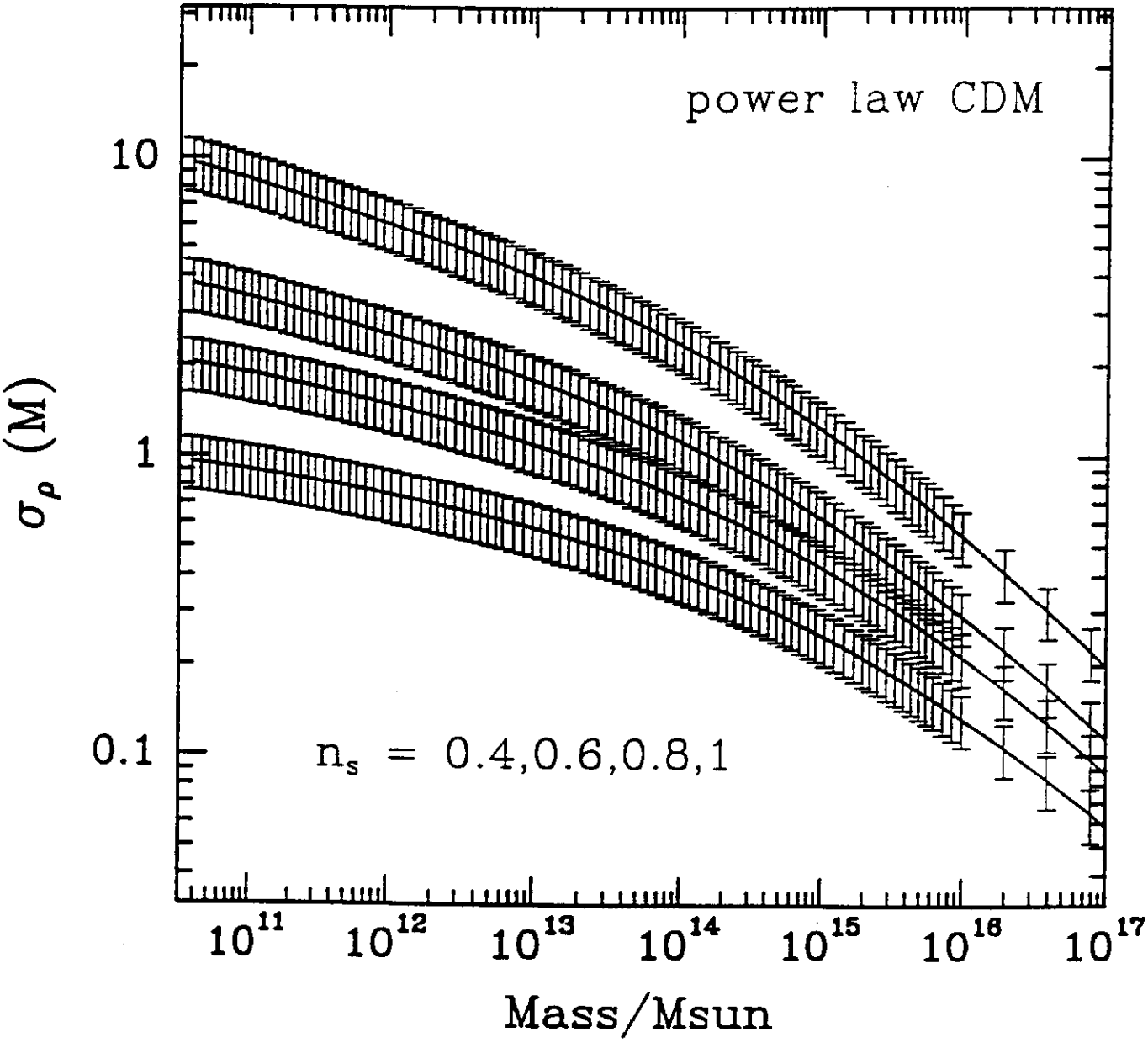
power law CDM
10
1
0.1
σ_ρ (M)
n_s = 0.4,0.6,0.8,1
10^{11}
10^{12}
10^{13}
10^{14}
10^{15}
10^{16}
10^{17}
Mass/Msun

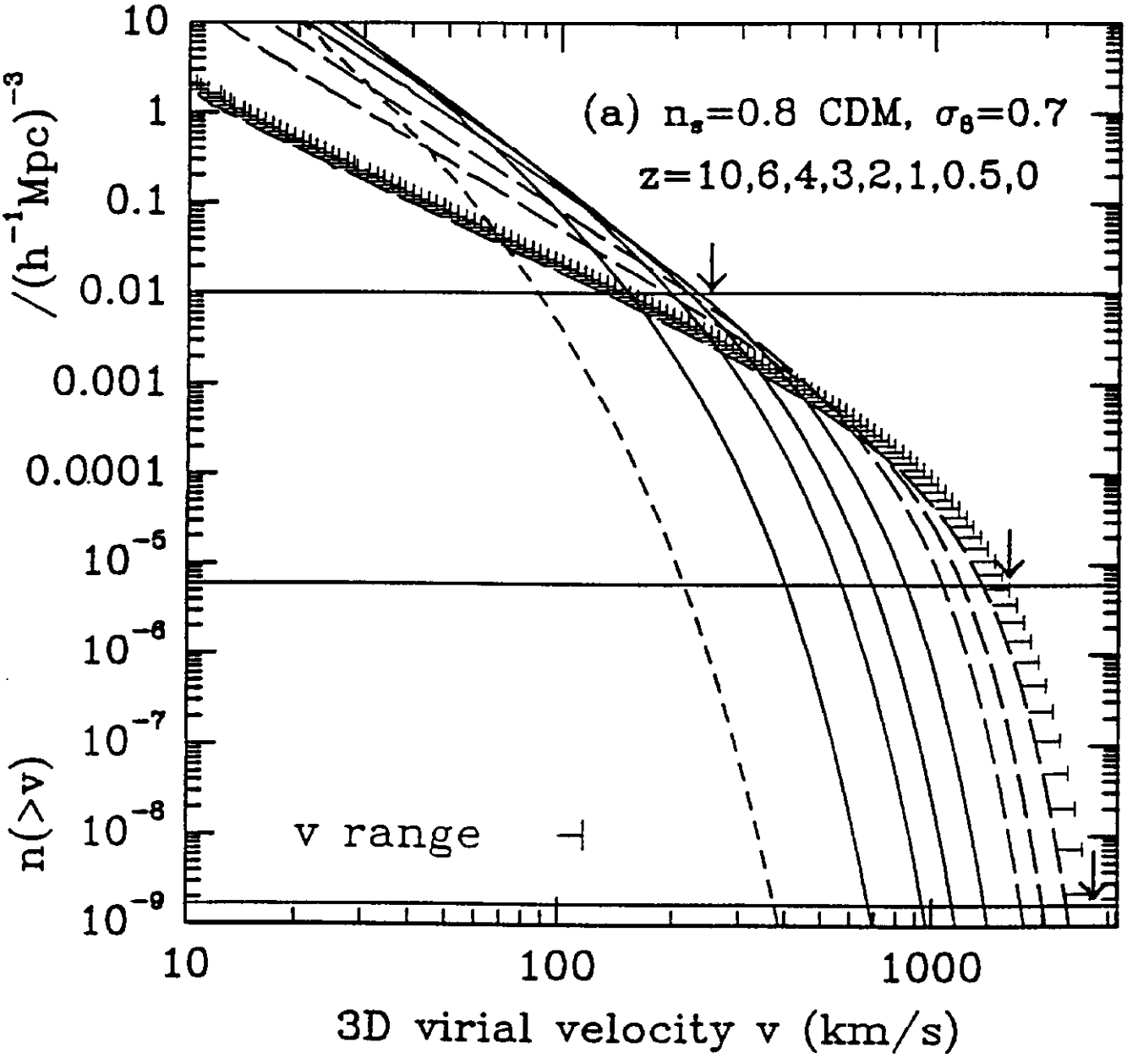
(a) n_s=0.8 CDM, σ_8=0.7
z=10,6,4,3,2,1,0.5,0
v range
n(>v) /(h^{-1}Mpc)$^{-3}$
10
1
0.1
0.01
0.001
0.0001
10^{-5}
10^{-6}
10^{-7}
10^{-8}
10^{-9}
10
100
1000
3D virial velocity v (km/s)

F. 8(a)

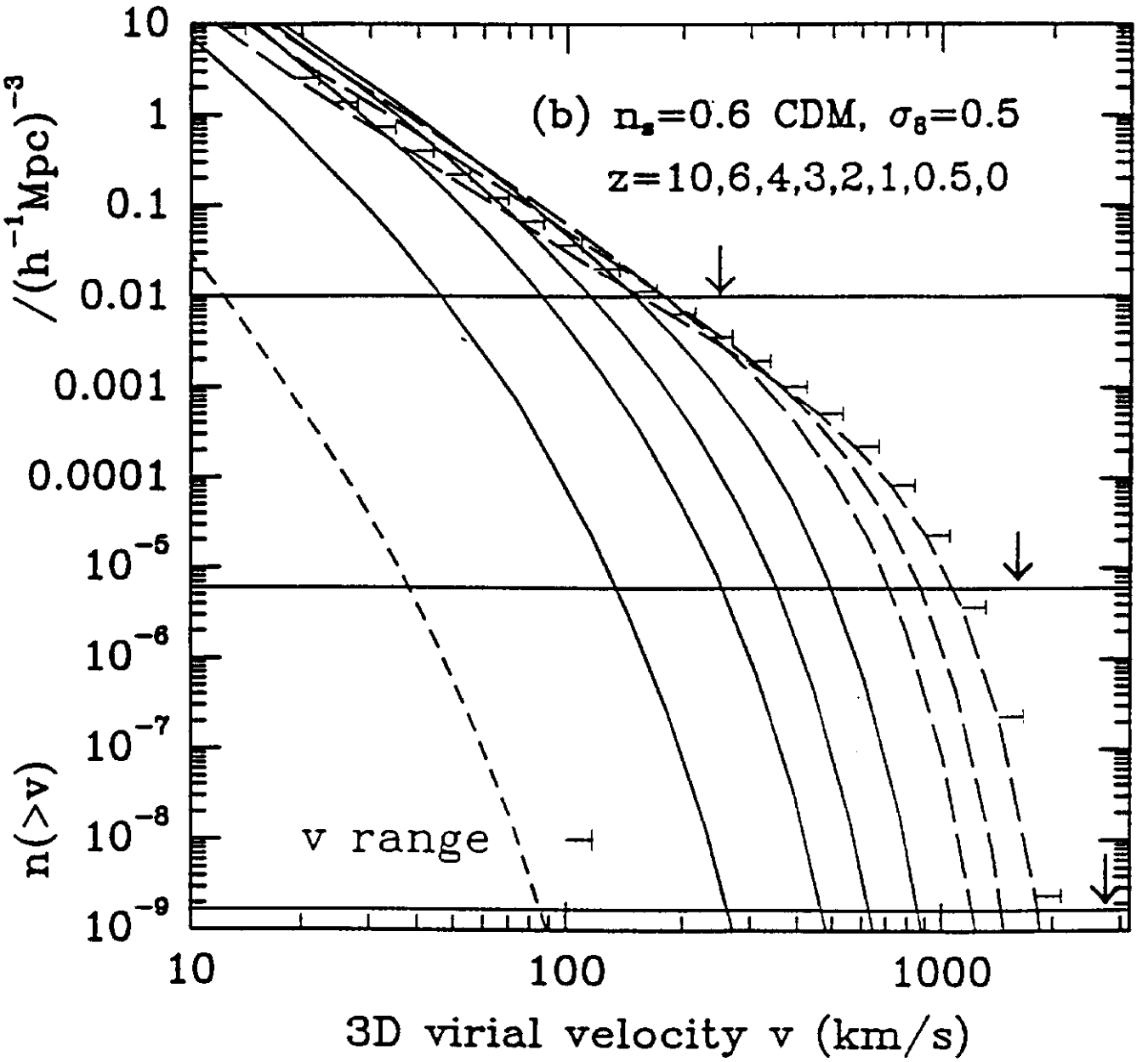
(b) n_s=0.6 CDM, σ_8=0.5
z=10,6,4,3,2,1,0.5,0
v range
n(>v) /(h^{-1}Mpc)$^{-3}$
10
1
0.1
0.01
0.001
0.0001
10^{-5}
10^{-6}
10^{-7}
10^{-8}
10^{-9}
10
100
1000
3D virial velocity v (km/s)

F. 8(b)

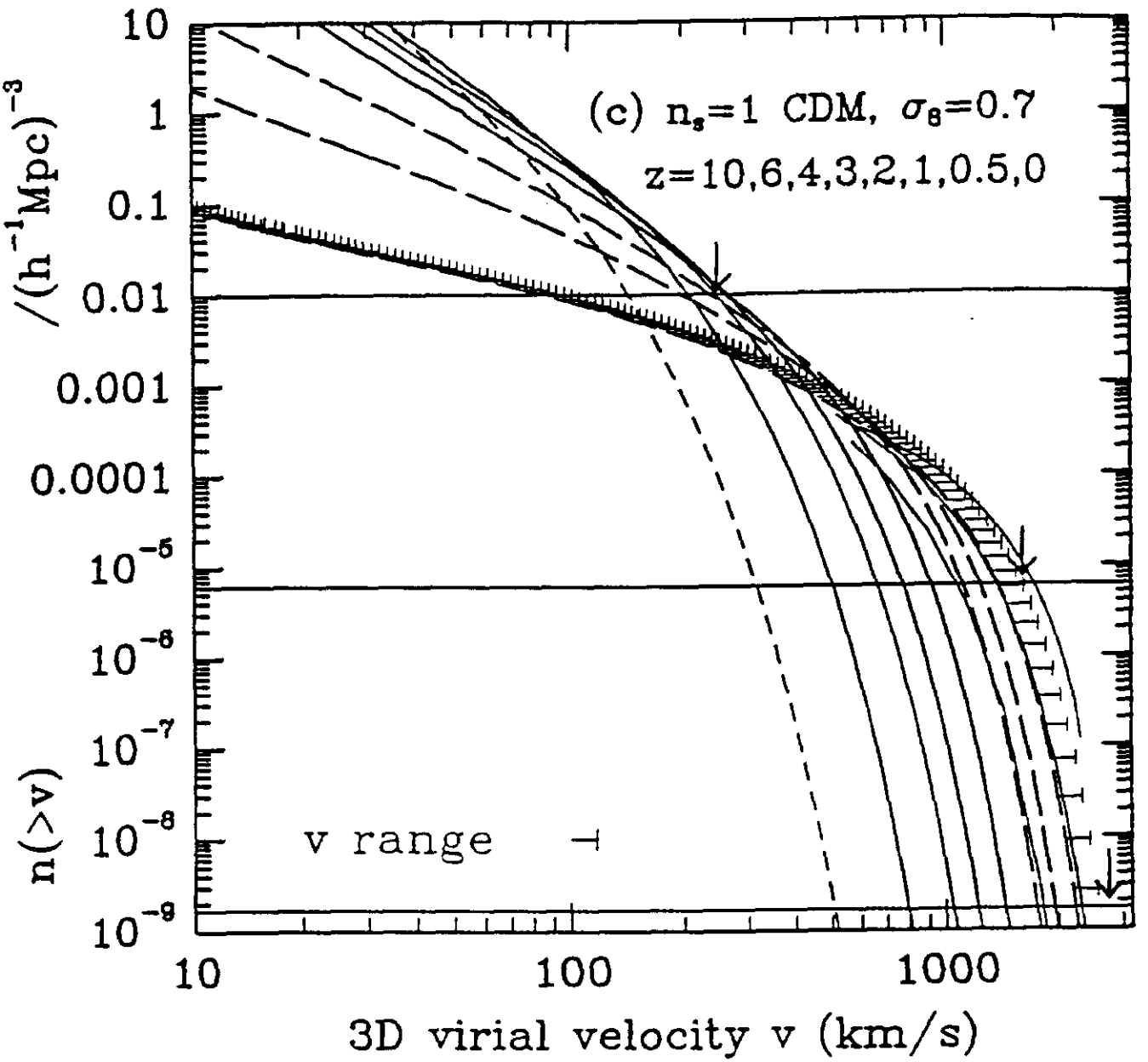
(c) n_s=1 CDM, σ_8=0.7
z=10,6,4,3,2,1,0.5,0
v range
n(>v) /(h^{-1}Mpc)$^{-3}$
10
1
0.1
0.01
0.001
0.0001
10^{-5}
10^{-6}
10^{-7}
10^{-8}
10^{-9}
10
100
1000
3D virial velocity v (km/s)

Fig 1(c)